Helsinki University of Technology Signal Processing Laboratory
Teknillinen korkeakoulu Signaalinkäsittelytekniikan laboratorio
Espoo 2006 Report 54

ADVANCED RECEIVER STRUCTURES FOR MOBILE MIMO MULTICARRIER COMMUNICATION SYSTEMS

Timo Roman

Dissertation for the degree of Doctor of Science in Technology to be presented with due permission of the Department of Electrical and Communications Engineering for public examination and debate in Auditorium S4 at Helsinki University of Technology (Espoo, Finland) on the 6th of April, 2006, at 12 o'clock noon.

Helsinki University of Technology
Department of Electrical and Communications Engineering
Signal Processing Laboratory

Teknillinen korkeakoulu
Sähkö- ja tietoliikennetekniikan osasto
Signaalinkäsittelytekniikan laboratorio

Distribution:
Helsinki University of Technology
Signal Processing Laboratory
P.O. Box 3000
FIN-02015 HUT
Tel. +358-9-451 3211
Fax. +358-9-452 3614
E-mail: Mirja.Lemetyinen@hut.fi

© Timo Roman

ISBN 951-22-8103-1 (Printed)
ISBN 951-22-8104-X (Electronic)
ISSN 1458-6401

Otamedia Oy
Espoo 2006

Abstract

Beyond third generation (3G) and fourth generation (4G) wireless communication systems are targeting far higher data rates, spectral efficiency and mobility requirements than existing 3G networks. By using multiple antennas at the transmitter and the receiver, multiple-input multiple-output (MIMO) technology allows improving both the spectral efficiency (bits/s/Hz), the coverage, and link reliability of the system. Multicarrier modulation such as orthogonal frequency division multiplexing (OFDM) is a powerful technique to handle impairments specific to the wireless radio channel. The combination of multicarrier modulation together with MIMO signaling provides a feasible physical layer technology for future beyond 3G and fourth generation communication systems.

The theoretical benefits of MIMO and multicarrier modulation may not be fully achieved because the wireless transmission channels are time and frequency selective. Also, high data rates call for a large bandwidth and high carrier frequencies. As a result, an important Doppler spread is likely to be experienced, leading to variations of the channel over very short period of time. At the same time, transceiver front-end imperfections, mobility and rich scattering environments cause frequency synchronization errors. Unlike their single-carrier counterparts, multi-carrier transmissions are extremely sensitive to carrier frequency offsets (CFO). Therefore, reliable channel estimation and frequency synchronization are necessary to obtain the benefits of MIMO OFDM in mobile systems. These two topics are the main research problems in this thesis.

An algorithm for the joint estimation and tracking of channel and CFO parameters in MIMO OFDM is developed in this thesis. A specific state-space model is introduced for MIMO OFDM systems impaired by multiple carrier frequency offsets under time-frequency selective fading. In MIMO systems, multiple frequency offsets are justified by mobility, rich scattering environment and large angle spread, as well as potentially separate radio frequency - intermediate frequency chains. An extended Kalman filter stage tracks channel and CFO parameters. Tracking takes place in time domain, which ensures reduced computational complexity, robustness to estimation errors as well as low estimation variance in comparison to frequency domain processing.

The thesis also addresses the problem of blind carrier frequency synchronization in OFDM. Blind techniques exploit statistical or structural properties of the OFDM modulation. Two novel approaches are proposed for blind fine CFO estimation. The first one aims at restoring the orthogonality of the OFDM transmission by exploiting the properties of the received signal covariance matrix. The second approach is a subspace algorithm exploiting the correlation of the channel frequency response among the subcarriers. Both methods achieve reliable estimation of the CFO regardless of multipath fading. The subspace algorithm needs extremely small sample support, which is a key feature in the face of time-selective channels. Finally, the Cramér-Rao (CRB) bound is established for the problem in order to assess the large sample performance of the proposed algorithms.

Preface

The research work for this doctoral thesis was carried out at the Signal Processing Laboratory, Helsinki University of Technology, during the years 2001-2005. The Statistical Signal Processing research group, led by Prof. Visa Koivunen, is a part of SMARAD (Smart and Novel Radios Research Unit) Center of Excellence in research nominated by the Academy of Finland.

First, I wish to express my gratitude to my supervisor, Prof. Visa Koivunen, for his continuous encouragement, guidance and support during the course of this work. It has been an honor to work with such a deeply dedicated scientist and outstanding group leader.

Then, I would like to thank the thesis pre-examiners, Prof. Mounir Ghogho and Dr. Jyri Hämäläinen for their constructive and helpful comments. Furthermore, Prof. Iiro Hartimo, the director of the Graduate School in Electronics, Telecommunications and Automation (GETA) and the GETA coordinator Marja Leppäharju are highly acknowledged. Lab secretaries Mirja Lemetyinen and Anne Jääskeläinen deserve also many thanks for assisting with all practical issues and arrangements.

I am grateful to my colleagues in the lab and especially co-workers Dr. Mihai Enescu and Dr. Samuli Visuri with whom I co-authored several publications, as well as Traian Abrudan, Maarit Melvasalo, Dr. Jan Eriksson and Dr. Marius Sirbu. Prof. Risto Wichman, Dr. Stephan Werner, Dr. Andreas Richter, Fabio Belloni, Eduardo Zacarias, Jussi Salmi and Cassio Ribeiro are also acknowledged for our valuable discussions.

This research work was funded by the Academy of Finland and the GETA Graduate School. Also, the financial support of Nokia Foundation, Tekniikan Edistämissäätiö, Emil Aaltosen Säätiö, HPY:n Tutkimussäätiö, and the Finnish Foundation for Economic and Technology Sciences - KAUTE is gratefully acknowledged.

I wish to express my warmest gratitude to my family in both France and Finland, my parents Alain and Marjo as well as my brothers Tommi and Johan for their permanent encouragement and support, despite the distance to France. Foremost, I would like to thank Mona, who has been by my side day after day, giving me understanding and love.

Espoo,
March 2006,

Timo Roman

Contents

List of original publications

(I) T. Roman, M. Enescu and V. Koivunen. Time-domain method for tracking dispersive channels in MIMO OFDM systems, in *Proceedings of the IEEE International Conference on Acoustics, Speech, and Signal Processing*, ICASSP 2003, Vol. 4, pp. IV 393-IV 396, Hong Kong, China, April 2003.

(II) T. Roman, M. Enescu and V. Koivunen. Joint time-domain tracking of channel and frequency offset for OFDM systems, in *Proceedings of the IEEE Workshop on Signal Processing Advances in Wireless Communications*, SPAWC 2003, pp. 605-609, Rome, Italy, June 2003.

(III) T. Roman, M. Enescu and V. Koivunen. Joint time-domain tracking of channel and frequency offsets for MIMO OFDM systems, *Wireless Personal Communications*, Kluwer, Vol. 31, Nos 3-4, pp. 181-200, December 2004.

(IV) T. Roman, S. Visuri and V. Koivunen. Blind frequency synchronization in OFDM via diagonality criterion, to appear in *IEEE Transactions on Signal Processing*.

(V) T. Roman, S. Visuri and V. Koivunen. Performance bound for blind CFO estimation in OFDM with real-valued constellations, in *Proceedings of the IEEE Semiannual Vehicular Technology Conference*, VTC 04 Fall, Vol. 6, pp. 3866-3870, Los-Angeles, USA, September 2004.

(VI) T. Roman and V. Koivunen. One-shot subspace based method for blind CFO estimation for OFDM, in *Proceedings of the IEEE International Conference on Acoustics, Speech, and Signal Processing*, ICASSP 2005, Vol. 3, pp. 809 - 812, Philadelphia, USA, March 2005.

(VII) T. Roman and V. Koivunen. Subspace method for blind CFO estimation for OFDM systems with constant modulus constellations, in *Proceedings of the IEEE Semiannual Vehicular Technology Conference*, VTC 05 Spring, Vol. 2, pp. 1253 - 1257, Stockholm, Sweden, May 2005.

List of abbreviations and symbols

Abbreviations

1-D	one-dimensional
2-D	two-dimensional
2G	second generation
3G	third generation
4G	fourth generation
3GPP	third generation partnership project
ADSL	asymmetric digital subscriber line
AFC	automatic frequency control
ANLS	approximate nonlinear least-squares
AOA	angle of arrival
AR	auto-regressive
APSB	added pilot semi-blind
AWGN	additive white Gaussian noise
B3G	beyond third generation
BER	bit error rate
BLUE	best linear unbiased estimator
BPSK	binary phase shift keying
EVD	eigenvalue decomposition
CDMA	code division multiple access
CFR	channel frequency response
CIR	channel impulse response
CM	constant modulus
CP	cyclic prefix
CP-OFDM	cyclic-prefix OFDM
CCRB	conditional Cramér-Rao bound
CRB	Cramér-Rao bound
CS	cyclostationarity
dB	decibel
DAB	digital audio broadcast
DD	decision-directed
DDCE	decision-directed channel estimation
DOA	direction of arrival
DS	deterministic subspace
DFE	decision-feedback equalization
DFT	discrete Fourier transform
DMT	discrete multi-tone
DVB	digital video broadcast

DVB-H	digital video broadcast - hand-held
DVB-T	digital video broadcast - terrestrial
EKF	extended Kalman filter
EM	expectation maximization
ESCA	extended Schmidl and Cox algorithm
FA	finite alphabet
FD	frequency domain
FDD	frequency division duplexing
FDM	frequency division multiplexing
FFT	fast Fourier transform
FIR	finite impulse response
HIPERLAN	high performance local area network
HOS	high-order statistics
HR	harmonic retrieval
HSDPA	high speed data packet access
IBI	inter-block interference
ICA	independent component analysis
ICI	intercarrier interference
IDFT	inverse Fourier transform
IFFT	inverse fast Fourier transform
IP	internet protocol
ISI	inter-symbol interference
i.i.d.	independent identically distributed
KF	Kalman filter
LAN	local area network
LMMSE	linear minimum mean square error
LMS	least mean squares
LO	local oscillator
LOS	line-of-sight
LS	least squares
MB-OFDM	multiband OFDM
MC-CDMA	multicarrier CDMA
MIMO	multiple-input multiple-output
MISO	multiple-input single-output
MKF	mixture Kalman filter
ML	maximum likelihood
MMSE	minimum mean square error
MOE	minimum output energy
MOV	minimum output variance
NLS	nonlinear least-squares
NSC	null subcarrier
OFDM	orthogonal frequency division multiplexing
OOB	out-of-band
OQAM	offset quadrature amplitude modulation
PAPR	peak-to-average power ratio
PIC	parallel interference cancellation
PDP	power-delay profile
PN	pseudo-noise
P/S	parallel-to-serial

PHN	phase noise
PLL	phase-locked loop
PSAM	pilot symbol-assisted modulation
PSD	power spectral density
PSK	phase shift keying
QAM	quadrature amplitude modulation
QPSK	quadrature phase shift keying
REP	repetitive slots
RF	radio frequency
RF-IF	radio frequency - intermediate frequency
RMS	root-mean-squared
SCA	Schmidl and Cox's algorithm
SCM	spatial channel model
SCME	spatial channel model extended
SFO	sampling frequency offset
SIMO	single-input multiple-output
SMC	sequential Monte-Carlo
SNR	signal-to-noise ratio
SOCS	second-order cyclostationary statistics
S/P	serial-to-parallel
SS	statistical subspace
SVD	singular value decomposition
TD	time domain
TDD	time domain duplexing
TDM	time division multiplexing
UWB	ultra wideband
VCMA	vector constant modulus algorithm
VSC	virtual subcarrier
WiBro	wireless broadband
WLAN	wireless local area network
WLS	weighted least squares
WSS	wide-sense stationary
ZF	zero-forcing
ZP	zero-padding
ZP-OFDM	zero-padded OFDM

Symbols

j	imaginary unit
$*$	convolution product
$\odot$	Hadamard (i.e., element-wise) product
$\| \ \|$	Euclidean norm
arg	argument of a complex number
arg min	minimizing argument
arg max	maximizing argument
E	expectation operator
E[|]	conditional expectation operator
mod N	modulo N operation
exp	exponential function
min	minimum
max	maximum
rank	rank of a matrix
span $\{\mathbf{A}\}$	column range of matrix $\mathbf{A}$
w. p. 1	convergence with probability 1
a	complex scalar
a^*	complex conjugate of scalar a
Re$\{a\}$	real part of complex scalar a
Im$\{a\}$	imaginary part of complex scalar a
$\hat{a}$	estimate of a
$\mathbf{a}$	complex-valued vector
$\hat{\mathbf{a}}$	estimate of vector $\mathbf{a}$
$\mathbf{a}^*$	complex conjugate of vector $\mathbf{a}$
$\mathbf{a}^T$	transpose of vector $\mathbf{a}$
$\mathbf{a}^H$	Hermitian transpose of vector $\mathbf{a}$
$\mathbf{A}$	complex-valued matrix
$\hat{\mathbf{A}}$	estimate of matrix $\mathbf{A}$
$\mathbf{A}^*$	complex conjugate of matrix $\mathbf{A}$
$\mathbf{A}^T$	transpose of matrix $\mathbf{A}$
$\mathbf{A}^H$	Hermitian transpose of matrix $\mathbf{A}$
$\mathbf{A}^{-1}$	inverse of matrix $\mathbf{A}$
$\mathbf{A}^{-T}$	inverse transpose of matrix $\mathbf{A}$
$\mathbf{A}^\dagger$	Moore-Penrose pseudo-inverse of matrix $\mathbf{A}$
$[\mathbf{A}]_{m,n}$	(m,n) element of matrix $\mathbf{A}$
$[\mathbf{A}]_{\{i_1:i_2,j_1:j_2\}}$	sub-matrix of $\mathbf{A}$ formed by the lines indexed by i_1 to i_2 and the columns indexed by j_1 to j_2
cov$(\mathbf{u})$	covariance matrix of $\mathbf{u}$
pcov$(\mathbf{u})$	pseudo-covariance matrix of $\mathbf{u}$
diag $\{\}$	diagonal matrix of the argument vector
vec	stacks columns of a matrix on top of each other
β_k	energy normalization factor accounting for null-subcarriers
Δf	intercarrier spacing [Hz]
ϵ	fractional CFO (normalized wrt. intercarrier spacing)
f_D	Doppler frequency
$\varphi_k(\nu)$	CFO-induced block dependent term
ϕ_D	angle of the impinging wavefront

λ	wavelength
ν	normalized CFO wrt. intercarrier spacing
$\hat{\nu}_K$	estimate of the carrier frequency offset with K observed blocks
ν_{tr}	CFO for MIMO branch tr
σ^2	variance of the noise
σ_s^2	average symbol energy
τ	timing offset
τ_d	delay spread
$\tau(k,l)$	time delay of the l^{th} path index at k^{th} block instance
b	bit rate [bit/s]
b_{sc}	subcarrier bit rate [bit/s]
B	total system bandwidth [Hz]
B_d	Doppler spread [Hz]
B_{sc}	subcarrier bandwidth [Hz]
$\mathcal{D}$	set of data subcarrier indices
E_s/N_o	SNR per symbol
J	number of repetitive slots in time domain for slot-based CFO estimators
k	OFDM block index
k_ν	integer CFO (normalized wrt. intercarrier spacing)
K	total number of OFDM blocks
L_h	channel length
L_h'	channel order
L_{CP}	cyclic prefix length
N	number of subcarriers
N_t	number of transmit antennas
N_r	number of receive antennas
N_p	total number of pilot symbols per OFDM block
N_d	total number of data symbols per OFDM block
N_z	number of null-subcarriers
N_v	number of virtual subcarriers
N_a	number of active subcarriers
N_n	number of equi-spaced null-subcarriers
$\mathcal{N}$	entire set of subcarrier indices
$\mathcal{N}_{\text{A}}$	set of active subcarrier indices
$\mathcal{N}_{\text{NSC}}$	set of null-subcarrier indices
$\mathcal{N}_{\text{VSC}}$	set of virtual subcarrier indices
$\mathbb{U}_{\text{A}}$	subspace of active subcarriers
$\mathbb{U}_{\text{N}}$	subspace of null-subcarriers
$\mathcal{P}$	set of pilot subcarrier indices
P	OFDM block length
Q	number of samples in each repetitive slot
$\mathcal{Q}$	size of symbol alphabet
r	receive antenna index
t	transmit antenna index
τ_c	continuous time-delay
t_s	duration of the OFDM sub-symbol
T_g	duration of the cyclic prefix
T_s	duration of the data part
T_{s+g}	duration of the OFDM block

v	velocity of the mobile terminal
x_{bps}	number of bits per symbol
a	data variable (excluding null-subcarriers)
$h^{(c)}(\tau_c)$	continuous time impulse response between the transmitter and the receiver
$h^{(tx)}(\tau_c)$	continuous time transmit pulse shaping filter
$h^{(rx)}(\tau_c)$	continuous time receive pulse shaping filter
$h^{(ch)}_{tr,k}(\tau_c)$	continuous time channel impulse response at block time instance k
$h(k,l)$	discrete-time channel impulse response at block instance k and path index l
$\tilde{h}_n$	value of the channel frequency response at the n^{th} subcarrier
s	symbol variable (may include null-subcarriers)
$s_{t,n}$	symbol variable at the t^{th} transmit antenna and n^{th} subcarrier
y	received signal sample in the time domain
$y_{\text{CP},n}$	n^{th} received signal sample in the time domain before CP removal
$y_{\nu,\text{CP},n}$	n^{th} received signal sample in the time domain before CP removal corrupted by CFO
$y_{\nu,n}$	n^{th} sample of the received signal in the time domain corrupted by CFO
$\tilde{y}$	received signal sample in the frequency domain
$\boldsymbol{\alpha}$	vector containing the symbols affected by channel fading and CFO-induced phase rotation
$\boldsymbol{\rho}$	parameter vector
$\boldsymbol{\nu}$	vector of CFOs
$\mathbf{a}$	data vector
$\bar{\mathbf{f}}_n$	n^{th} column vector of the DFT matrix $\mathbf{F}^H$
$\mathbf{f}_n$	n^{th} column vector of the IDFT matrix $\mathbf{F}$
$\mathbf{g}$	nonlinear vector function of the state vector in the EKF measurement equation
$\mathbf{h}$	channel impulse response vector
$\tilde{\mathbf{h}}$	channel frequency response vector
$\tilde{\mathbf{h}}_p$	channel frequency response vector at pilot subcarriers
$\tilde{\mathbf{h}}_d$	channel frequency response vector at data subcarriers
$\mathbf{s}$	symbol vector
$\mathbf{s}_t$	symbol vector at the t^{th} transmit antenna
$\mathfrak{s}$	state vector for Kalman filtering / extended Kalman filtering
$\mathfrak{s}_{(k\|k-1)}$	predicted estimate of the state vector
$\mathfrak{s}_{(k\|k)}$	filtered estimate of the state vector
$\mathbf{u}_{\mathbf{w},i}$	i^{th} column vector of matrix $\mathbf{U}_{\mathbf{w}}$
$\mathbf{u}_{\text{ZF}}$	equalized symbol vector (ZF equalizer)
$\mathbf{u}_{\text{MMSE}}$	equalized symbol vector (MMSE equalizer)
$\mathbf{v}$	state noise vector for KF/EKF
$\mathbf{v}_{\hat{\nu}\nu}$	CFO-compensated received vector in the frequency domain using the estimate $\hat{\nu}$ of the true CFO ν
$\mathbf{w}$	noise vector in the time domain
$\tilde{\mathbf{w}}$	noise vector in the frequency domain
$\tilde{\mathbf{w}}_p$	noise vector at pilot subcarriers (in the frequency domain)
$\tilde{\mathbf{w}}_d$	noise vector at data subcarriers (in the frequency domain)
$\tilde{\mathbf{x}}_t$	modulated symbol vector at the t^{th} transmit antenna

$\tilde{\mathbf{x}}_{\mathrm{CP},t}$	modulated symbol vector at the t^{th} transmit antenna with cyclic prefix
$\mathbf{y}$	received signal vector in the time domain
$\mathbf{y}_\nu$	received signal vector in the time domain corrupted by CFO
$\tilde{\mathbf{y}}$	received signal vector in the frequency domain
$\tilde{\mathbf{y}}_\nu$	received signal vector in the frequency domain corrupted by CFO
$\tilde{\mathbf{y}}_\theta$	received signal in the frequency domain impaired by phase noise
$\tilde{\mathbf{y}}_p$	received signal vector in the frequency domain at pilot subcarriers
$\tilde{\mathbf{y}}_d$	received signal vector in the frequency domain at data subcarriers
$\mathbf{0}_{N\times M}$	matrix of zeros of size $N \times M$
$\mathbb{1}_N$	matrix of 1's of size $N \times N$
$\mathbf{I}_N$	identity matrix of size $N \times N$
$\mathbf{A}$	DFT/IDFT pair of transforms
$\mathbf{A}_{\mathfrak{s}}$	state transition matrix for KF/EKF
$\mathbf{C}(\nu)$	CFO matrix
$\mathbf{C}_{\mathrm{PHN}}$	phase noise matrix
$\mathbf{D}_{\tilde{\mathbf{h}}}$	diagonal channel frequency response matrix
$\mathbf{D}_p$	diagonal matrix of pilot symbols
$\mathbf{D}_d$	diagonal matrix of data symbols
$\mathbf{F}$	IDFT matrix of size $N \times N$
$\mathbf{F}^H$	DFT matrix of size $N \times N$
$\mathbf{G}_{\mathfrak{s}}$	Jacobian matrix of $\mathbf{g}(\mathfrak{s})$ with respect to $\mathfrak{s}$
$\mathbf{H}$	Toeplitz channel matrix
$\tilde{\mathbf{H}}$	circulant channel matrix
$\mathbf{J}$	matrix linking the complete second-order statistics to the parameter vector $\boldsymbol{\rho}$
$\mathbf{K}_{(k)}$	Kalman gain matrix
$\mathbf{M}$	MIMO transmission matrix
$\mathbf{M}_{tr}$	transmission matrix between transmit antenna t and receive antenna r
$\mathbf{P}_{(k\|k-1)}$	covariance matrix of the prediction error
$\mathbf{P}_{(k\|k)}$	covariance matrix of the filtering error
$\mathbf{Q}_{\mathbf{v}}$	state noise covariance matrix for KF/EKF
$\mathbf{Q}_{\mathbf{h}}$	state noise covariance matrix associated to channel coefficients
$\mathbf{Q}_{\boldsymbol{\nu}}$	state noise covariance matrix associated to CFOs
$\mathbf{Q}(\mu)$	time domain received signal covariance matrix given a CFO compensation by μ
$\tilde{\mathbf{Q}}(\mu)$	frequency domain received signal covariance matrix given a CFO compensation by μ
$\widehat{\tilde{\mathbf{Q}}}_K(\mu)$	sample estimate of $\tilde{\mathbf{Q}}(\mu)$ with K vector observations
$\hat{\mathbf{R}}$	sample covariance matrix
$\mathbf{R}_{\mathbf{ss}}$	source signal covariance matrix
$\mathbf{R}_{\mathbf{rr}}$	received signal covariance matrix
$\mathbf{R}_{\mathrm{CP}}$	cyclic prefix removal matrix
$\mathbf{T}_{\mathrm{CP}}$	cyclic prefix insertion matrix
$\mathbf{U}_{\mathbf{s}}$	matrix containing the basis vectors for the signal subspace
$\mathbf{U}_{\mathbf{w}}$	matrix containing the basis vectors for the noise subspace
$\boldsymbol{\mathcal{U}}_{\mathbf{w},i}$	Toeplitz convolution matrix generated from the vector $\mathbf{u}_{\mathbf{w},i}$
$\mathbf{V}_{\mathrm{NSC}}$	matrix introducing null-subcarriers
$\tilde{\mathbf{X}}_t(k)$	circular convolution matrix of modulated symbols at transmit antenna t
$\tilde{\mathbf{X}}_{tr}^{(\nu)}$	circular convolution matrix of CFO-corrupted modulated symbols on MIMO

	branch tr
$\tilde{\mathbf{X}}^{(\nu)}$	matrix of CFO-corrupted modulated symbols in the MIMO case
$\mathbf{\Pi}_{\text{NSC}}$	projection matrix to subspace of null-subcarriers
$\mathbf{\Pi}_{\text{A}}$	projection matrix to subspace of active subcarriers
$\partial \mathbf{g}/\partial \mathfrak{s}^T$	derivative of $\mathbf{g}$ with respect to $\mathfrak{s}^T$
$\mathcal{C}$	cost function for the proposed projection-based CFO estimator
$\mathcal{G}$	basis for the column subspace of channel squared amplitude frequency responses
$\mathcal{J}$	cost function minimizing the total off-diagonal power of frequency domain signal covariance matrix
$\widehat{\mathcal{J}}_K$	sample estimate of $\mathcal{J}$ with K vector observations
$\mathcal{J}_{\text{CM}}$	cost function exploiting the CM assumption for blind CFO estimation
$\mathcal{J}_{\text{VSC}}$	cost function exploiting VSC's for blind CFO estimation
$\mathcal{J}_{\text{VSC+CM}}$	cost function exploiting both VSC's and the CM assumption for blind CFO estimation
D_{PHN}	degradation in SNR due to phase noise
D_{CFO}	degradation in SNR due to carrier frequency offset
$\text{CRB}_K(\nu)$	Cramér-Rao bound on the CFO assuming a total of K vector observations
FIM_K	Fisher information matrix assuming a total of K vector observations
MSE_K	MSE after K received blocks

Chapter 1

Introduction

1.1 Motivation of the thesis

Third generation (3G) wireless services are currently being deployed. While 3G networks outperform their second generation (2G) predecessors, they still may not be sufficient to meet the requirements for future high data rate applications like multimedia, video streaming, wireless teleconferencing and web browsing. Hence, there exists the need for a wireless network technology that improves 3G throughput performance by one order of magnitude at least. Major requirements of future beyond third generation (B3G) and fourth generation (4G) wireless communication systems are thus higher user data rates, improved coverage and spectral efficiency, as well as enhanced user mobility. Low latency and improved radio link quality are also desired. The future trend is the convergence to all digital IP-based packet networks, with both voice and data capabilities. All those enhancements will allow bringing to mobile users Internet services and multimedia applications that consume lot of resources. Figure 1.1 below illustrates the past and future evolution of wireless cellular systems (2G,3G), local area networks (WLAN) and digital broadcast services (DVB-T,DVB-H) toward 4G.

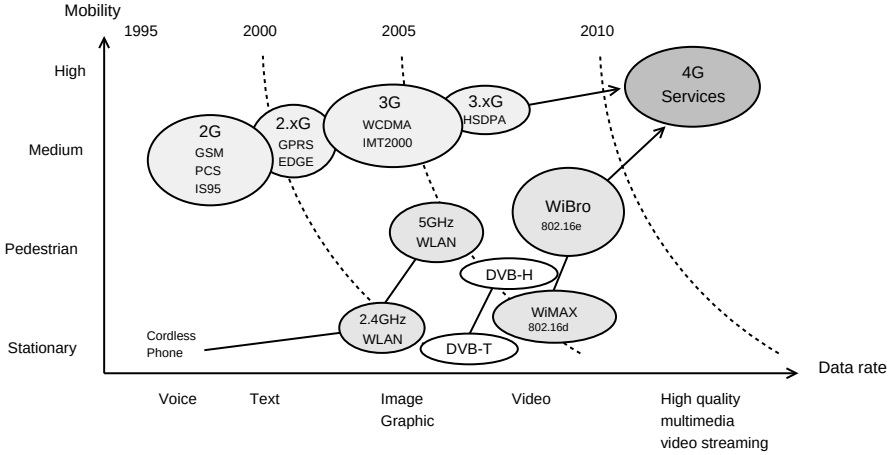

Figure 1.1: Evolution of existing wireless systems toward 4G in terms of mobility and data rates.

The radio spectrum is a scarce resource, and should therefore be utilized efficiently. By using several antennas at the transmitter and the receiver, multiple-input multiple-output

(MIMO) systems allow improving both the spectral efficiency (bits/s/Hz), the coverage, and link reliability of the system. Therefore, MIMO systems are a key technology in order to fulfill the requirements for future 4G communication networks. Increased capacity may be obtained through spatial multiplexing where independent data streams are launched from each antenna. It requires appropriate antenna placement so that spatially independent channels are observed. Independent channels are encountered in rich scattering environments. Theoretically, multi-antenna systems allow a linear improvement in capacity over their single-antenna counterparts proportional to $\min(N_t, N_r)$, where N_t is the number of deployed transmit antennas and N_r is the number of receive antennas [261]. This fundamental result of information theory led to a spur of research in this area. As example, the capacity curves corresponding to different antenna configurations are plotted in Figure 1.2. The selectivity of the wireless channel in time, frequency and space is also a benefit. It provides diversity which may be exploited to improve the reliability of the radio link [126]. Space-time codes were developed for this purpose. There is a trade-off between the transmission rate and the diversity. Figure 1.3 illustrates the benefits of diversity through a simple example where a mobile user is experiencing a fast fading channel.

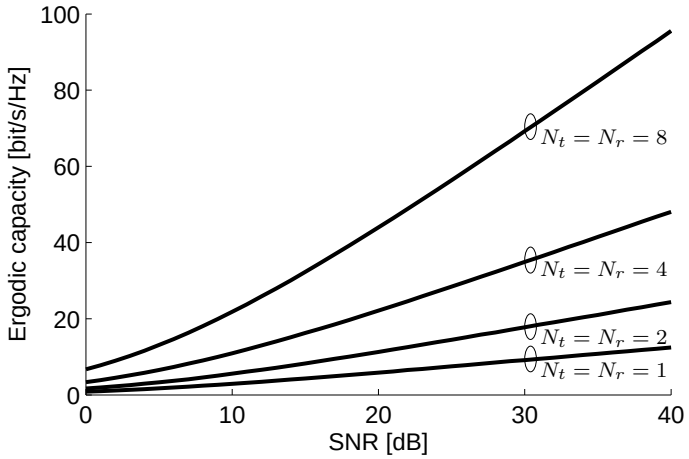

Figure 1.2: The MIMO ergodic capacity [bit/s/Hz] for i.i.d. Rayleigh fading channel coefficients as a function of the signal-to-noise ratio [dB] and the antenna configuration. N_t and N_r are the number of transmit and receive antennas, respectively.

Multicarrier modulation such as orthogonal frequency division multiplexing (OFDM) is a powerful technique to handle impairments specific to the wireless radio channel [33]. The idea is to turn the wideband frequency-selective wireless channel into a set of frequency flat narrowband channels [119, 273]. As a consequence, the complexity of the equalization task reduces considerably [113, Ch.2], and receiver design is thereby simplified significantly. Also, multicarrier systems exploit the transmission spectrum more efficiently because they allow a spectral overlap between the sub-channels. While the concept of OFDM has been known since the 1960's [44], it gained interest in the 1980's [64] and began to emerge in standards starting from the 1990's only [17, 85, 86]. Since then, OFDM and multicarrier technology in general have reached sufficient technical maturity. The ease of implementation achieved by using Discrete Fourier Transform (DFT) together with the cyclic prefix leads to simple transceiver structures. Consequently, practical real-world OFDM systems are deployed, such as digital audio (DAB) and digital video broadcast (DVB) [85,86] as well as wireless local area network (WLAN) standards [84,130]. Another successful application

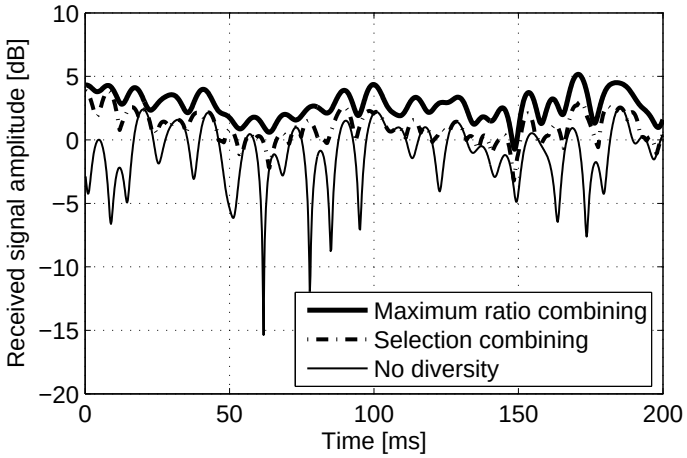

Figure 1.3: Benefits of diversity. Received signal amplitude in a single antenna system compared to a system with four receive antennas applying either selection combining or maximum ratio combining. Diversity techniques smooth out deep channel fades and thus improve significantly the link quality.

of multicarrier modulation is found in wireline communications (ADSL) [17]. OFDM is also a key part of the WiMAX technology for fixed broadband wireless access [1].

Both multi-antenna systems and multicarrier modulation are feasible candidates for future fourth generation broadband wireless networks. Indeed, by using single-carrier modulation, system requirements envisioned for B3G and 4G communications are significantly more difficult to fulfill. However, the benefits of MIMO and OFDM may not be fully achieved in broadband mobile applications because the channels are time and frequency selective. High data rates require larger bandwidth and also higher carrier frequencies compared to existing 2G and 3G systems. Therefore, a significant Doppler spread may be experienced, leading to time-variations of the radio channel over very short period of time. Multipath propagation makes the channel frequency selective and causes inter-symbol interference (ISI) [220]. The channel characteristics change in time due to the mobility of the transmitter and/or receiver as well as of the scatterers. Moreover, selectivity in space domain may be encountered in multi-antenna systems, if the antennas are placed further than the coherence distance apart. As a result, wireless communication channels are characterized by impulse responses that change as a function of time, frequency and location [220]. However, channel selectivity provides also diversity and should not always be viewed as a source of impairment [126]. A feedback channel may be used to provide the transmitter with knowledge about the channel state information [126]. In such case, closed-loop transmit diversity techniques may be deployed. Open-loop transmit diversity methods also exist but are less efficient. Also, uplink and downlink transmissions may be separated either in time or frequency, using time or frequency division duplexing (TDD and FDD), respectively. Since high data rates together with low probability of error are targeted in 4G, coherent detection and high-order symbol modulations are a natural choice. The knowledge of the channel impulse response (CIR) is therefore needed at the receiver in order to recover the transmitted data. Typically, no prior knowledge on the channel is available. Hence, it needs to be estimated and the estimates updated in a regular basis [113, Ch.4,14-16]. In this way, equalizer coefficients may be updated periodically and error rates may be kept below targets. Training data may be inserted among informa-

tion bearing symbols on the time-frequency grid. This may avoid loosing the track of the channel coefficients, if the channel is highly time and/or frequency selective. The training overhead should be kept as small as possible in order to maintain high effective data rates.

OFDM as well as multicarrier modulations in general are extremely sensitive to carrier frequency synchronization errors caused by oscillator inaccuracies and Doppler shifts due to mobility [113, 119, 273]. Moreover, multiple frequency shifts may be simultaneously encountered in MIMO systems because of the rich scattering environment and potentially separate radio frequency - intermediate frequency (RF-IF) chains. These result in intercarrier interference (ICI), leading to severe performance losses especially at high data-rates. The degradation is significant because the number of subcarriers is typically large and the intercarrier spacing is small. Thus, estimation of the carrier frequency offset (CFO) is a crucial task for any multicarrier transceiver. In OFDM systems, frequency synchronization is often accomplished by using series of identical pilot blocks transmitted prior to the information frame [130]. Blind carrier frequency synchronization without any training symbols is also feasible and is an important field of research [101]. Frequency synchronization proceeds generally in two steps. Coarse synchronization brings the residual synchronization error within the range of the intercarrier spacing. Then, fine synchronization aims at estimating the fractional CFO which causes ICI. In general, time and frequency synchronization tasks are performed prior to channel estimation. This allows restoring the orthogonality of the transmission. Finally, frequency offsets may be time-varying because of mobility. Hence, for successful multicarrier transmission, CFO parameters need to be estimated and tracked over time similarly to channel coefficients [225].

1.2 Scope of the thesis

The scope of this thesis is to develop novel receiver structures for mobile multi-antenna OFDM systems. The thesis contributes to beyond 3G and 4G wireless physical layer research. In particular, the problems of channel estimation and carrier frequency synchronization are addressed. The proposed work applies to mobile wireless multicarrier communication systems.

The goal of this thesis is to develop advanced receiver structures that allow providing the benefits of MIMO OFDM in mobile wireless systems. Estimators for time-varying MIMO channel coefficients and CFO parameters are derived. Low complexity algorithms are developed. Statistical large sample properties of the estimators are established. Other issues of the receiver front-end in digital multicarrier communications (time synchronization, carrier phase noise, peak-to-average power issues, etc.) are important but are not considered in this thesis. Also, channel coding as well as optimization of the equalization task are not considered.

In order to achieve high effective data rates, the derived algorithms should exploit any useful information or property of the communication system. Moreover, they should require as little pilot information as possible for processing observations, while achieving either substantial performance improvements over the existing methods or equal performance with a lower degree of computational complexity. Estimation range and identifiability conditions for the parameters of interest should be specified as well. The performance studies should be conducted by computer simulations in a realistic manner.

1.3 Contributions and structure of the thesis

This dissertation contributes to the field of channel estimation and carrier frequency synchronization for wireless communication systems using OFDM modulation and MIMO technology.

The estimation and tracking of channel and frequency offset parameters in mobile MIMO OFDM is considered first. An algorithm is proposed based on a state-space model of the transmission assuming multiple carrier frequency offsets. Each transmitter-receiver pair is assumed to introduce its own carrier frequency offset. This is justified by separate RF-IF chains which lead to several different oscillator frequency mismatches. Mobility together with the large angle spread and rich scattering environment typically assumed in MIMO systems lead to several frequency shifts as well. Papers [225, 251] as well as Publication III were among the first ones to promote this type of modeling for MIMO OFDM. With a single CFO parameter per multi-antenna receiver, it is shown that channel equalization and CFO compensation tasks decouple, leading to low complexity equalization.

A time domain estimation and tracking stage stemming from extended Kalman filtering is the key component of the proposed techniques. Estimation and tracking are performed in the time domain while equalization takes place in the frequency domain. At the beginning of the transmission, a few known training symbols are used to initialize the channel and CFO tracker. Then, the algorithm may switch to decision-directed mode and use the decoded symbols for keeping the track. If pilot information is available, it may be used to improve the estimation performance. The MMSE equalizer is chosen for its simplicity as well as to provide some indication about the bit error rate performance. The equalizer performance is by no means optimized. The proposed algorithm is shown to capture both time and frequency domain as well as spatial characteristics of mobile broadband MIMO channels. Variations of the CFO parameters are also tracked over time. Moreover, time domain processing allows a significant reduction in computational complexity. Fewer number of estimated parameters leads also to lower variance of the estimator. Estimation errors are spread over the whole frequency band, and not concentrated on a given set of subcarriers, which is another key benefit. Simulation studies demonstrate that recursive estimation using extended Kalman filter offers a viable and reliable solution for tracking time-varying channel and frequency offset parameters in MIMO OFDM systems, under slow to moderate fading conditions. Fast fading may be handled as well if sufficient amount of pilot information is included.

A blind method is proposed for fine carrier frequency synchronization. No a priori knowledge of the transmitted data or the multipath channel is required. Effective data rates remain high as no pilot or null-subcarrier are required. It is shown that the sample covariance matrix of the received signal contains information on the carrier frequency offset in cyclic-prefix OFDM transmissions. The algorithm is based on the property that perfect carrier frequency synchronization implies a diagonal covariance matrix for the received signal in the frequency domain. A cost function minimizing the total off-diagonal power induced by intercarrier interference in the frequency domain is introduced. Minimization of the cost function is accomplished in a closed-form, which leads to low complexity and accurate computational solution. The theoretical performance analysis of the algorithm demonstrates that consistent estimation of the carrier frequency offset is achieved under frequency selective fading. The algorithm is shown to perform reliably in simulations almost regardless of the signal-to-noise ratio.

Novel approaches in blind subspace-based fine carrier frequency synchronization for OFDM are introduced as part of this thesis work. It is shown that a low rank model arises

in almost any OFDM transmission, because of the DFT/IDFT operations and the FIR communication channels. In practice, the channel is much shorter than the number of subcarriers, which leads to a low rank model. By exploiting the frequency correlation of the channel among the subcarriers, blind subspace-based carrier frequency synchronization becomes feasible. Constant modulus symbol constellations need to be assumed but null-subcarriers are not necessarily required. The method is shown to be closely related to maximum likelihood estimation [97]. Close to optimal performance is achieved with a single block of observations. The fact that only a small sample support is required is obviously a key advantage in time selective channels.

Finally, the Cramér-Rao bound (CRB) is established for the blind CFO estimation problem in OFDM. The CRB is a useful measure of the large sample performance because it gives the minimum variance an unbiased estimator may achieve. The CRB is derived under the Gaussian approximation for the received signal corrupted by CFO. As the received signal may be non-circular, e.g. when real-valued modulations are used, the derivation of the CRB needs to include complete second order statistics. Those require both signal covariance and pseudo-covariance matrices. It is shown that there is a significant difference between CRBs in the circular and non-circular cases.

This thesis is organized as follows. Chapter 2 gives an overview of orthogonal frequency division multiplexing systems. The system model is introduced, assuming a multi-antenna OFDM setup with multiple carrier frequency offsets. The chapter presents a common framework for channel and carrier frequency offset parameter estimation that will be followed throughout the thesis. In Chapter 3, a literature survey on channel estimation in OFDM systems is provided. Chapter 4 is a review of carrier frequency synchronization techniques specific to OFDM. In Chapter 5, a recursive algorithm derived in this thesis for the estimation and tracking of channel and CFO parameters in mobile MIMO OFDM systems is described. Chapter 6 introduces two novel approaches for blind carrier frequency synchronization in OFDM systems. The CRB for the blind synchronization problem in OFDM is provided as well. Finally, Chapter 7 summarizes the results and the contributions of the thesis.

1.4 Summary of the publications

This thesis consists of an introductory part and seven original publications. The publications are listed at page ix, and appended at the end of the manuscript starting from page 121. The first three publications are dealing with the estimation and tracking of channel coefficients and carrier frequency offsets in MIMO OFDM systems. The last four of them introduce novel approaches to blind carrier frequency offset estimation in OFDM. References to other publications by the author of this thesis are also included in the following summary, where appropriate.

In Publication I, estimation and tracking of channel coefficients in a MIMO OFDM system is addressed. A Kalman filter based recursive estimator is proposed. The estimation and tracking stage is running in the time domain, whereas equalization is performed in the frequency domain. Time domain processing leads to lower computational complexity even though additional DFTs are needed. Robustness against estimation errors is improved, as those are spread over the entire frequency band. The special case of recursive channel estimation in single-input single-output (SISO) OFDM systems is studied in [226].

In Publication II, joint estimation and tracking of channel coefficients and carrier frequency offset is proposed for SISO OFDM systems. The derived algorithm stems from extended Kalman filter, and operates in the time domain. Since CFO induces a nonlinear

distortion, the state-space model for the OFDM transmission must be linearized prior to Kalman filtering. Reliable tracking of time-varying frequency selective channels and frequency offsets is achieved for a wide range of signal-to-noise ratios. Additionally, sequential Monte-Carlo estimation is an appealing technique for non-linear state-space models. It was also investigated for carrier frequency synchronization in OFDM [200].

Publication III is one of the main publications of this dissertation. The state-space models introduced in Publications I-II are extended to cope with arbitrary number of transmit and receive antennas as well as with multiple carrier frequency offsets in MIMO systems. The resulting modeling extends the preliminary derivation of [225]. Time domain processing allows a significant reduction in computational complexity. This is due to the smaller parameter space compared to frequency domain estimation. Moreover, estimation errors are spread over the entire frequency band and improved robustness is thus achieved. Extensive simulations studies are conducted for various noise conditions and terminal velocities. A technique for refining the obtained estimates is proposed. Both the estimation error and the tracking capability of the algorithm are improved in this way. Channel estimation and tracking in spatially correlated MIMO OFDM systems are studied in detail in [82], whereas the estimation and tracking of real-world measured MIMO channels are addressed in [78, 81].

Publication IV is the other main publication of this doctoral thesis. A blind fine CFO estimator based on the received signal covariance matrix is introduced. The algorithm is based on the property that perfect carrier frequency synchronization leads to a diagonal covariance matrix for the received signal in the frequency domain. The method does not require a priori knowledge of the transmitted data or the multipath channel. Effective data rates rates remain high as no pilot or null-subcarrier are needed. A closed-form is found for the cost function, which allows reliable and low-complexity CFO estimation. An analysis of theoretical and asymptotic properties of the estimator is provided. The proposed algorithm is shown to be a consistent estimator of the CFO in the range of $[-1/2, 1/2[$ with respect to the intercarrier spacing. As a consequence, it is asymptotically unbiased. It is shown that the estimator converges in the mean square error at the rate $1/K$, where K is the sample size. Finally, simulation results show good performance with respect to the Cramér-Rao bound established in Publication V. Furthermore, reliable estimation of the CFO is achieved at low SNR regime, where decision-directed methods are likely to fail.

In Publication V, the stochastic Cramér-Rao bound is established for the blind CFO estimation problem in OFDM. The CRB is derived under the Gaussian approximation for the received signal corrupted by CFO. Such approximation is widely used in the OFDM literature, and is justified by the central limit theorem [281]. As the received signal may be non-circular, e.g. when real-valued modulations are used, the derivation of the CRB needs to include complete second order statistics. Those require both signal covariance and pseudo-covariance matrices. Channel parameters are treated as deterministic nuisance parameters, and are assumed to be constant over the observation period. Simulation results highlight significant differences between the CRBs in the circular and non-circular cases. As a result, the performance of blind CFO estimation algorithms may be significantly improved in the non-circular case by exploiting a complete second order statistics.

In Publication VI, a novel subspace-based approach is introduced for blind carrier frequency offset estimation under time and frequency selective fading. The method applies to OFDM systems using real-valued constant modulus modulations such as binary phase shift keying. Correlation in the squared spectrum of the channel is exploited and low rank signal model is thereby obtained without null-subcarriers. The estimator may be

interpreted geometrically as minimizing the projection of the squared received signal to the subspace of channel squared spectrum as a function of the CFO compensation factor. The proposed estimator accomplishes fine frequency synchronization with a single OFDM block in the range of $[-1/2, 1/2[$ with respect to the intercarrier spacing. No extensive time averaging is needed, which makes the approach very attractive for time-varying scenarios. The method is statistically very efficient since close to optimal performance is achieved with respect to the Cramér-Rao bound with a single received block.

Publication VII extends the algorithm derived Publication VI to the case of complex-valued constant modulus modulations. An accurate description of the subspace structure related to the CFO estimation problem with constant modulus modulations is provided. Because the subspaces are known a priori, there is no need for estimating them. The computational complexity is significantly reduced as no subspace decomposition is required. The relationship to an existing algorithm in the literature [97] exploiting the constant modulus property is established in Chapter 6 of this thesis. Both algorithms are shown to be closely related to maximum likelihood estimation. As a result, close to optimal performance is achieved.

All the simulation software for all the original publications included in this dissertation was written solely by the author.

In Publications I-III, the original time domain channel and CFO estimator stemming from Kalman filter was the idea of the first author. Most of the simulations were performed by the first author as well. The co-authors provided guidance in the theoretical modeling, in the design of the experiments, and helped in writing the papers.

The algorithms in Publications IV-V were derived by the author of this thesis. The co-authors collaborated in the derivation of the theoretical performance bounds and in the establishing the asymptotic performance of the related algorithms. They also provided guidance for the author proofs and contributed to the writing of the final version of each paper.

The algorithms in Publications VI-VII were derived by the author of this thesis. The theoretical results presented were also established by the author. The co-author provided guidance during the development, and contributed to the writing as well.

Chapter 2

Overview of orthogonal frequency division multiplexing systems

This chapter gives an overview of orthogonal frequency division multiplexing (OFDM) systems. The main objective is to provide a formal description of MIMO OFDM communications in mobile environments. Single antenna OFDM systems are viewed as a particular case. Both SISO and MIMO system models are used throughout the thesis. Imperfections and their impact on the overall system performance are reviewed at the end of the chapter.

2.1 Short history of OFDM

The first OFDM scheme dates back to 1966 when Chang published his pioneering work on the synthesis of band-limited signals for multichannel transmission [44]. The main idea in OFDM is to divide the frequency selective channel into a number of parallel, frequency flat subchannels. By making all the subchannels narrowband, they experience almost flat fading, which makes receiver design very simple. In classical parallel data systems, the total signal frequency band is divided into non-overlapping frequency subchannels. Avoiding spectral overlap eliminates inter-channel interference [273, Ch.1]. However, this leads to inefficient use of the available spectrum. To obtain a high spectral efficiency, the frequency responses of the subchannels are designed to overlap and be orthogonal, hence the name OFDM. The power spectral density (PSD) of a typical OFDM signal is depicted in Figure 2.1.

In 1971, Weinstein and Ebert made an important contribution by proposing the use of the discrete Fourier transform (DFT) to perform baseband modulation and demodulation [283]. In this way, the complexity of OFDM modems is significantly reduced since there is no need for a bank of subcarrier oscillators anymore. The inter-symbol interference (ISI) and intercarrier interference (ICI) were mitigated by using a guard time between the symbols and raised-cosine windowing in time domain. Even though the proposed system did not achieve perfect orthogonality among the subcarriers over dispersive channels, it was nevertheless an important contribution to OFDM. In 1980, Peled and Ruiz solved the orthogonality problem by introducing the cyclic prefix (CP) [208]. Instead of having zero-padding, they filled it with a cyclic extension of the OFDM symbol. The latter manipulation converts the linear convolutive channel into a circular convolutive one. This ensures orthogonality among the subcarriers as long as the CP remains longer than the impulse response of the channel. However, the cyclic prefix induces a loss in effective

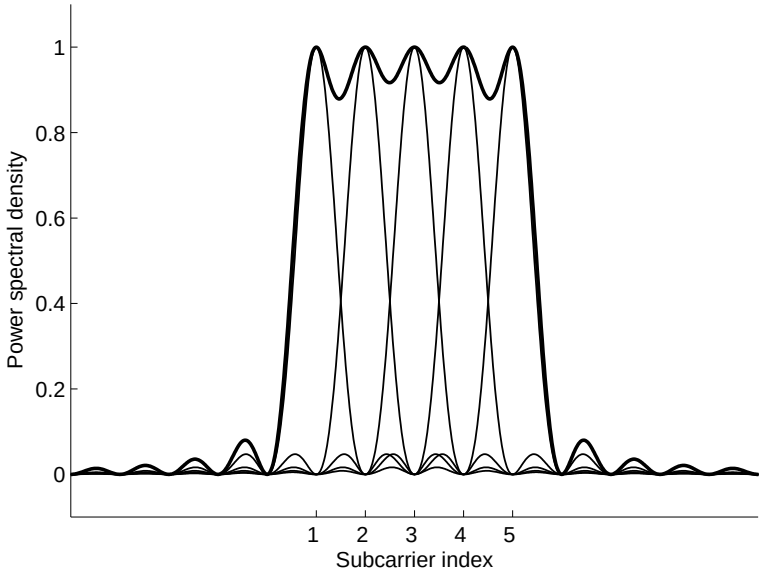

Figure 2.1: Power spectral density of an OFDM signal with $N = 5$ subcarriers (thick line). PSD of the individual subcarriers (thin lines).

data rates, but the zero ICI generally compensates for this loss. During the early years of development of OFDM, contributions by Saltzberg, Hirosaki, Cimini, Kalet [64, 121, 140, 230] are significant as well.

As a proof of its maturity, OFDM was included in the European digital audio broadcast (DAB) [85] as well as digital video broadcast (DVB) [86] standards. OFDM was selected as transmission technique for the high performance local area network HIPERLAN [84] [119, Ch.8] and is also part of the IEEE 802.11 [130] Wireless Local Area Network (WLAN) standard. An excellent overview of OFDM receivers for WLANs may be found in [119]. Also, asymmetric digital subscriber loop (ADSL) [17] is an important application of OFDM modulation for high data rate wireline transfers. Moreover, two out of the three air interfaces specified in the IEEE 802.16 [1] standard for broadband wireless access (also known as WiMAX) are based on OFDM [103]. Finally, OFDM is considered for the long term evolution of 3G [2, 3, 285] as well as fourth generation (4G) mobile wireless systems [38, 138, 207].

2.2 System model for MIMO OFDM

This section presents the system model for multiple-input multiple-output (MIMO) OFDM based wireless communication systems. Single-input single-output (SISO) OFDM systems are viewed as a special case of the latter. The following description will serve as a common framework throughout the thesis in order to address issues in both channel estimation and frequency synchronization.

2.2.1 MIMO channel model

Continuous time channel impulse response

Let us consider a wireless communication system with N_t transmit and N_r receive antennas. This is referred to as a $N_t \times N_r$ MIMO system. In the following, the index

$t = 1, \ldots, N_t$ refers to transmit antennas and $r = 1, \ldots, N_r$ to receive antennas. Let us denote the continuous-time impulse response between transmit antenna t and receive antenna r by

$$h_{tr,k}^{(c)}(\tau_c) = h_t^{(tx)}(\tau_c) * h_{tr,k}^{(ch)}(\tau_c) * h_r^{(rx)}(\tau_c), \tag{2.1}$$

where $*$ stands for the convolution operator, and $h_t^{(tx)}(\tau_c)$ and $h_r^{(rx)}(\tau_c)$ are the transmit and receive pulse shaping filters, respectively. We denote by τ_c the continuous time-delay. In the above equation, $h_{tr,k}^{(ch)}(\tau_c)$ is the impulse response of the propagation channel corresponding to MIMO branch tr, sampled at time kT_{s+g} and delay lag τ_c. The channel is assumed to be constant within the time duration of one OFDM block, which is equal to T_{s+g}. This assumption is called block fading model. The index k refers to the OFDM block number. OFDM systems are usually designed using rectangular pulse shape. However, other pulse shapes may be useful, for instance, to lower side lobes in frequency domain [254, 269]. This is beneficial in reducing interference as OFDM with a cyclic prefix can prevent intercarrier interference but does not combat inter-channel interference if rectangular pulses are used.

Discrete time channel impulse response

Taking samples at $t_s = 1/(NB_{\text{sc}})$, where B_{sc} is the subcarrier bandwidth and N the total number of subcarriers, the discrete-time channel impulse response (CIR) for MIMO branch tr is obtained as

$$h_{tr}(k,l) = \left. h_{tr,k}^{(c)}(\tau_c) \right|_{\tau_c = lt_s}, \quad l = 0, \ldots, P-1, \quad k \in \mathbb{N}, \tag{2.2}$$

where P denotes the total length of the OFDM block in samples, including the cyclic prefix. Indices k and l correspond to OFDM block and tap numbers, respectively. For a given block index k, the quantity $h_{tr}(k,l)$ is referred to as the l^{th} channel tap and is linked to the physical propagation environment. Under the idealistic assumption of sample-spaced CIRs, $h_{tr}(k,l)$ corresponds to a single propagation path. In practice, this assumption does not always hold, and consequently $h_{tr}(k,l)$ contains energy from multiple physical paths. This introduces correlation among the channel taps and may affect channel estimation algorithms if they assume uncorrelated channels [113, 16.4.2].

Due to the block fading assumption, the channel taps are constant within the time duration of one OFDM block, which is equal to $T_{s+g} = Pt_s$. Furthermore, we assume that the CIR has L_h non-zero taps and is no longer than the cyclic prefix of length L_{CP}. At block time instance k, one may express the CIR corresponding to MIMO branch tr as the following vector of size $L_h \times 1$:

$$\mathbf{h}_{tr}(k) = \left[h_{tr}(k,0),\, h_{tr}(k,1),\, \ldots,\, h_{tr}(k,L_h-1)\right]^T. \tag{2.3}$$

The channel coefficients in time domain $h_{tr}(k,l)$, for $l = 0, \ldots, L_h - 1$, are assumed to be zero-mean complex circular Gaussian random variables, which leads to Rayleigh fading. Channel taps are considered to be correlated in time, and may be dependent or independent from each other. The average power and delay profiles, $\left\{\mathrm{E}\left[|h_{tr}(k,l)|^2\right]\right\}_{l=0}^{L_h-1}$ and $\{\tau_{tr}(k,l)\}_{l=0}^{L_h-1}$, respectively, are determined by the propagation environment. Note that the multipath nature of the channel leads to frequency selectivity, while the mobility-induced Doppler spectrum translates into time-selectivity and correlation over time [220, Ch.14]. Thus, one is dealing with time-frequency dispersive/selective channels, which need to be estimated and tracked over time for successful data transmission. The Ricean

and Nakagami-m distributions are among other well-known and frequently used statistical models for fading [220, Ch.14]. The Rice model includes a line-of-sight (LOS), unlike Rayleigh fading. Both models can be considered as special cases of the Nakagami fading model. Simulation studies in this work have been conducted with independent Rayleigh fading, with correlation over time. The Doppler spectrum is assumed to follow Jakes' model [134].

Practical implementations in both wireless and wireline transmissions experience quite long CIRs. In this case, channel shortening is an interesting option to improve effective data rates as a smaller guard interval (i.e., cyclic prefix) may be used. The idea is to linearly equalize the CIR to a much shorter target impulse response which length may be fixed a priori [30, 204].

Discrete time MIMO channel vector

We may stack the MIMO channel coefficients at time instance k into a column vector of size $N_t N_r L_h \times 1$ as follows:

$$\mathbf{h}(k) = \left[\mathbf{h}_{11}^T(k), \ldots, \mathbf{h}_{N_t 1}^T(k), \ldots, \mathbf{h}_{1r}^T(k), \ldots, \mathbf{h}_{N_t r}^T(k), \ldots, \mathbf{h}_{1N_r}^T(k), \ldots, \mathbf{h}_{N_t N_r}^T(k)\right]^T. \tag{2.4}$$

Channels corresponding to different transmit and receive antenna pairs in MIMO systems usually exhibit similar delay profiles. In this thesis, CIR vectors in each branch are assumed to be independent and identically distributed. In practice this means that the scattering environment is rich and the antennas are placed further apart than the coherent distance. High correlation in MIMO channel branches is detrimental in terms of reduced capacity and higher bit error rates, and leads to lower system performance.

Correlation among MIMO branches

MIMO channel models, especially the ones validated by measurement campaigns [143, 282], are of great importance in algorithm design. In the Kronecker model [143], the channel correlation matrix is given by the Kronecker product between the transmitter and receiver correlation matrices. The main assumption is that the correlation properties at the two link ends are separable. The Kronecker model has become popular, despite its limitations. Indeed, it was shown recently to under-estimate the MIMO channel capacity [282]. The Weichselberger model (W-model) [282] provides more advanced modeling and differs from the Kronecker model in the sense that correlation features at the link ends are not necessarily decoupled. In realistic scenarios, both uncorrelated and correlated channels are encountered. Recently, the third generation partnership project (3GPP) proposed the spatial channel model (SCM) and extended SCM (SCME) [285]. The IEEE task group in charge of 802.11n addresses channel modeling issues as well [131].

MIMO systems allow improving the spectral efficiency (bits/s/Hz) tremendously as they promise a linear improvement in the capacity proportional to the number of antennas. Indeed, channel capacity was shown to be proportional to $\min\{N_t, N_r\}$ [207, 261]. Spatial multiplexing allows creating multiple data streams between transmitter and receiver arrays without additional bandwidth or increased total power. Channel diversity of order up to $N_t \times N_r$ may be obtained via transmit diversity techniques such as, e.g., space-time coding [126]. This results in improved quality of the radio link. Finally, increased array gain over SISO systems allows improving the coverage and SNR. Both multi-antenna systems and multicarrier modulation are needed for filling the technology gaps for future broadband wireless networks.

2.2.2 Frequency offsets in mobile MIMO systems

Frequency offsets are mainly caused by two different factors [168]: Doppler shifts and carrier frequency mismatches between transmit and receive oscillators.

Carrier frequency mismatches occur when oscillators at the transmitter and receiver experience drifts from their nominal frequency. Therefore, a frequency offset is introduced. In multi-antenna systems, each transmitter and receiver typically requires its own radio frequency - intermediate frequency (RF-IF) chain. Consequently, each transmitter-receiver pair has its own mismatch parameter and hence separate frequency offset. In a $N_t \times N_r$ MIMO system this leads to $N_t \times N_r$ mismatch parameters and offsets. If transmit or receive antennas share RF-IF chains, fewer carrier frequency mismatch parameters are needed.

In wireless mobile communications, Doppler shift of the received signal spectrum arises from relative motion between the transmitter and the receiver. The shift depends on the carrier frequency, the velocity of the mobile terminal and the angle of arrival. For instance, a sinusoidal transmitted waveform with wavelength λ [m] and impinging at angle $\phi_D \in [0, 2\pi[$ experiences a shift in frequency $f_D = v \cos \phi_D / \lambda$, resulting from the relative motion at velocity v [m/s] with respect to the receiver. The shift f_D [Hz] is referred to as Doppler shift. In reality, the signal experiences a complete Doppler spread instead of a single frequency shift [220, Ch.14], [134]. Hence, in theory, separate offset parameter is needed for each propagation path [8, 65, 110, 135, 136]. In MIMO wireless communication systems, rich scattering environment and large angle spread are required in order to obtain improved spectral efficiency and link quality. Therefore, each channel branch introduces its own Doppler shift. Papers [32, 225] as well as Publication III presented in Chapter 5 of this thesis were among the first ones to advocate the use of multiple CFO parameters in mobile MIMO OFDM. However, most of the existing work in the literature still assumes single CFO parameter per multi-antenna receiver or for the whole MIMO system. The assumption of a single offset per multi-antenna receiver is valid only in the case when multipath components impinge the antennas with the same angle of arrival (AOA) [32, 168, 252], e.g. in LOS situation, for instance in the case of a Rician channel with very few dominant AOA's.

As a result, in a general case of a $N_t \times N_r$ MIMO system, it is necessary to compensate for $N_t \times N_r$ different Doppler shifts. Such approach has be adopted in this thesis. At time instance k, assume that MIMO branch tr experiences a frequency shift $\nu_{tr}(k)$, for $t = 1, \ldots, N_t$ and $r = 1, \ldots, N_r$. All the $N_t N_r$ values of the CFOs may be stacked in vector form as

$$\boldsymbol{\nu}(k) = [\nu_{11}(k), \ldots, \nu_{N_t 1}(k), \ldots, \nu_{1r}(k), \ldots, \nu_{N_t r}(k), \ldots, \nu_{1N_r}(k), \ldots, \nu_{N_t N_r}(k)]^T . \quad (2.5)$$

2.2.3 MIMO OFDM input-output relationships

There exist several versions of OFDM. The focus in this thesis is on discrete time MIMO OFDM systems employing a cyclic prefix. In the following, the MIMO OFDM transmission is described in a formal way [174,279]. A $N_t \times N_r$ MIMO OFDM system with $N_t N_r$ separate carrier frequency offsets is depicted in Figure 2.2.

MIMO OFDM modulation

In MIMO OFDM, there is one OFDM modulator per transmit antenna. In spatial multiplexing, independent data streams are transmitted from each antenna. Modulation and demodulation operations in OFDM are performed by IDFT and DFT, respectively. Both

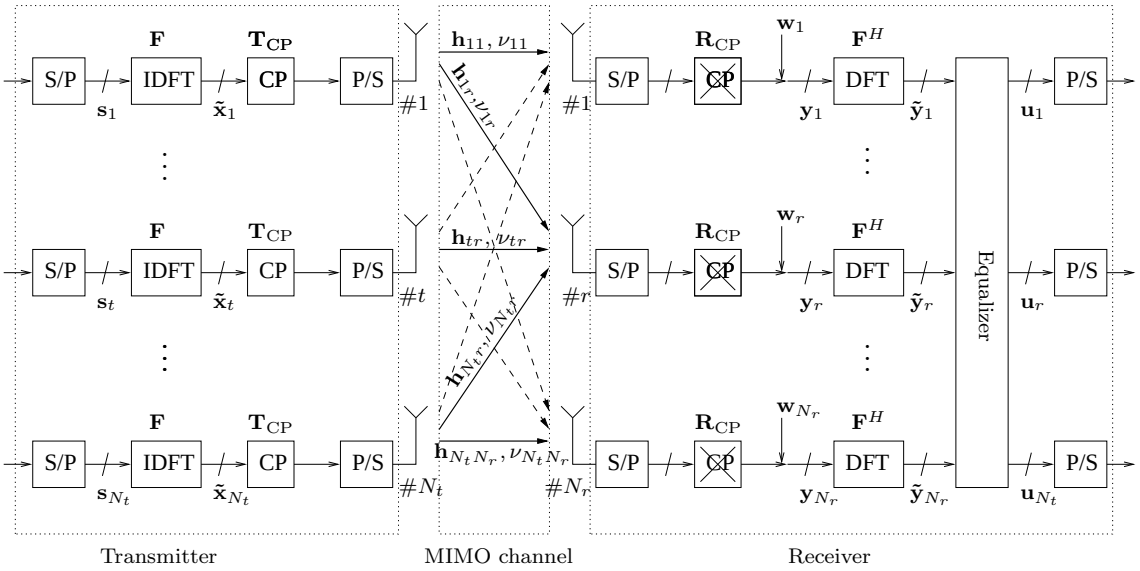

Figure 2.2: Baseband model of the MIMO OFDM model with $N_t N_r$ separate carrier frequency offsets considered in this thesis.

tasks may be accomplished with computationally efficient fast Fourier transform (FFT) algorithms. This played an important role in the deployment of OFDM systems in practical applications.

At time instance k, the original data stream at antenna t, $s_{t,0}(k), \ldots, s_{t,N-1}(k)$, is drawn from a symbol constellation and serial-to-parallel (S/P) converted to form the k^{th} data vector $\mathbf{s}_t(k)$ of size $N \times 1$. Some subcarriers may be left unmodulated and hence some components of $\mathbf{s}_t(k)$ may be set to zero. Those are referred to as null-subcarriers, and their use is discussed later in this section.

An N-point IDFT (inverse discrete Fourier transform) is then applied to N complex data symbols at the t^{th} transmitter creating the k^{th} modulated block $\tilde{\mathbf{x}}_t(k)$. A cyclic prefix of length L_{CP} is added to form $\tilde{\mathbf{x}}_{\mathrm{CP},t}(k)$. As a result, the total length of the OFDM symbol with CP is $P = N + L_{\mathrm{CP}}$. The CP is a copy of the last part of the OFDM symbol which is inserted in front of the transmitted symbol. The benefits of a cyclic prefix are twofold:

1. It allows avoiding inter-block interference (IBI) since it acts as a guard space between two consecutive OFDM symbols. A CP of length L_{CP} may accomodate a channel of order up to L_{CP}, i.e., with up to $L_{\mathrm{CP}} + 1$ non-zero taps.

2. It prevents from intercarrier interference (ICI) as it maintains the orthogonality between the subcarriers as long as its length is longer than the delay spread of the channel.

The structure of the OFDM block together with CP is depicted in Figure 2.3.

The above operations (see Figure 2.2) may be conveniently represented in matrix-vector product form as follows:

$$\mathbf{s}_t(k) = [s_{t,0}(k), \ldots, s_{t,N-1}(k)]^T \tag{2.6}$$

$$\tilde{\mathbf{x}}_t(k) = \mathbf{F}\mathbf{s}_t(k) \tag{2.7}$$

$$\tilde{\mathbf{x}}_{\mathrm{CP},t}(k) = \mathbf{T}_{\mathrm{CP}}\tilde{\mathbf{x}}_t(k), \quad t = 1, \ldots, N_t, \tag{2.8}$$

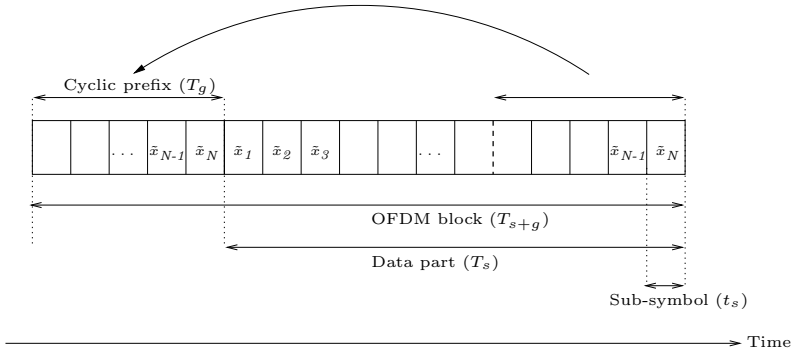

Figure 2.3: Structure of the OFDM block. The CP is a copy of the last part of the OFDM block. T_g, T_s, T_{s+g} and t_s refer to the durations of the cyclic prefix, the data part, the whole OFDM block and the OFDM sub-symbol, respectively. The transmit antenna index is omitted, for simplicity.

where the matrix $\mathbf{T}_{\text{CP}}$ of size $P \times N$ performs the cyclic prefix insertion and $\mathbf{F}$ is the IDFT matrix of size $N \times N$:

$$\mathbf{T}_{\text{CP}} = \begin{bmatrix} \mathbf{0}_{L_{\text{CP}} \times (N-L_{\text{CP}})} & \mathbf{I}_{L_{\text{CP}}} \\ \mathbf{I}_{N-L_{\text{CP}}} & \mathbf{0}_{(N-L_{\text{CP}}) \times L_{\text{CP}}} \\ \mathbf{0}_{L_{\text{CP}} \times (N-L_{\text{CP}})} & \mathbf{I}_{L_{\text{CP}}} \end{bmatrix} \tag{2.9}$$

$$[\mathbf{F}]_{m,n} = \frac{1}{\sqrt{N}} \exp\left(j \frac{2\pi mn}{N}\right), \quad m, n = 0, \ldots, N-1. \tag{2.10}$$

The notation $\mathbf{I}_K$ refers to the identity matrix of size $K \times K$, and $\mathbf{0}_{K \times L}$ to the matrix of size $K \times L$ filled with zeros. The resulting sequence $\tilde{\mathbf{x}}_{\text{CP},t}(k)$ is successively parallel-to-serial converted (P/S), converted to analog, modulated on a carrier and sent through the channel through transmit antenna t. See, Figure 2.2.

MIMO OFDM demodulation

At the receiver, the received signal is first down-converted to baseband and sampled. The CP is discarded, which suppresses IBI assuming the CP is sufficiently long. Under perfect time synchronization, the CFO-corrupted received signal in time domain at the r^{th} receive antenna after cyclic prefix removal may be expressed as

$$\mathbf{y}_r(k) = \sum_{t=1}^{N_t} e^{j2\pi(kP+L_{\text{CP}})\nu_{tr}(k)/N} \mathbf{C}(\nu_{tr}(k)) \tilde{\mathbf{H}}_{tr}(k) \tilde{\mathbf{x}}_t(k) + \mathbf{w}_r(k), \quad r = 1, \ldots, N_r, \tag{2.11}$$

where:

1. The matrix $\tilde{\mathbf{H}}_{tr}(k)$ of size $N \times N$ is defined as $\tilde{\mathbf{H}}_{tr}(k) = \mathbf{R}_{\text{CP}} \mathbf{H}_{tr}(k) \mathbf{T}_{\text{CP}}$, where the matrix $\mathbf{R}_{\text{CP}} = [\ \mathbf{0}_{N \times L_{\text{CP}}} \quad \mathbf{I}_N\ ]$ of size $N \times P$ discards the CP. The matrix $\mathbf{H}_{tr}(k)$ models the wireless environment at time instance k between the t^{th} transmit and r^{th} receive antennas. It is a Toeplitz convolution matrix of size $P \times P$ built from the channel vector $\mathbf{h}_{tr}(k)$ defined in (2.3). Now, cyclic prefix insertion at the transmitter followed by CP removal at the receiver side turns the linear convolutive channel into a circular convolutive one [76, 279]. Hence, the matrix $\tilde{\mathbf{H}}_{tr}(k)$ of size $N \times N$ is

circulant, i.e., its elements are of the form:

$$\left[\tilde{\mathbf{H}}_{tr}(k)\right]_{m,n} = \begin{cases} h_{tr}(k,l), & l = (m-n) \bmod N \leq L_h - 1 \\ 0, & \text{otherwise} \end{cases}, \; m,n = 0,\ldots,N-1. \tag{2.12}$$

2. At time instance k, the distortion specific to MIMO branch tr caused by the CFO $\nu_{tr}(k)$ is modeled by both the block dependent term $e^{j2\pi(kP+L_{\text{CP}})\nu_{tr}(k)/N}$ and the $N \times N$ diagonal matrix $\mathbf{C}(\nu_{tr}(k))$ defined as

$$\mathbf{C}(\nu_{tr}(k)) = \text{diag}\left\{\left[1, e^{j\frac{2\pi\nu_{tr}(k)}{N}}, \ldots, e^{j\frac{2\pi(N-1)\nu_{tr}(k)}{N}}\right]\right\}. \tag{2.13}$$

The quantity $\nu_{tr}(k)$ is referred to as normalized frequency offset with respect to intercarrier spacing. The effective frequency deviation is equal to $\nu_{tr}(k)\,\Delta f$ [Hz], where $\Delta f = B/N$ is the intercarrier spacing and B [Hz] is the bandwidth allocated to the system.

3. The $N \times 1$ vector $\mathbf{w}_r(k)$ is a zero-mean complex circular additive white Gaussian vector with covariance matrix $\sigma^2\mathbf{I}_N$.

OFDM demodulation is performed using DFT at each receive antenna. Taking the DFT of $\mathbf{y}_r(k)$ in (2.11) yields

$$\tilde{\mathbf{y}}_r(k) = \sum_{t=1}^{N_t} e^{j2\pi(kP+L_{\text{CP}})\nu_{tr}(k)/N}\mathbf{F}^H\mathbf{C}(\nu_{tr}(k))\tilde{\mathbf{H}}_{tr}(k)\mathbf{F}\mathbf{s}_t(k) + \tilde{\mathbf{w}}_r(k) \tag{2.14}$$

$$= \sum_{t=1}^{N_t} e^{j2\pi(kP+L_{\text{CP}})\nu_{tr}(k)/N}\mathbf{F}^H\mathbf{C}(\nu_{tr}(k))\mathbf{F}\mathbf{D}_{\tilde{\mathbf{h}}_{tr}}(k)\mathbf{s}_t(k) + \tilde{\mathbf{w}}_r(k), \tag{2.15}$$

where $r = 1,\ldots,N_r$ and $\tilde{\mathbf{w}}_r(k) = \mathbf{F}^H\mathbf{w}_r(k)$. The matrix $\mathbf{D}_{\tilde{\mathbf{h}}_{tr}}(k)$ of size $N \times N$ is defined as $\mathbf{D}_{\tilde{\mathbf{h}}_{tr}}(k) = \mathbf{F}^H\tilde{\mathbf{H}}_{tr}(k)\mathbf{F}$. It is a diagonal matrix because $\tilde{\mathbf{H}}_{tr}(k)$ is circulant and is thus diagonalized by DFT/IDFT matrices. Moreover, the matrix $\mathbf{D}_{\tilde{\mathbf{h}}_{tr}}(k)$ contains the channel frequency response $\tilde{\mathbf{h}}_{tr}(k)$ at subcarrier frequencies, i.e.,

$$\mathbf{D}_{\tilde{\mathbf{h}}_{tr}}(k) = \text{diag}\left\{\tilde{\mathbf{h}}_{tr}(k)\right\} \tag{2.16}$$

$$\tilde{\mathbf{h}}_{tr}(k) = \left[\tilde{h}_0,\ldots,\tilde{h}_{N-1}\right]^T \tag{2.17}$$

$$\tilde{h}_n = \sum_{l=0}^{L_h-1} h_{tr}(k,l)\exp\left(-j\frac{2\pi nl}{N}\right), \quad n = 0,\ldots,N-1. \tag{2.18}$$

Now, stacking N_r equations of the form (2.15) in a vector we obtain:

$$\tilde{\mathbf{y}}(k) = \mathbf{M}(k)\mathbf{s}(k) + \tilde{\mathbf{w}}(k), \tag{2.19}$$

with the following notation:

$$\mathbf{M}(k) = \begin{bmatrix} \mathbf{M}_{11}(k) & \dots & \mathbf{M}_{N_t 1}(k) \\ \vdots & \mathbf{M}_{tr}(k) & \vdots \\ \mathbf{M}_{1N_r}(k) & \dots & \mathbf{M}_{N_t N_r}(k) \end{bmatrix}_{N_r N \times N_t N} \tag{2.20}$$

$$\mathbf{M}_{tr}(k) = e^{j2\pi(kP+L_{\mathrm{CP}})\nu_{tr}(k)/N}\mathbf{F}^H\mathbf{C}(\nu_{tr}(k))\mathbf{F}\mathbf{D}_{\tilde{\mathbf{h}}_{tr}}(k) \tag{2.21}$$

$$\mathbf{s}(k) = \left[\mathbf{s}_1^T(k), \dots, \mathbf{s}_{N_t}^T(k)\right]^T \tag{2.22}$$

$$\tilde{\mathbf{w}}(k) = \left[\tilde{\mathbf{w}}_1^T(k), \dots, \tilde{\mathbf{w}}_{N_r}^T(k)\right]^T. \tag{2.23}$$

Finally, given the knowledge of both the MIMO channel coefficients and CFO parameters, the channel may be equalized. ZF or MMSE equalizers may be found in the frequency domain respectively as

$$\mathbf{u}_{\mathrm{ZF}}(k) = \left[\mathbf{M}^H(k)\mathbf{M}(k)\right]^{-1}\mathbf{M}^H(k)\,\tilde{\mathbf{y}}(k) \tag{2.24}$$

$$\mathbf{u}_{\mathrm{MMSE}}(k) = \sigma_s^2\left[\sigma_s^2\mathbf{M}^H(k)\mathbf{M}(k) + \sigma^2\mathbf{I}_{N_tN}\right]^{-1}\mathbf{M}^H(k)\,\tilde{\mathbf{y}}(k), \tag{2.25}$$

where σ^2 is the variance of the noise and σ_s^2 is the average symbol energy. Then, decisions are carried out on $\mathbf{u}_{\mathrm{ZF}}(k)$ or $\mathbf{u}_{\mathrm{MMSE}}(k)$ in order to obtain the estimate of the transmitted symbol vector $\hat{\mathbf{s}}(k)$. In order to ensure data symbol detectability with zero forcing equalizer, $\mathbf{M}^H\mathbf{M}$ has to be full rank, i.e., $N_tN = \mathrm{rank}\{\mathbf{M}^H\mathbf{M}\} = \mathrm{rank}\{\mathbf{M}\} \leq \min(N_tN, N_rN)$. Hence, $\min(N_tN, N_rN) = N_tN$, i.e., the number of receive antennas must be at least equal to the number of transmit antennas.

MMSE and zero-forcing equalization schemes were presented due to their simplicity and to provide some indication on the bit error rate performance. The equalization and detection stages are by no means optimized in this thesis, since the scope is in channel and CFO estimation. More advanced equalizers lead to better performance, i.e., lower data error rates. The maximum likelihood (ML) approach leads to the optimal detector from a statistical viewpoint [113, 17.3.3]. However, the computational complexity of ML detection is of order $O\left(\mathcal{Q}^{N_t}\right)$ per subcarrier, where $\mathcal{Q}$ refers to the constellation size. Hence, it is prohibitive for high order modulation schemes in practice. Then, one distinguishes linear sub-optimal approaches such as the previously discussed ZF and MMSE detectors. Low-complexity MMSE and MMSE decision-feedback equalization (DFE) are addressed in [229] and [228], respectively. Finally, there exist nonlinear sub-optimal techniques known as parallel interference (PIC) or serial interference (SIC) cancellation. A thorough review of the literature associated to both optimal and sub-optimal detection in MIMO OFDM may be found in [113, Ch.16-17]. An excellent reference book on signal detection and estimation principles is [218].

Special case of SISO OFDM

Single-input single-output OFDM transmissions are considered in Publications II, IV-VII. Moreover, a model for SISO OFDM is needed later in this thesis in order to describe most of the existing work in channel and frequency offset estimation. In the case of SISO transmission, i.e., $N_t = N_r = 1$, the expression in (2.11) for the received signal in time domain after CP removal reduces to

$$\mathbf{y}(k) = e^{j2\pi(kP+L_{\mathrm{CP}})\nu(k)/N}\mathbf{C}(\nu(k))\tilde{\mathbf{H}}(k)\mathbf{F}\mathbf{s}(k) + \mathbf{w}(k) \tag{2.26}$$

$$= e^{j2\pi(kP+L_{\mathrm{CP}})\nu(k)/N}\mathbf{C}(\nu(k))\mathbf{F}\mathbf{D}_{\tilde{\mathbf{h}}}(k)\mathbf{s}(k) + \mathbf{w}(k), \tag{2.27}$$

where the circulant matrix $\tilde{\mathbf{H}}(k)$ of size $N \times N$ performs the circular convolution with the channel impulse response vector $\mathbf{h}(k)$, and the diagonal matrix $\mathbf{D}_{\tilde{\mathbf{h}}}(k) = \text{diag}\{\tilde{\mathbf{h}}(k)\}$ contains the channel frequency response (CFR) at subcarrier frequencies. Similarly, the received signal after the DFT operation in (2.14)-(2.15) becomes

$$\begin{aligned} \tilde{\mathbf{y}}(k) &= e^{j2\pi(kP+L_{\text{CP}})\nu(k)/N}\mathbf{F}^H\mathbf{C}(\nu(k))\tilde{\mathbf{H}}(k)\mathbf{F}\mathbf{s}(k) + \tilde{\mathbf{w}}(k) \quad (2.28) \\ &= e^{j2\pi(kP+L_{\text{CP}})\nu(k)/N}\mathbf{F}^H\mathbf{C}(\nu(k))\mathbf{F}\mathbf{D}_{\tilde{\mathbf{h}}}(k)\mathbf{s}(k) + \tilde{\mathbf{w}}(k). \quad (2.29) \end{aligned}$$

Equalization may then be performed as in (2.24)-(2.25). Now, in the absence of CFO, i.e., $\nu(k) = 0$, the transmission equation (2.29) reduces to

$$\tilde{\mathbf{y}}(k) = \mathbf{D}_{\tilde{\mathbf{h}}}(k)\mathbf{s}(k) + \tilde{\mathbf{w}}(k). \quad (2.30)$$

As a result, OFDM modulation together with CP is able to turn a frequency selective channel into a set of parallel narrowband frequency flat channels. This assumes perfect time and frequency synchronization. Consequently, the equalization of frequency selective channels becomes extremely simple as a single-tap equalizer in the frequency domain is needed only. Another option to eliminate IBI is to add zeros at the end/beginning of the OFDM block. This is referred to as zero-padding (ZP) [279]. At the receiver, the corresponding samples are dropped, eliminating the IBI. Unlike the CP, the ZP does not enjoy the property of transforming the linear convolution with the channel into a circular one. However, relatively simple equalization may still be achieved if the received signal is overlap-added first and then equalized in the frequency domain [279, 303].

Null subcarriers

In practical OFDM systems, not all the subcarriers are used in order to avoid interference between adjacent OFDM systems [101]. Some of the subcarriers at the edges of the OFDM block are not modulated, and those are referred to as virtual subcarriers (VSC). Their number is dictated by system design requirements and they may represent up to 10% of the total number of subcarriers. Some other subcarriers may be deactivated as well. For instance, those which experience deep fades may be left unmodulated if the transmitter possesses knowledge of the channel state. In the following, deactivated subcarriers will be referred to as null-subcarriers (NSC), and those include VSCs.

Let $\mathcal{N} = \{0, \ldots, N-1\}$ denote the entire set of subcarriers indices, and let $\mathcal{N}_{\text{A}}$ denote the subset of $\mathcal{N}$ that contains the N_a modulated subcarriers. Similarly, $\mathcal{N}_{\text{NSC}}$ denotes the subset of $\mathcal{N}$ that contains the N_z NSCs. The $N \times 1$ vector modulating the entire set of subcarriers at time instance k may be expressed as

$$\mathbf{s}(k) = \beta_k \mathbf{V}_{\text{NSC}}(k)\, \mathbf{a}(k), \quad (2.31)$$

where $\mathbf{a}(k) = [a_1(k), \ldots, a_{N_a}(k)]^T$ is the $N_a \times 1$ symbol vector drawn from a complex symbol constellation. The normalization factor $\beta_k = \sqrt{N/N_a}$ ensures that the total transmitted power is constant regardless of N_a. The (m,n) element of the $N \times N_a$ tall permutation matrix $\mathbf{V}_{\text{NSC}}(k)$ is 1 if the n^{th} symbol is transmitted on the m^{th} subcarrier during the k^{th} OFDM block, and zero otherwise [101].

Choosing OFDM parameters

The choice of OFDM parameters is a tradeoff between various and often conflicting requirements [273, Ch.2]. There are three key parameters to begin with: the bandwidth B,

the bit rate b and the delay spread τ_d. The delay spread directly dictates the guard time T_g. In practice, the guard time is chosen between two to four times the root-mean-squared (RMS) delay spread. Once the guard time is set, the total symbol duration T_{s+g} may be determined (see Figure 2.3). In order to minimize the loss in signal-to-noise ratio (SNR)

Channel parameters	Symbol	Unit
Delay spread	τ_d	[s]
Doppler spread	B_d	[Hz]

System parameters	Symbol	Unit	Requirement	Cross links
Guard time	T_g	[s]	$T_g > \tau_d$	
System bandwidth	B	[Hz]	$B_d \ll B$	$B = NB_{\text{sc}} = 1/t_s$
Subcarrier bandwidth	B_{sc}	[Hz]		$B_{\text{sc}} = B/N = 1/T_s$
System bit rate	b	[bit/s]		$b = Nb_{\text{sc}} = x_{\text{bps}}/t_s$
Subcarrier bit rate	b_{sc}	[bit/s]		$b_{\text{sc}} = b/N = x_{\text{bps}}/T_s$
Block duration	T_{s+g}	[s]	$T_{s+g} = T_s + T_g$	
Data part duration	T_s	[s]	$T_s > T_g$	$T_s = Nt_s$
Sub-symbol duration	t_s	[s]		$t_s = T_s/N$
Number of subcarriers	N	integer	$N = \lceil B/B_{\text{sc}} \rceil$	$N = \lceil b/b_{\text{sc}} \rceil$

Table 2.1: Choice and dependencies among OFDM system and channel parameters.

induced by the guard time, it is advised to have the data symbol duration T_s as long as possible. However, it cannot be extended indefinitely for mainly two reasons:

1. The channel is assumed to remain (approximately) constant over the total duration $T_{s+g} = T_s + T_g$ of the OFDM block. Hence the condition $B \gg B_d$, where B_d is the Doppler spread of the channel. Otherwise, the orthogonality among the subcarriers gets compromised, which leads to ICI and significantly degrades the performance of the whole system.

2. A larger symbol duration implies a narrower subcarrier bandwidth, which in turn requires having more subcarriers with smaller intercarrier spacing. Increasing N requires FFTs of larger size which means a higher implementation complexity and peak-to-average power ratio (PAPR). Moreover, extremely closely spaced subcarriers put tight requirements on the frequency synchronization and makes the system highly sensitive to carrier frequency offsets.

Consequently, a practical design rule is to make the symbol duration at least five times the guard time, which implies a 1 decibel (dB) loss in SNR.

When the symbol duration and the guard time are fixed, the number of subcarriers N follows from the required -3 dB system bandwidth B divided by the subcarrier spacing $B_{\text{sc}} = 1/T_s$. The number of subcarriers may be found as well as the ratio between the required bit rate b and the bit rate per subcarrier b_{sc}. The parameter b_{sc} is determined by the modulation scheme in use and the symbol rate $1/T_s$. Assuming x_{bps} bits per symbol and the same modulation for all subcarriers, one gets $b_{\text{sc}} = x_{\text{bps}}/T_s$.

An additional requirement is to have an integer number of samples (typically a power of 2 to allow the use of radix-2 or -4 FFTs) within the DFT/IDFT interval and/or in the whole symbol interval. A typical solution is to modify one of the other system parameters to meet the requirement. Alternatively, null or virtual subcarriers allow meeting the

integer constraint and provide oversampling needed to avoid aliasing as well. The main requirements and design rules for OFDM system parameters are summarized in Table 2.1.

2.3 Imperfections in OFDM systems

Real-world OFDM systems suffer from various imperfections and limitations. In particular, they are extremely sensitive to frequency synchronization similarly to any multicarrier system. On the other hand, they are more tolerant to timing errors unlike single-carrier systems. In this section, we first review issues related to symbol synchronization including symbol timing and phase noise effects. Then, carrier frequency synchronization is addressed. Finally, we discuss high peak-to-average power ratios inherent to OFDM which put tight requirements on the power amplifier design. Many aspects regarding OFDM transceivers such as time synchronization or the peak power problem are only described briefly here, since they are beyond the scope of this thesis.

2.3.1 Symbol synchronization

One of the arguments against OFDM is its sensitivity to synchronization errors, especially frequency errors. Time and frequency synchronization techniques applied to OFDM are reviewed in [113, Ch.5]. In this section, we make a brief overview of issues related to timing, symbol phase errors, carrier frequency synchronization, the peak-to-average power problem and their impact on the OFDM system performance.

Timing errors

While carrier frequency offsets and phase noise (jitter) introduce ICI, OFDM is robust with respect to timing offsets. Indeed, OFDM is not sensitive to timing errors as long as those remain within the boundaries of the cyclic prefix. In this case, the orthogonality of the transmission is maintained and the symbol timing delay can be viewed as a phase shift introduced by the channel. The latter may be estimated and compensated by performing channel estimation followed by equalization. ISI and ICI occur only when the DFT interval extends over the OFDM block boundaries [273, Ch.4.4]. The latter is illustrated in Figure 2.4. However, to achieve the maximal robustness to multipath, the timing instant should

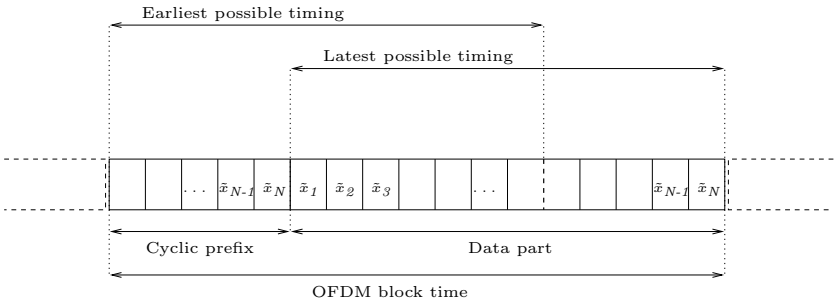

Figure 2.4: Boundaries for symbol timing instants in OFDM.

be the earliest possible one. Otherwise, the system can accommodate less delay spread than the value it was initially designed for. Therefore, the timing error should remain small compared to the guard interval. There exist mainly two classes of synchronization strategies for OFDM in the literature: the ones based on the redundancy introduced by

the cyclic prefix [272] and those using pilot symbols [153]. Combination of CP and pilot data may be used as well [153]. Correlation based methods seek for the time shift which maximizes the correlation of the received signal after equalization with the reference synchronization signal [280]. They usually consist of three distinct phases: power detection, coarse synchronization and fine synchronization. Also, a time and frequency synchronization algorithm exploiting a special pilot structure with two identical halves in time domain is considered in [238]. Blind synchronization in OFDM is also feasible by exploiting a special signal structure on top of the OFDM modulation: the delay information is not preserved in the second order statistics of a pure OFDM signal. Then, one may exploit the CP, the cyclostationarity of pulse-shaped signals [35] or the presence of virtual subcarriers [28]. A thorough review of time synchronization algorithms for OFDM may be found in [113, Ch.5] and [247, Ch.5].

Phase noise

Carrier phase noise (PHN) stems from imperfections in both transmitter and receiver oscillators, which translate in baseband into an additional phase and amplitude modulation of the received samples. Phase noise has two detrimental effects. First, it introduces a random phase variation common to all subcarriers. In addition, it causes ICI as subcarriers are not placed anymore $1/T_s$ apart in the frequency domain. Phase noise is an important factor that may limit the OFDM system performance [113, Ch.3].

Looking now at the SISO system model with phase noise in a CFO-free case ($\nu = 0$), the received signal in the frequency domain in equation (2.26) becomes:

$$\tilde{\mathbf{y}}_\theta(k) = \mathbf{F}^H \mathbf{C}_{\text{PHN}}(k)\, \mathbf{F} \mathbf{D}_{\tilde{\mathbf{h}}}(k) \mathbf{s}(k) + \tilde{\mathbf{w}}(k), \tag{2.32}$$

where we denote by $\mathbf{C}_{\text{PHN}}(k) = \text{diag}\{\exp(j\theta_0(k)), \ldots, \exp(j\theta_{N-1}(k))\}$ the phase noise matrix of size $N \times N$ and by $\theta_0(k), \ldots, \theta_{N-1}(k)$ the discrete time PHN sequence at block instance k. For non-zero PHN, the matrix $\mathbf{F}^H \mathbf{C}_{\text{PHN}}(k)\, \mathbf{F}$ is non-diagonal. Hence, phase noise destroys the orthogonality of the OFDM transmission and introduces ICI. Consequently, PHN statistics should be estimated.

There exist two different models for PHN in the literature [213]. The first type assumes the local oscillator (LO) is controlled by a phase-locked loop (PLL) and approximates the PHN by a process with finite power and low-pass shaped spectrum. The second type of PHN is obtained when the LO is tuned to the carrier frequency and free-running, i.e., the system is frequency-locked only. The modeling results in a Wiener process for the phase noise with Lorentzian power density spectrum. Assuming the second type of model for PHN, Pollet *et al.* estimate in [217] the resulting degradation in SNR as

$$D_{\text{PHN}} \cong \frac{11}{6 \ln 10} \left(4\pi N \frac{\beta}{B} \right) \frac{E_s}{N_0} \quad [\text{dB}], \tag{2.33}$$

where B denotes the system bandwidth, β (in Hz) is the one-sided 3 dB linewidth of the Lorentzian power density spectrum, and E_s/N_0 is the SNR per symbol. Notice that the degradation increases with the number of subcarriers. It also depends on the ratio $\beta/B = \beta T_s$, where T_s is the duration of the OFDM block. While the literature related to PHN focuses to date on SISO OFDM systems, the influence and suppression of phase noise in multi-antenna OFDM was analyzed in [237].

2.3.2 Carrier frequency synchronization

In Section 2.2.2, the Doppler spread and the local oscillators drifts were identified as the two main sources of carrier frequency offset. In the following, we analyze the impact of imperfect frequency synchronization on OFDM system performance.

Let us consider the SISO case, for simplicity. First, we recall the expression in (2.29) for the received signal in the frequency domain corrupted by carrier frequency offset:

$$\tilde{\mathbf{y}}(k) = e^{j2\pi(kP+L_{\mathrm{CP}})\nu/N}\mathbf{F}^H\mathbf{C}(\nu)\mathbf{F}\mathbf{D}_{\tilde{\mathbf{h}}}(k)\mathbf{s}(k) + \tilde{\mathbf{w}}(k). \tag{2.34}$$

From (2.34), it is clear that performing the DFT before correcting the CFO introduces ICI in the frequency domain as the matrix $\mathbf{F}^H\mathbf{C}(\nu)\mathbf{F}$ is not the identity matrix for non-zero frequency offset. The CFO may be several times larger than the subcarrier spacing. It is usually divided into an integer part k_ν and fractional part ϵ, as follows:

$$\nu = k_\nu + \epsilon, \tag{2.35}$$

with $k_\nu \in \mathbb{N}$ and $\epsilon \in [-1, 1[$. The integer part causes a circular shift of the transmitted symbols, while the fractional part is source of ICI. As seen in Figure 2.5, fractional CFO shifts the ideal sampling positions with zero-ICI in the frequency domain, leading to intercarrier interference. The amplitude loss occurs because the desired subcarriers are no longer sampled at the peak of the $\mathrm{sinc}(x) = \sin(x)/x$ function. Adjacent subcarriers cause interference, as they are not sampled at the zero-crossing of their sinc functions anymore. Figure 2.6 depicts the transmission matrix $\mathbf{F}^H\mathbf{C}(\nu)\mathbf{F}\mathbf{D}_{\tilde{\mathbf{h}}}$ for $\nu = 0$, 5.4 and a

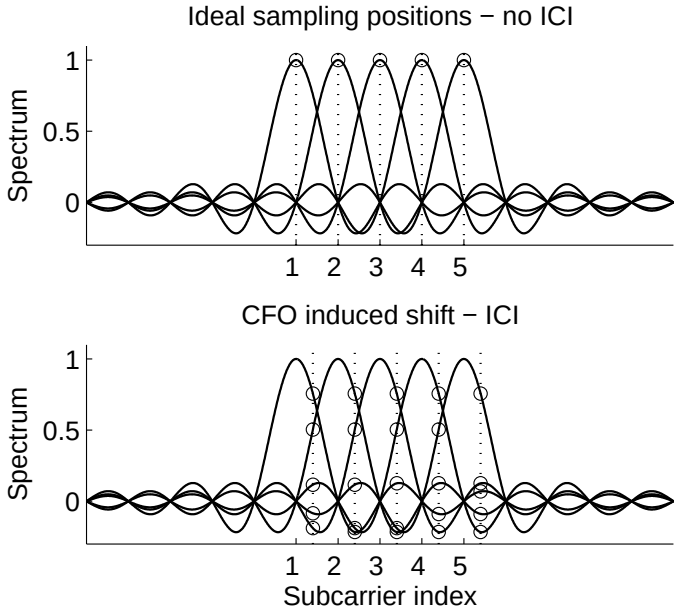

Figure 2.5: Effect of CFO on OFDM transmission with $N = 5$ subcarriers. Upper plot: Perfect synchronization, no ICI is observed ($\nu = 0$). Lower plot: CFO is present ($\nu = 0.4$). CFO shifts the ideal sampling positions in the frequency domain, introducing severe intercarrier interference.

random channel with $L_h = 8$ non-zero propagation paths. It is seen from the figure that the transmission matrix becomes clearly non-diagonal for non-zero frequency offset. This

may be treated as an equalization problem as the impulse response of the ICI may be expressed in terms of the CFO [101]. However, the number of parameters to be estimated increases and the benefit of low-complexity equalization is lost. Also, synchronization in

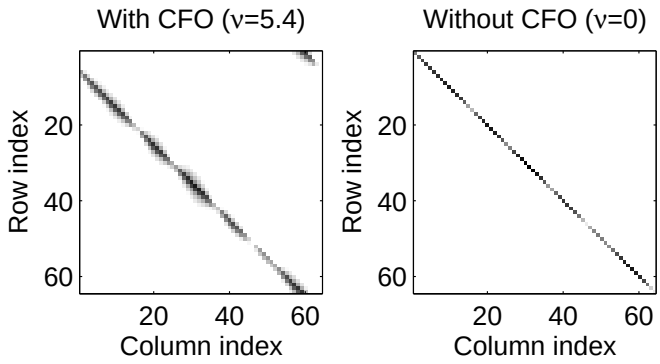

Figure 2.6: Effect of CFO on OFDM transmission with $N = 64$ subcarriers. Plot of the absolute values of the elements of the transmission matrix $\mathbf{F}^H\mathbf{C}(\nu)\mathbf{F}\mathbf{D}_{\tilde{\mathbf{h}}}$ in a logarithmic scale, for a random channel with $L_h = 8$ non-zero propagation paths. On the left: $\nu = 5.4$. The integer part of the CFO shifts the subcarriers by five while the fractional CFO equal to 0.4 introduces severe ICI. On the right: $\nu = 0$, i.e., perfect synchronization which leads to an orthogonal transmission. Dark colors correspond to high values.

the uplink is more difficult than in the downlink, as each user has a separate frequency offset. Moreover, in a mobile MIMO system in a rich scattering environment and with possibly separate IF-RF chains, one CFO parameter is needed for each MIMO branch as discussed earlier. CFO estimation in MIMO OFDM systems is further addressed in detail in Chapter 5.

Seminal work by Pollet et al. [217] quantified the degradation in SNR caused by the CFO as

$$D_{\text{CFO}} \cong \frac{10}{3\ln 10} 4 \left(\frac{\pi\nu N}{B}\right)^2 \frac{E_s}{N_0} \quad \text{[dB]}. \tag{2.36}$$

From (2.36), one notices that the degradation is proportional to the signal-to-noise ratio and quadratic in both the number of subcarriers and the value of the CFO itself. A more accurate analysis of the CFO-induced degradation may be found in [235]. It can be seen that carrier frequency offset is a critical issue for successful OFDM transmission, especially when high data rates with increased number of subcarriers together with narrow intercarrier spacing are used. OFDM systems are commonly considered to tolerate synchronization errors up to a few percents of the carrier spacing [273]. For instance, QPSK modulation can tolerate up to 5% error whereas 64QAM requires at least 1% accuracy for a loss of 0.5 dB in SNR [119]. The IEEE 802.16 standard specifies a tolerance of maximum 2% of the intercarrier spacing [1, 8.3.12]. For instance, in an OFDM system operating at 5 GHz carrier frequency with a subcarrier spacing of 300 kHz, the oscillator accuracy needs to be about 3 kHz (i.e., 1% of the intercarrier spacing) or $0.6 \cdot 10^{-6}$ (denoted 0.6 ppm). Low-cost oscillators do not generally meet those requirements. Typically, cristals controlling the oscillators have an accuracy around 1-20 ppm. Temperature control and other sophisticated techniques may allow further increasing the accuracy. However, due to their high cost, those solutions are likely to be deployed in base-stations only. Hence, additional frequency synchronization mechanisms have to be applied at the mobile receiver prior to

the DFT operation [273, Ch.4].

To conclude, OFDM and multicarrier systems in general are much more sensitive to carrier frequency offsets than single-carrier systems. CFO gives rise to intercarrier interference and reduction in amplitude for the desired subcarriers [273]. The issue is critical when higher data rates are required, and a relatively large number of subcarriers and very narrow guard bands are used [198, 311]. Imperfect CFO estimation has also a detrimental impact on channel estimation [206]. Consequently, frequency offset estimation and compensation must be accomplished with high fidelity. An extensive review of CFO estimation in OFDM may be found in Chapter 4. Frequency synchronization algorithms proposed in this thesis work are introduced in Chapters 5-6.

2.3.3 Peak power issues

OFDM modulated signals exhibit high peak-to-average power ratios since they are the superposition of a high number of modulated subchannel signals. Based on the central limit theorem, such a random process should be close to Gaussian [273, Ch.6]. Wei et al. established the result that the complex envelope of an OFDM modulated signal converges in distribution to a Gaussian random process as the number of subcarriers becomes infinitely large [281]. Therefore, OFDM signals put a high demand on power amplifiers as they may exhibit high instantaneous signal peaks compared to the average level. Practical amplifiers have a finite amplitude range in which they can be considered close to linear. Non-linearities in amplifiers may cause both ISI and ICI in the system. Clipping of the signal occurs when the amplifier is driven to saturation, which leads to out-of-band (OOB) emissions to both adjacent subchannels and systems.

Two families of solutions have been suggested in the literature to mitigate these problems. The first one consists of reducing the PAPR by various means such as coding techniques. They aim at lowering the probability of high signal crests prior to signal amplification. They operate either prior to OFDM modulation or by post-processing the time domain OFDM signal. Another option is to improve the amplification stage of the transmitter or to operate it with sufficient back-off, which leaves enough room for the signal peaks and reduces the risk of amplifier saturation. An overview of the peak power problem and the associated literature may be found in [273, Ch.6], [113, 3.1.1.1].

2.4 Discussion

Orthogonal frequency division multiplexing and more generally multicarrier transmission are tailored for multipath propagation. Hence, typical applications may be found in demanding wireless or wireline environments. Cyclic prefix together with DFT baseband modulation ensure simple equalization and low complexity of OFDM modems. OFDM found already its way in both wireless broadcasting (DAB and DVB) and wireline systems (ADSL). OFDM is the leading technique in digital subscriber lines. In this case, it is often referred to as discrete multi-tone (DMT) modulation. Spectrally efficient transmission may be achieved by allocating different number of bits to different subcarriers depending on their individual SNR, similarly to the water-filling principle. The use of OFDM in multiuser systems has gained increasing interest over the last few years. For instance, OFDMA [19, 150] yields a straightforward extension of OFDM to the multi-user case where users are assigned disjoint sets of subcarriers. The IEEE 802.16 standard specifies physical interfaces based on OFDM [1, 8.3] and OFDMA as well [1, 8.4] [150]. Multicarrier CDMA (MC-CDMA) [113, Ch.11] [114] is another way to provide multiple

access together with a stronger immunity to interference and deep channel fades. MC-CDMA builds on OFDM technology, with DFT-based modulators and cyclic prefix. The CDMA component allows for multiple users with coding across time and/or frequency. Though diversity is not obtained through the equalizer, it arises from the possibility to interleave in the frequency domain. Thus, MC-CDMA is a potential candidate for future beyond third generation mobile wireless communication systems. In January 2004, the IEEE formed a new task group to develop 802.11n [131], a new amendment to the 802.11 standard [130] for local-area wireless networks. The real data throughput is estimated to reach a theoretical 540 Mbit/s, and should be up to 10 times faster than 802.11a or 802.11g, and nearly 40 times faster than 802.11b, with as well a better operating distance than current networks. 802.11n builds upon previous 802.11 standards by adding MIMO and OFDM. MIMO technology allows for increased data throughput through spatial multiplexing and increased range by exploiting the spatial diversity. In addition, both the 3GPP [3] and WINNER projects [285] contribute to the development of future beyond 3G radio access [2].

Synchronization issues as well as the peak power problem are major challenges in OFDM and multicarrier system design. Excellent treatment of many other challenges encountered during the design of OFDM systems may be found in [83, 113, 119, 273]. High peak-to-average power ratios put high demand on linearity in power amplifiers and require also efficient pre- or post-processing of the OFDM data stream to lower the PAPR. Otherwise, ICI and OOB are produced. From the synchronization standpoint, the use of the cyclic prefix handles multipath delay spread efficiently and relaxes in a way timing requirements compared to single-carrier systems. However, due to the time-frequency duality, the problem translates to the frequency domain where synchronization requirements become extremely strict. If not compensated for, carrier frequency offsets are extremely harmful to OFDM transmissions as they destroy the orthogonality of the system. As a consequence, they cause intercarrier interference. Frequency synchronization mismatches may arise from both inaccuracies in local oscillators and Doppler shifts induced by mobility. Accurate frequency synchronizers are therefore needed for OFDM operation in future high data rate mobile wireless applications.

Then, as in any digital communication system, there exist two options for modulation: coherent or differential. The European DAB system employs differential QPSK while the DVB standard uses coherent high-order modulation (e.g., 64QAM). Differential modulation may be suitable for low data rates and allows much simpler receiver design, which may be important for low cost consumer products. However, differential encoding suffers from a 3 dB degradation in SNR compared to coherent modulation. Whenever high data rates together with low probability of error are targeted, coherent modulation is a natural choice. Thanks to OFDM modulation, equalization is greatly simplified compared to single-carrier systems. However, accurate channel estimation plays an important role in achieving the high capacity of MIMO OFDM systems. If the transmitter has partial or full knowledge of the transmission channel, adaptive modulation yields a powerful way of increasing the transmission efficiency [113, Ch.12].

To conclude, accurate frequency synchronization and channel estimation are major challenges for the deployment of multi-antenna high data rate mobile wireless multicarrier transmission systems. Therefore, those two major issues have been chosen as the main research topics of this thesis work.

Chapter 3

Channel estimation in OFDM systems

In wireless mobile communications, the channels are time, frequency and space selective [113, Ch.4]. The transmitted signal propagating via multiple paths experiences various delays due to different lengths of the paths. This makes the channel frequency selective and causes inter-symbol interference (ISI) [220]. The ISI may distort the received signal so severely that the transmitted symbols cannot be recovered [273]. Coherence bandwidth measures the frequency selectivity of the channel [220, Ch.14]. Multicarrier modulation such as OFDM is a powerful technique to turn the frequency selective wireless channel into a set of frequency flat narrowband channels [119, 273]. This reduces the complexity of the equalization task considerably [113, Ch.2]. Mobility causes the channel impulse response to be time-varying. Hence, it needs then to be tracked over time. The coherence time describes how time selective the channel is [220, Ch.14]. Moreover, selectivity in space domain may be encountered in multi-antenna systems, if the antennas are placed further than the coherence distance apart. The knowledge of the CIR is needed at the receiver in order to recover the transmitted data. Typically, no prior knowledge on the channel is available, and it may vary over time. Hence, it needs to be estimated and the estimates updated in a regular basis [113, Ch.4,14-16].

This chapter considers channel estimation in OFDM transmissions. In communication systems, channel estimation methods may be classified as *blind*, *semi-blind* or *pilot-aided* [31, Ch.8]. Blind algorithms do not require any training data and exploit statistical or structural properties of communication signals. Pilot-aided methods on the other hand rely on a set of known symbols interleaved with data in order to acquire the channel estimate [113, Ch.14-16]. Semi-blind methods combine a blind criterion with limited amount of pilot data, which improves both effective data rates and convergence speed. They also benefit from a larger sample support since both pilot and data are used for channel estimation. Blind, semi-blind and pilot-aided channel estimation in OFDM are successively reviewed in the following.

3.1 Blind channel estimation in OFDM

The need for higher data rates motivates the search for blind channel identification and equalization methods. In OFDM, cyclic prefix occupies generally up to 20% of the transmitted data [273, Ch.2]. Furthermore, if pilot symbols are used for channel estimation and synchronization purposes, those may require another 15-20% of the remaining data

symbols [113, 119]. Therefore, blind estimators are of interest, especially in the case of continuous transmissions (e.g. DVB-T) or slowly time-varying channels (e.g. ADSL). The term blindness means that the receiver has no knowledge of the transmitted sequence and the channel impulse response. Channel identification, equalization or demodulation is then performed using only some statistical or structural properties of communication signals, e.g. cyclostationarity, high-order statistics, or the finite-alphabet property [31, Ch.8]. Training data can then be either completely excluded or significantly reduced, and information symbols transmitted instead. The processing in blind receivers is typically nonlinear. Common design goals for blind receivers algorithms are the following: *capability to identify any type of channel, fast convergence to the desired solution, capability of tracking channel variations, and low computational complexity.*

There are quite a few underlying assumptions needed in deriving blind receivers. The signals may be assumed to be either random or deterministic. Random sequences are typically assumed to be white and wide-sense stationary when sampled at the symbol rate. For efficiently source coded signals where the redundancy is removed, this is a reasonable assumption. It also holds for many widely used channel coding schemes [179]. In case of deterministic data models, the sequences are typically required to have linear complexity and sufficient excitation to ensure channel identifiability. In practice, it follows that the sample covariance matrix of the sequence is not rank deficient. The pulse-shape employed at the transmitter as well as an upper-bound on the channel order are typically assumed to be known too.

In the following, we first review the main criteria used in blind channel estimation for OFDM. Those may be classified as follows: *correlation-based methods, subspace methods, methods exploiting the finite alphabet property and maximum likelihood estimation.* The section ends with a short survey of other possible criteria. Sequential estimation techniques such as, e.g. particle filters and Kalman filters, are also briefly reviewed.

3.1.1 Criteria for blind channel estimation in OFDM

Correlation-based methods

Correlation-based blind methods are among the most commonly used in OFDM. The main reason to this is the cyclic prefix (CP) and its periodic nature, which naturally introduces redundancy as well as cyclostationarity (CS). CS in communications and signal processing is a popular and extensively studied field [92]. Cyclostationary signals have the property that statistics, such as mean or autocorrelation function, are periodical. Linear time-invariant filtering does not affect cyclostationarity. Consequently, periodicity is expected in the time-varying correlation at the output of the channel. Cyclostationary statistics carry information on channel amplitude and phase. Hence, they allow blind channel estimation.

Heath and Giannakis proposed to exploit CS in OFDM transceivers [118]. In order to improve the performance and more specifically the channel identifiability (no restrictions on channel zeros), Bölcskei introduced the idea of periodic non-constant modulus precoding [37] for CP-based OFDM. In MIMO systems, the method assumes a non-constant modulus linear precoder at the transmitter array. User separation is ensured by providing each transmit antenna with different signatures in the cyclostationarity domain. The use of CP itself yields already redundant precoding in some sense, but the performance of blind identification based on CP only suffers from both high variance and low convergence speed [112, 120]. Moreover, redundant periodic precoding leads to a loss in effective data rates. In general, channel estimation via second-order cyclostationary statistics (SOCS)

allows identifying the CIR coefficients up to a complex scalar ambiguity [118].

Another approach led by Petropulu *et al.* is to employ non-redundant precoding at the transmitter side in SISO [166, 211, 212] or MIMO systems [294, 295]. With non-redundant precoding, the block length remains unchanged, but a specific correlation structure is induced at the transmitter, e.g. by correlating each carrier with a reference carrier. The method is computationally simpler than [37], and converges also faster. A proper balance must be found between the level of transmitter-induced correlation, leading to ICI, and a low channel estimation variance which may in turn improve the system performance.

Cyclostationarity may be introduced by means of pulse-shaping in OFDM systems, for example by using offset quadrature amplitude modulation (OFDM/OQAM) [36]. Overlapping pulse-shaping filters act as a form of precoder that induces CS, without the need for CP. A loss in data rates is the price to be paid for both modulation and pulse-shaping induced CS. Also, receive antenna diversity may be useful for blind channel recovery [99]. Two diversity branches are shown to be sufficient for channel identifiability, provided that any common roots to all the diversity channels are either at the origin or on the unit circle. In addition, data recovery requires that common unit-modulus roots must not coincide with any subcarrier frequency.

Statistical subspace methods

In general, subspace methods rely on a block formulation of the input-output relationship of the form

$$\mathbf{r}_{N_{ss}\times 1}(k) = \mathbf{H}_{N_{ss}\times L_{ss}}\mathbf{s}_{L_{ss}\times 1}(k) + \mathbf{w}_{N_{ss}\times 1}(k), \quad L_{ss} < N_{ss}, \tag{3.1}$$

where $\mathbf{r}_{N_{ss}\times 1}$, $\mathbf{H}_{N_{ss}\times L_{ss}}$, $\mathbf{s}_{L_{ss}\times 1}$ and $\mathbf{w}_{N_{ss}\times 1}$ denote the received vector, the channel matrix, the transmitted signal vector and the noise vector, respectively. Note that subscripts refer to dimensions of matrices and vectors. The transfer matrix $\mathbf{H}$ is a tall matrix, hence the signal subspace has a smaller dimension L_{ss} compared to the dimension N_{ss} of the observation (low rank model).

Let $\mathbf{R_{ss}} = \mathrm{cov}(\mathbf{s})$ be the source signal covariance matrix. If matrices $\mathbf{R_{ss}}$ and $\mathbf{H}$ are of full column rank, then $\mathrm{span}\{\mathbf{H}\} = \mathrm{span}\left\{\mathbf{H}\mathbf{R_{ss}}\mathbf{H}^H\right\}$. Thus, the columns of the channel matrix span the signal subspace, which is also spanned by L_{ss} eigenvectors of the received signal covariance matrix $\mathbf{R_{rr}} = \mathrm{cov}(\mathbf{r})$. Usually, signal and noise subspaces are not known a priori to the receiver, as they are determined by the unknown transfer matrix $\mathbf{H}$. However, they may be estimated by performing an eigenvalue decomposition (EVD) on $\mathbf{R_{rr}}$. Alternatively, one may perform a singular value decomposition (SVD) directly on the signal matrix [51, 227, 243]. This results in a reduced estimation error in theory, as signal and especially noise components are not squared. Let the matrices $\mathbf{U_s}$ and $\mathbf{U_w}$ of size $N_{ss} \times L_{ss}$ and $N_{ss} \times (N_{ss} - L_{ss})$ include the basis vectors for the orthogonal signal and noise subspaces, respectively. The orthogonality property between the signal and noise subspaces asserts that

$$\mathbf{u}_{\mathbf{w},i}^H \mathbf{H} = 0, \quad i = 1, \ldots, N_{ss} - L_{ss}, \tag{3.2}$$

where $\mathbf{u}_{\mathbf{w},i}$ denotes the i^{th} column vector of $\mathbf{U_w}$. Usually, $\mathbf{H}$ has some specific structure. For instance, let us assume, it is a Toeplitz convolution matrix made out from the $L_h \times 1$ channel vector $\mathbf{h}$. As the convolution operation is commutative, condition (3.2) may be rewritten as

$$\boldsymbol{\mathcal{U}}_{\mathbf{w},i}\mathbf{h} = 0, \quad i = 1, \ldots, N_{ss} - L_{ss}, \tag{3.3}$$

where the Toeplitz convolution matrix $\boldsymbol{\mathcal{U}}_{\mathbf{w},i}$ of size $N_{ss} \times L_{ss}$ is generated from the vector

$\mathbf{u}_{\mathbf{w},i}$. It can be shown that the set of equations in (3.3) determines the channel up to a complex scalar ambiguity.

In practice, the output covariance matrix $\mathbf{R}_{\mathbf{rr}}$ is unknown to the receiver and replaced by its sample estimate $\hat{\mathbf{R}}_{\mathbf{rr}}$. Hence, one does not have an exact knowledge of the true signal and noise subspaces, and the orthogonality conditions in (3.3) may not hold exactly in practice. Therefore, in order to solve for the channel vector $\mathbf{h}$, one resorts to minimize the following quadratic criterion

$$\hat{\mathbf{h}} = \arg\min_{\|\mathbf{h}\|=1} \sum_{i=1}^{N_{ss}-L_{ss}} \|\boldsymbol{\mathcal{U}}_{\mathbf{w},i}\mathbf{h}\|^2 \tag{3.4}$$

$$= \arg\min_{\|\mathbf{h}\|=1} \mathbf{h}^H \boldsymbol{\Psi}^H \boldsymbol{\Psi} \mathbf{h}, \tag{3.5}$$

where $\boldsymbol{\Psi} = \left[\boldsymbol{\mathcal{U}}_{\mathbf{w},1}^T, \ldots, \boldsymbol{\mathcal{U}}_{\mathbf{w},N_{ss}-L_{ss}}^T\right]^T$. Notice that the constraint $\|\mathbf{h}\| = 1$ avoids the trivial solution $\mathbf{h} = \mathbf{0}$. It is well known that the unit-norm eigenvector corresponding to the smallest eigenvalue of $\boldsymbol{\Psi}^H\boldsymbol{\Psi}$ yields a solution to (3.5) up to a complex scalar phase rotation.

Various statistical subspace-based methods have been proposed for blind channel estimation in OFDM systems [16, 24, 25, 42, 49, 74, 75, 192, 287, 300, 302, 303, 305, 316]. The main task is to cast the OFDM transmission equations in the form of a low rank model as in (3.1). Then, in most of the existing subspace methods, the channel estimate is found by minimizing a criterion similar to (3.5). The remaining scalar ambiguity is removed with the help of some pilot symbols.

Intuitively, the redundancy introduced by CP makes the system of equations overdetermined. By stacking a sufficient number of consecutive cyclic-prefixed blocks, the transmission matrix becomes tall, and subspace blind channel estimation becomes feasible [42]. The blind subspace channel estimator by Muquet *et al.* relies on the cyclic prefix as well [192]. The identifiability conditions were established by Zeng and Ng for this specific case [302]. Most of the existing methods require the cyclic prefix for subspace estimation [25,42,75,192,287,302,316]. Some of them cope with channel orders larger than the CP [316], while some others do not assume any CP [16, 24]. However, in that case, redundancy has to be introduced in the system in one way or another in order to maintain a low rank model. Zero-padding may be chosen instead of CP [74,300,301,303], which is not as spectrally efficient. This is also the case for redundant precoding at the transmitter [305]. Low rank model may also be obtained by exploiting NSCs with or without the CP [51,243]. It is observed that CP is more advantageous for noise subspace-based estimators than NSCs alone [51]. Oversampling the channel output in time and/or spatial domains by employing multiple antennas at the receiver side is another option [16, 24, 49, 227].

Statistical subspace methods exhibit a performance comparable to SOCS-based algorithms, at the price of an increased computational complexity. Eigenvalue or singular value decompositions require in the order of $\mathcal{O}(N_{ss}^2 L_{ss})$ operations [105, p.254]. This is significantly higher compared to correlation-based methods typically in $\mathcal{O}(N_{ss})$. Adaptive algorithms yield a potential way to reduce the computational complexity of subspace decompositions [74]. Moreover, the subspace dimensions are related to the channel length and need to be known. An upper-bound on the maximum channel length is usually sufficient as subspace based algorithms generally suffer less from over- than under-determined channels. In the case of CP-OFDM, the CP length provides a safe upper-limit in practice. In general, statistical subspace-based methods suffer from low convergence speeds due to the averaging needed in the estimation of the output covariance matrix. A few hundreds

of blocks are commonly needed in order to achieve satisfactory performance, which limits the use to the estimation of stationary channels. Finite sample sizes also result in error floor effects.

Deterministic subspace methods

In a few cases, signal and noise subspaces may be known a priori to the receiver [52, 107, 219, 276]. The statistical methods on the other hand rely on estimated signal and noise subspaces. For instance, a known redundant coding scheme [107] or NSCs at known locations may be present in the system by design. Receiver diversity offers also means to build a low rank model [52, 276]. In the above cases, the projection matrix to the noise subspace may be built beforehand and channel estimates may be obtained upon the first received block of data. Moreover, an exact solution up to a scalar ambiguity is guaranteed in the noise-free case with finite sample support. Deterministic techniques generally outperform statistical approaches for small sample sizes.

Finite-alphabet property based methods

Finite-alphabet (FA) based methods were introduced for CP- and ZP-OFDM by Zhou and Giannakis [313]. Assuming equiprobable symbols $a_n(k)$ drawn from a finite symbol alphabet of size $\mathcal{Q}$, there exists a non-zero integer $J_{\text{FA}} \leq \mathcal{Q}$ such that

$$\mathrm{E}\left[a_n^{J_{\text{FA}}}(k)\right] = -(J_{\text{FA}}/\mathcal{Q})\alpha_{\text{FA}} \neq 0,\ \alpha_{\text{FA}} \in \mathbb{C}, \tag{3.6}$$

where k and n refer to block and subcarrier indices, respectively. For instance $J_{\text{FA}} = 2$ for BPSK, $J_{\text{FA}} = 4$ for QPSK and QAM modulations with $\mathcal{Q}$ signaling points. In addition, any PSK symbol possesses the deterministic property $a_n^{J_{\text{FA}}}(k) = -1$. Starting from the J_{FA}^{th} moment of the received signal in the frequency domain, one obtains in the noiseless case

$$\mathrm{E}\left[\tilde{y}_n^{J_{\text{FA}}}(k)\right] = \tilde{h}_n^{J_{\text{FA}}}\,\mathrm{E}\left[a_n^{J_{\text{FA}}}(k)\right], \tag{3.7}$$

where $\tilde{h}_n$ is the channel frequency response at the n^{th} subcarrier. The channel is assumed to be time-invariant. In practice, the channel should remain constant over a sufficiently large number of consecutive blocks. By substituting (3.6) into (3.7), we may write

$$\tilde{h}_n^{J_{\text{FA}}} = -\frac{\mathcal{Q}}{J_{\text{FA}}\alpha_{\text{FA}}}\,\mathrm{E}\left[\tilde{y}_n^{J_{\text{FA}}}(k)\right]. \tag{3.8}$$

Setting the OFDM block length as $P \geq J_{\text{FA}}L'_h + 1$, where L'_h is the channel order, equation (3.8) allows us to the find channel coefficients uniquely. The first step is to solve for the $J_{\text{FA}}L'_h + 1$ time domain coefficients corresponding to the J_{FA}^{th} power of the channel spectrum. Those time domain coefficients correspond to the J_{FA}-fold convolution of the CIR with itself. The second and last step is the find out the CIR by solving the J_{FA}-fold convolution equation.

FA-based methods need only a few symbols. In PSK transmissions, channel estimation may be performed with a single OFDM block at high SNR. The scalar ambiguity is reduced to have unit-amplitude and phase values belonging to a finite set depending on the symbol constellation. Hence, ambiguity may be easily resolved, which is another advantage. Also, channel estimation decouples from symbol estimation. The major drawback of FA-based techniques is the high computational complexity. Recent attempts to lower the complexity are reported in [94, 210], at the cost of a significant loss in performance.

Non-CM modulations lead to error floor effects. Moreover, the use of J_{FA}^{th} order statistics implies slow convergence in practice for values of $J_{\text{FA}} \geq 4$.

Maximum likelihood methods

Let us recall the model in (2.29) and consider a single block of data. Let us assume that both the CIR vector $\mathbf{h}$ and the symbol vector $\mathbf{a}$ are deterministic but unknown, and the noise term is complex circular Gaussian. Then, the ML estimate of both CIR and data vectors is obtained as [56]

$$\left[\hat{\mathbf{h}}_{\text{ML}}\,,\,\hat{\mathbf{a}}_{\text{ML}}\right] = \arg\min_{\mathbf{h},\mathbf{a}} \left\| \tilde{\mathbf{y}} - \sqrt{N}\,\text{diag}\{\mathbf{a}\}\left[\mathbf{F}^H\right]_{\{:,1:L_h\}}\mathbf{h}\right\|^2, \tag{3.9}$$

where $\mathbf{a}$ is a $N \times 1$ vector of transmitted symbols belonging to a CM constellation of size $\mathcal{Q}$, and $\mathbf{h}$ is the $L_h \times 1$ CIR vector. The minimization problem in (3.9) turns out to be separable, assuming CM modulations. Then, ML estimates for data and channel vectors are computed as [56]

$$\hat{\mathbf{a}}_{\text{ML}} = \arg\max_{\mathbf{a}\in\mathcal{Q}^N} \left\{ \mathbf{a}^T\,\text{diag}\{\tilde{\mathbf{y}}^*\}\left[\mathbf{F}^H\right]_{\{:,1:L_h\}}\mathbf{F}_{\{1:L_h,:\}}\,\text{diag}\{\tilde{\mathbf{y}}\}\mathbf{a}^* \right\} \tag{3.10}$$

$$\hat{\mathbf{h}}_{\text{ML}} = \frac{1}{\sqrt{N}}\mathbf{F}_{\{1:L_h,:\}}\,\text{diag}\{\hat{\mathbf{a}}_{\text{ML}}^*\}\tilde{\mathbf{y}}. \tag{3.11}$$

The extension to SIMO systems is found in [26]. The maximization in (3.10) in often non-tractable because it involves a search over $\mathcal{Q}^N$ modulation symbols. In practice, the ML estimator can be run on a limited set of subcarriers only [56]. However, (3.10) may be solved sub-optimally, assuming PSK symbols and moderate frequency selective fading [194].

Other criteria

There exist few other criteria for blind channel estimation purposes in OFDM systems. The concept of *blind Viterbi decoding* is described in [172]. Minimum output energy equalization (MOE) is performed in [111]. An approach based on linear smoothing methods is reported in [299]. Vector constant mean energy (VCMA) has been employed together with user-decorrelation in the MIMO case [4]. The energy of out-of-band signals [70] may also serve as error criterion for blind channel estimation. In practice, the chosen criterion is often minimized iteratively (block-wise) by using a stochastic gradient algorithm. Another option is to perform blind adaptive equalization. Such methods adjust the coefficients of a time domain equalizer adaptively, in order to minimize the error criterion [4, 70, 112, 120]. Also, a blind source separation approach based on a natural gradient learning algorithm was developed in [108].

3.1.2 Sequential estimation techniques

Sequential Monte-Carlo (SMC) techniques, also know as particle filters, are applied in [292], without using any training/pilot symbols or decision feedback. Bayesian inference is made from the observation of a single OFDM block. The method happens to be relatively robust in the face of channel order mismatch. The computational complexity is high, as around 50 particles at least are needed at each iteration step. Kalman filtering (KF) applied to blind channel estimation was studied in [306]. A vector Kalman filter may be used

for this purpose, but has to operate in training or decision-directed mode (see Publication I), as KF needs information symbols to perform channel tracking. Otherwise, mixture Kalman filter (MKF) may be employed to estimate channel coefficients and information symbols jointly [306]. MKF combines in a way the principles of KF and particle filtering. Hence, the complexity remains extremely high.

3.1.3 Summary

Blind channel estimators rely in general on statistical or structural properties of communication signals. They are appealing because they do not need any dedicated pilot information, and data may be transmitted instead. Blind channel estimation appears to be especially suitable for fixed wireless OFDM transmissions, as the overhead caused by both pilots and CP may be too severe. This is especially true for time-invariant channels, where blind channel estimators perform at best. Blind methods allow updating the equalizer using information symbols continuously [49, 74, 192, 212, 233], which brings some advantage in time-varying channels. Pilot-based techniques on the other hand need to wait until next pilot symbol to get updated. A few blind estimators (ML, SMC, KF and to some extent FA with PSK) are suited to block fading channels [107, 172, 194, 276, 306]. The cost is though a much higher computational complexity. SOCS-based algorithms possess the lowest complexity but suffer from low convergence speeds. Subspace methods provide a little improvement in convergence speed but are significantly more complex. One should note that the ML estimator in [56] is of pure theoretical interest because of its prohibitive complexity. Also, if relatively high number of subcarriers (typically from 64 to 2048) is used, close to Gaussian transmitted signals are produced, which makes the application of both blind source separation techniques and higher order statistics (HOS) difficult.

However, blind methods suffer from ambiguity problems. The most common way to resolve the ambiguities is to require a little training or the use of differential encoding. Also, ambiguities may be avoided by a proper design of the signal constellation [193, 194, 233]. One may choose asymmetric constellation arrangements [233] or the combination of different modulation schemes on adjacent subcarriers [194], e.g., 3- and 5-PSK. The key idea is to have unique angles between any pair of constellation points. Hence, no ambiguity can exist anymore. In the MIMO case, the ambiguity matrix after the equalizer may be modeled as an instantaneous MIMO system, and solved using independent component analysis (ICA) [275].

A comparison of the techniques reviewed in this chapter is summarized in Table 3.1. Comparison is made in terms of four criteria: computational complexity, variance of the estimates, speed of convergence and the type of remaining ambiguity. Blind techniques typically have worse performance compared to their pilot-based counterparts and lower convergence speed as well. The energy required per information bit should be the figure of merit, to assess the potential gain of blind versus pilot-based approaches for given system specifications. The increased receiver complexity inherent to blind signal processing must also be kept in mind. Finally, a blind criterion is always at the core of any semi-blind algorithm. Hence, development in blind methods is important for semi-blind estimation as well.

3.2 Semi-blind channel estimation in OFDM

Limited training data in conjunction with blind algorithms leads to semi-blind methods. Increased sample support leads to lower estimation error. Convergence speeds are im-

		Compl.	Var.	Conv. speed	Ambiguity
SOCS	[36, 37, 99, 118] [212]	$*$	$*$	$*$	Complex scalar
SS	[16, 24, 42, 49, 74] [192,287,300,302] [305, 316]	$***$	$*$	$**$	Complex scalar
DS	[52, 107, 276]	$***$	$**$	$**$	Complex scalar
FA	[94, 177, 210, 313]	$**$	$**$	$**$	Phase in finite set
ML	[26, 56, 194]	$****$	$***$	$***$	Complex scalar
SMC, KF	[292, 306]	$***$	$***$	$***$	None[1]

Table 3.1: Comparative chart of blind channel estimation techniques for OFDM ($*$: low, $**$: moderate, $***$: high, $****$: extremely high). [1] Differential encoding is assumed. Compl.: complexity; Var.: variance of the estimate; Conv. speed: speed of convergence.

proved as well. Furthermore, semi-blind techniques allow updating the channel estimate and equalizer coefficients for both information and pilot symbols. Hence, semi-blind methods are better suitable for tracking time selective channels than their blind counterparts and provide a more feasible solution to practical communication systems [31, ch.8]. The following paragraphs detail how previously presented statistical subspace and maximum likelihood blind channel estimators may be adjusted to benefit from little pilot information. Added-pilot and decision-directed methods are reviewed as well.

3.2.1 Statistical subspace-based algorithms

In [192], Muquet *et al.* state several principles that may be applied in general to statistical subspace methods in semi-blind context [16, 24, 25, 42, 49, 74, 75, 192, 287, 300, 302, 305, 316]. The training is limited in the sense that training symbols alone are not sufficient to estimate the channel. If there are fewer pilots than parameters to be estimated, the problem may not be solved uniquely in the conventional least squares (LS) sense. Instead, a regularization procedure may be followed [12].

First, the slow convergence inherent to blind statistical subspace methods may be improved up by proper initialization of the output covariance matrix as follows:

$$\hat{\mathbf{R}}_{\mathbf{rr}}^{(0)} = \mathbf{H}(\hat{\mathbf{h}}^{(0)})\mathbf{R}_{\mathbf{ss}}\mathbf{H}(\hat{\mathbf{h}}^{(0)})^H, \tag{3.12}$$

where $\mathbf{H}(\hat{\mathbf{h}}^{(0)})$ is an estimate of the channel matrix in (3.1) constructed using an initial channel estimate $\hat{\mathbf{h}}^{(0)}$ obtained from the pilots. The covariance matrix of source symbols $\mathbf{R}_{\mathbf{ss}}$ is assumed to be known a priori.

Second, the output covariance matrix may be refined iteratively each time a new block of symbols is received. Both an adaptive update with a weighting factor [192] or a sliding window approach [314] allow tracking time variations of the output covariance matrix. Let $\hat{\mathbf{R}}_{\mathbf{rr}}^{(K)}$ be the resulting estimate of the covariance matrix, assuming K observed blocks. The

window size or the weighting factor should be properly set depending of the Doppler frequency. There is a clear tradeoff between improved channel tracking and noise suppression capability.

Third and last, the statistical subspace algorithm may be run based on $\hat{\mathbf{R}}_{\mathbf{rr}}^{(K)}$. Alternatively, if pilot information is present in each received block, it may be included in a composite criterion which comprises of a blind part and another component based on pilot symbols [192].

3.2.2 Semi-blind maximum likelihood methods

ML type of estimators also benefit from some pilot data. As the complexity of ML blind channel estimation is prohibitive in the case of OFDM [56], the expectation-maximization (EM) approach is often followed [10, 13, 181]. Pilots are used to initialize the channel estimation procedure, though they may not be sufficient for standalone estimation. However, the major problem of EM-based methods is that they may converge to local optima. Several different initial estimates may be needed. Alternatively, gradient-based approach may be followed to solve the ML optimization problem [262].

3.2.3 Added-pilot based methods

Added-pilots (or superimposed-pilots) schemes [47, 122, 201, 202] are closer to pilot-aided channel estimation than to blind techniques. The idea is to add pilot symbols directly to data symbols in time [47] or frequency domain [122, 201, 202]. In this way, no dedicated slot needs to be allocated to pilots, and the whole OFDM block may be used for information bearing symbols. The major drawback in added pilot semi-blind (APSB) channel estimation is that data interferes with pilots, and vice-versa. Thus, the influence of data should be minimized while estimating the channel, and conversely, the pilots have to be removed prior to data detection. Also, superimposed pilots contribute to increasing the peak-to-average power ratio.

3.2.4 Decision-directed methods

After detection, the detected symbols themselves may be used to refine channel estimates obtained using blind, semi-blind or pilot-assisted methods [12, 222, 262, 291] (see also Publication I). This is referred to as decision-directed (DD) processing, which is typically highly effective at moderate to high SNRs, when reliable symbol decisions are available to the receiver. In decision-directed channel estimation (DDCE), all the sliced and remodulated subcarrier data symbols are considered as pilot information. Reliable channel estimates may be obtained in case there are no decision errors and depending on the rate of channel variation. As an example, preamble based channel estimation schemes in both HIPERLAN/2 and IEEE 802.11a systems cannot fulfill the requirements in scenarios with moderate to high velocities. However, DDCE may allow a little mobility to wireless LAN (WLAN) systems [222]. Iterative and alternating estimation of channel and data is another option [12]. In this case, the DD algorithm iterates between using the channel estimate to detect the data, and using the data estimates to further improve the channel estimate. Pilots are needed for the initial channel estimation. Also, added-pilots may be combined together with decision-directed processing [291]. For this purpose, three types of symbols are used (see Figure 3.2): *i) full pilot, ii) partial pilot (i.e., pilot superimposed to data), iii) data symbol.*

Time-selectivity of the channel is clearly a limitation of pure DDCE schemes that do not use pilot information. With highly time-varying channels, past symbol decisions may not be correct anymore and lead to errors in channel estimation. Pure DDCE is prone to error propagation in highly time selective channels. The track of the channel coefficients may be totally lost. To avoid this, linear prediction techniques well known from the speech coding literature may be used. Those allow improving the past channel estimates prior to symbol detection and hence have fewer decision errors as well [15]. A review of OFDM-specific DDCE schemes may be found in [113], for both SISO [113, Ch.15] and MIMO [113, Ch.16] cases.

3.2.5 Summary

Semi-blind techniques combine the information contained in few known symbols with the statistical and structural properties of the communication signals. They possess three benefits over blind methods: *the ambiguities inherent to blind methods may be resolved, convergence speeds are improved, and more effective and robust tracking of time-varying channels is achieved*. Also, the increased sample support leads to lower estimation error. Consequently, lower variance estimates of the unknown channel may be obtained, or larger number of parameters may be estimated with reasonable variance. The channel estimate and equalizer coefficients may be updated for both information and pilot symbols. Hence, semi-blind methods provide a more feasible solution to practical communication systems [31, Ch.8]. Semi-blind techniques combine the benefits of both blind and pilot-based algorithms. Semi-blind processing may be implemented by using adaptive channel estimators and equalizers in a decision-directed mode. In order to ensure convergence, a small training sequence has to be transmitted first. This allows the estimator to acquire the channel rapidly. Blind methods are, however, an important research topic because the core of each semi-blind method is a powerful blind method.

3.3 Pilot-aided channel estimation in OFDM

One solution for channel estimation in OFDM is to transmit known pilot symbols on certain subcarriers [113,119,263,273]. Pilot symbol-assisted modulation (PSAM) schemes obtain the CFR estimate on the basis of known frequency domain pilot symbols that are interleaved among the transmitted data symbols. These pilot subcarriers facilitate the sampling of the channel frequency response. The corresponding sampling frequency needs to be higher than the Nyquist frequency required for the alias-free representation of the CFR at the Doppler frequency encountered. Errors in channel estimation influence the total system performance significantly, especially for systems employing multilevel modulation and coherent detection. A thorough overview of pilot-aided channel estimation for OFDM and PSAM in general may be found in [113] and [263], respectively.

A total of N_p pilot symbols are inserted in the OFDM block at known locations indexed by the set $\mathcal{P}$. Conversely, we assume N_d data symbols belonging to the set of indices $\mathcal{D}$, disjoint from $\mathcal{P}$. The total number of subcarriers is N and $N_d + N_p = N_a \leq N$, where equality holds when no null-subcarriers are used. Pilot allocation schemes as well as optimal rules of placement are discussed later in this chapter in Section 3.3.5. Let us rewrite the OFDM input-output relationships, in order to incorporate the pilot and data parts into the system model. After the DFT operation at the receiver and assuming that perfect time and frequency synchronization are achieved, the baseband signal in frequency

domain decouples into distinct pilot and data subchannels, as follows:

$$\tilde{\mathbf{y}}_d(k) = \mathbf{D}_d(k)\tilde{\mathbf{h}}_d(k) + \tilde{\mathbf{w}}_d(k) \quad (3.13)$$

$$\tilde{\mathbf{y}}_p(k) = \mathbf{D}_p(k)\tilde{\mathbf{h}}_p(k) + \tilde{\mathbf{w}}_p(k), \quad (3.14)$$

where $\tilde{\mathbf{y}}_d(k)$ and $\tilde{\mathbf{y}}_p(k)$ are the received signal vectors of sizes $N_p \times 1$ and $N_d \times 1$, respectively at pilot and data subcarriers. Diagonal matrices $\mathbf{D}_d(k)$ and $\mathbf{D}_p(k)$ contain data and pilot symbols on their main diagonal, respectively. Then, vectors $\tilde{\mathbf{h}}_d(k)$ and $\tilde{\mathbf{h}}_p(k)$ correspond to the channel frequency response at data and pilot subcarriers, respectively. Finally, $\tilde{\mathbf{w}}_d(k)$ and $\tilde{\mathbf{w}}_p(k)$ are the associated noise components in the frequency domain.

Therefore, if the CFR is well estimated, the equalization is easily performed by multiplying the received data on each subcarrier with the inverse of the corresponding CFR. The latter approach amounts to single-tap zero-forcing frequency domain equalization. Non-coherent data demodulation based on differential encoding may be employed as an alternative. Such an approach has the advantage that the channel estimation is not needed. However, a loss of 3 dB in SNR is experienced when compared to coherent demodulation. Moreover, coherent demodulation offers better performance over its non-coherent counterpart in the case of high-order modulations [273]. Hence, coherent demodulation is preferable for high data rate applications.

In this section, we review channel estimation procedures for PSAM-OFDM, which generally proceeds in the two following steps: *i) Channel estimation at pilot symbol locations. ii) Interpolation between CFR estimates at the pilot locations.* Finally, the problem of placing pilot symbols optimally is addressed.

3.3.1 Channel estimation at pilot symbol locations

Least-squares estimation

The first step in channel estimation in OFDM is generally to obtain an estimate of the CFR at pilot subcarriers. In most of the existing work in the literature, this task is usually accomplished via least-squares estimation [29,43,66,109,127,144,178,184,232,245,249,288, 289]. From now on, we drop the time index k, for simplicity, as we process a single OFDM block at the time. The least-squares estimate $\hat{\tilde{\mathbf{h}}}_{p,\mathrm{LS}}$ of the CFR at pilot symbols $\tilde{\mathbf{h}}_p$ may be obtained as

$$\hat{\tilde{\mathbf{h}}}_{p,\mathrm{LS}} = \mathbf{D}_p^{-1}\tilde{\mathbf{y}}_p. \quad (3.15)$$

The subcarriers are processed independently as $\mathbf{D}_p$ is a diagonal matrix. Hence, (3.15) amounts to perform single tap frequency domain ZF equalization on each subcarrier.

Linear minimum mean square error estimation

The LS estimate of (3.15) neglects the channel correlation among the subcarriers because it processes them independently. Because the CFR at data subcarriers are obtained later on by interpolation between the estimates at pilot subcarriers, the performance of the corresponding OFDM system will be highly dependent on the estimation error [127]. Thus, an improved estimate is desirable, such as the linear minimum mean square error (LMMSE) estimator of pilot signals derived in [77, 127] as

$$\hat{\tilde{\mathbf{h}}}_{p,\mathrm{LMMSE}} = \mathbf{R}_{\tilde{\mathbf{h}}_p,\tilde{\mathbf{h}}_p}\left(\mathbf{R}_{\tilde{\mathbf{h}}_p,\tilde{\mathbf{h}}_p} + \sigma^2_{\tilde{\mathbf{w}}}\left(\mathbf{D}_p\mathbf{D}_p^H\right)^{-1}\right)^{-1}\hat{\tilde{\mathbf{h}}}_{p,\mathrm{LS}}, \quad (3.16)$$

where $\tilde{\hat{\mathbf{h}}}_{p,\mathrm{LS}}$ is the LS estimate of $\tilde{\mathbf{h}}_p$ as shown in (3.15), and the channel covariance matrix at pilot locations is defined as $\mathbf{R}_{\tilde{\mathbf{h}}_p,\tilde{\mathbf{h}}_p} = \mathrm{E}[\tilde{\mathbf{h}}_p\tilde{\mathbf{h}}_p^H]$. It is easy to see from (3.16) that the LMMSE leads to the LS estimator at infinitely high SNR.

First, the LMMSE estimator above requires the knowledge of channel statistics at pilot symbol locations, which may be difficult to obtain in practice. Second, the method is highly complex because a matrix inversion needs to be performed every block in (3.16). The latter problem may be solved by using a static pilot pattern [127]. A simpler approach is to average over the transmitted data, and obtain a simplified LMMSE estimator [43,77,127]. To further reduce the complexity, low rank estimators may be derived [77,162]. However, they suffer from irreducible error floors due to the residual part of the channel outside the subspace. One also needs to make sure that the chosen rank is sufficiently large to eliminate the error floor up to a given SNR. Typically, the magnitude of the singular values of $\mathbf{R}_{\tilde{\mathbf{h}}_p,\tilde{\mathbf{h}}_p}$ should become small after about $L_{\mathrm{CP}}+1$ values. Generic low-rank estimators independent from the channel statistics may be constructed, with a nominal design tailored for a uniform correlation and a relatively high SNR [77]. The design at high SNR makes sense because channel estimation error is concealed in noise at low SNR.

Maximum likelihood estimation

Let us consider equation (3.14) assuming complex circularly symmetric AWGN and a deterministic but unknown CIR vector $\mathbf{h}$. Following Morelli and Mengali's derivation [191], the deterministic ML estimate of the CFR at pilot subcarriers may be obtained as

$$\tilde{\hat{\mathbf{h}}}_{p,\mathrm{ML}} = \left[\mathbf{F}^H\right]_{\{\mathcal{P},1:L_h\}} \left(\mathbf{F}_{\{1:L_h,\mathcal{P}\}} \left[\mathbf{F}^H\right]_{\{\mathcal{P},1:L_h\}}\right)^{-1} \mathbf{F}_{\{1:L_h,\mathcal{P}\}} \tilde{\hat{\mathbf{h}}}_{p,\mathrm{LS}}, \tag{3.17}$$

where $\left[\mathbf{F}^H\right]_{\{\mathcal{P},1:L_h\}}$ represents the DFT matrix truncated to the first L_h columns and with lines picked up from the set of pilot symbol indices $\mathcal{P}$. Similar expression is found in [71]. It is seen from (3.17) that ML estimation amounts to performing an orthogonal projection on the column space of $\left[\mathbf{F}^H\right]_{\{\mathcal{P},1:L_h\}}$. Note that the existence of the ML estimator above is conditioned upon the invertibility of the matrix $\mathbf{F}_{\{1:L_h,\mathcal{P}\}} \left[\mathbf{F}^H\right]_{\{\mathcal{P},1:L_h\}}$. Such a condition is met if and only if $N_p \geq L_h$, which means that there must be at least as much pilot symbols than channel parameters in the time domain. On the other hand, the LMMSE estimator still exists if $N_p < L_h$. The performance will degrade, though. The ML estimator achieves the Cramér-Rao bound (CRB), and no further improvement in MSE is possible if the estimator is unbiased, and the CIR is viewed as a *deterministic but unknown* vector. In practice, the ML estimator is computed in a case there is uncertainty on the CIR. On the other hand, LMMSE estimation is based on the Bayesian approach and exploits prior information on the channel and noise statistics. This explains the slight gain of LMMSE over deterministic ML observed in simulations [191].

Both ML and LMMSE estimators have the same form, which amounts to perform a linear filtering on the LS estimate. They outperform the LS estimator in frequency domain because the latter processes the components of the CFR independently. Hence, the correlation among subcarriers remains unexploited. The ML estimator restores the correlation via a deterministic subspace approach, while the LMMSE follows a statistical way. The LMMSE has higher complexity though.

MIMO channel estimation

The channel estimators presented so far are applicable to PSAM SISO OFDM systems, as they were all designed to extract parameters of a single CFR at pilot symbol locations. In a $N_t \times N_r$ MIMO system, there are $N_t \times N_r$ CFRs to be estimated, i.e., one per MIMO branch. This leads to $N_t N_r L_h$ channel parameters in time domain, where L_h upper-bounds the lengths of the CIRs. Second, with spatial multiplexing, several data streams are sent across the transmit antennas in the same frequency band, and they cause co-channel interference at the receiver array.

Assuming perfect synchronization in time and frequency, the $N \times 1$ received post-DFT signal vector at receiver antenna r in (2.15) may be rewritten as:

$$\tilde{\mathbf{y}}_r(k) = \sum_{t=1}^{N_t} \sqrt{N} \left(\mathbf{D}_{d,t}(k) + \mathbf{D}_{p,t}(k) \right) \left[\mathbf{F}^H \right]_{\{:,1:L_h\}} \mathbf{h}_{tr} + \tilde{\mathbf{w}}_r(k), \quad r = 1, \ldots, N_r, \tag{3.18}$$

where diagonal matrices $\mathbf{D}_{d,t}(k)$ and $\mathbf{D}_{p,t}(k)$ of size $N \times N$ contain data and pilot symbols at time instance k on their main diagonal and zeros elsewhere. Assuming training over K consecutive OFDM blocks, i.e., $k = 1, \ldots, K$, we may write the data model

$$\tilde{\mathbf{y}}_r = \mathbf{T}_d \mathbf{h}_r + \mathbf{T}_p \mathbf{h}_r + \tilde{\mathbf{w}}_r, \tag{3.19}$$

where $\tilde{\mathbf{y}}_r = \left[\tilde{\mathbf{y}}_r^T(1), \ldots, \tilde{\mathbf{y}}_r^T(K) \right]^T$, $\mathbf{h}_r = \left[\mathbf{h}_{1r}^T, \ldots, \mathbf{h}_{N_t r}^T \right]^T$, $\tilde{\mathbf{w}}_r = \left[\tilde{\mathbf{w}}_r^T(1), \ldots, \tilde{\mathbf{w}}_r^T(K) \right]^T$, and matrices $\mathbf{T}_p$ and $\mathbf{T}_d$ of size $KN \times L_h N_t$ are defined as

$$\mathbf{T}_{\mathrm{q}} = \sqrt{N} \begin{bmatrix} \mathbf{D}_{\mathrm{q},1}(1) \left[\mathbf{F}^H \right]_{\{:,1:L_h\}} & \cdots & \mathbf{D}_{\mathrm{q},N_t}(1) \left[\mathbf{F}^H \right]_{\{:,1:L_h\}} \\ \vdots & & \vdots \\ \mathbf{D}_{\mathrm{q},1}(K) \left[\mathbf{F}^H \right]_{\{:,1:L_h\}} & \cdots & \mathbf{D}_{\mathrm{q},N_t}(K) \left[\mathbf{F}^H \right]_{\{:,1:L_h\}} \end{bmatrix}, \quad \mathrm{q} = p, d. \tag{3.20}$$

Notice that the modeling in (3.18)-(3.19) assumes constant channel coefficients over K OFDM blocks. Then, based on (3.19), the LS estimate of $\mathbf{h}_r$ is obtained as [29]

$$\hat{\mathbf{h}}_{r,\mathrm{LS}} = \mathbf{T}_p^{\dagger} \tilde{\mathbf{y}}_r \tag{3.21}$$

$$= \mathbf{h}_r + \mathbf{T}_p^{\dagger} \mathbf{T}_d \mathbf{h}_r + \mathbf{T}_p^{\dagger} \tilde{\mathbf{w}}_r, \tag{3.22}$$

where $\mathbf{T}_p^{\dagger} = (\mathbf{T}_p^H \mathbf{T}_p)^{-1} \mathbf{T}_p^H$ is the left pseudo-inverse of $\mathbf{T}_p$, if it exists. The existence of $\mathbf{T}_p^{\dagger}$ requires the pilot sequences to be designed in such a way that the matrix $\mathbf{T}_p$ of size $KN \times L_h N_t$ is of full column rank $L_h N_t$ and $KN \geq L_h N_t$. To eliminate the interference term due to the data, the matrix $\mathbf{T}_p$ of pilot symbols must fulfill the following condition

$$\mathbf{T}_p^{\dagger} \mathbf{T}_d = \mathbf{0}_{L_h N_t \times L_h N_t}, \tag{3.23}$$

which holds when $\mathbf{D}_{d,t}^H(k) \mathbf{D}_{p,t'}(k) = \mathbf{0}_{N \times N}$, $\forall\ t, t' = 1, \ldots, N_t$, and $\forall\ k = 1, \ldots, K$. One way of satisfying (3.23) is by choosing disjoint sets of subcarriers for training and data in each OFDM block, i.e., zeros in $\mathbf{D}_{d,t}(k)$ where $\mathbf{D}_{p,t}(k)$ contains non-zero elements, and vice-versa [29]. Pilot symbols are not necessarily the same for each OFDM block. For zero-mean noise and when (3.23) is fulfilled, $\hat{\mathbf{h}}_{r,\mathrm{LS}}$ is an unbiased estimate of $\mathbf{h}_r$. A similar form for the MIMO LS channel estimate is found in [184, 244].

Li *et al.* investigate MMSE channel estimation in MIMO OFDM [163]. A low-complexity version of their estimator is found in [161]. The method is sensitive to time-

selectivity of the channel. MMSE MIMO channel estimation is also considered in [173,256]. As the receiver usually lacks the knowledge on channel statistics, the LS approach is often preferred in practice. Also, estimators in [161, 163] assume a whole block of training is made available to the receiver, whereas training may only be transmitted on a limited set of subcarriers in practical systems. Channel estimation in space-time coded MIMO OFDM is considered in [164]. Channel estimators for MISO, MISO and SIMO OFDM systems are introduced respectively in [22, 155], [221] and [160].

3.3.2 Channel interpolation

Once the CFR estimates have been obtained at the pilot subcarrier frequencies, they are extended to data subcarriers by interpolation. This will further allow equalization. The CFR may be seen as a two-dimensional process over the time-frequency grid, sampled at pilot symbol locations. Early publications on pilot-assisted channel estimation in OFDM considered one-dimensional (1-D) pilot patterns spanning the frequency or time direction only [66, 127, 144, 223, 249, 260, 288, 315]. Later on, the theory of two-dimensional sampling was invoked, in an effort to both reduce pilot symbol rates and improve channel estimation performance. When the channel is probed simultaneously in both time and frequency domains, the overhead of pilot symbols may be reduced significantly [123], as two-dimensional (2-D) processing captures simultaneously the correlation of the channel transfer function in both time and frequency [113, ch.14].

1-D Interpolation

When pilot symbols are distributed within the OFDM block using, e.g, comb-type pilot structure, interpolation in the frequency direction is mandatory to obtain the CFR at data subcarriers. Piecewise-linear and piecewise-constant interpolation are among the simplest approaches [223]. Higher-order interpolation such as piecewise second-order polynomial interpolation [127], low-pass and cubic-spline methods [66] offer improved channel interpolation. The Wiener filter achieves the best performance, but also has the highest complexity [141, 142]. The spacing between pilots or the amount of pilots are determined by the frequency selectivity of the channel [144], which relates to the maximum delay spread of the channel in time domain. With block-type of pilots, interpolation in the time domain is needed instead. Time-selectivity of the channel dictates the rate of retraining. It should be chosen smaller than the coherence time [249].

Most of the channel estimation methods presented so far process the data in the frequency domain. Time domain interpolation based on zero-padding and DFT/IDFT yields a simple and reliable approach [162,271]. It is also referred to as the direct-cut method (see Figure 3.1(a)). An upper-bound on the channel order is required. The number of channel parameters in time domain may be further reduced by selecting the most significant taps and neglecting the ones with low energy [163, 185] (see Figure 3.1(b)). This is also termed as denoising. Estimating and tracking the delay-subspace over time may be also beneficial to channel estimation [245].

2-D Interpolation

Hoeher *et al.* derive the two-dimensional time-frequency Wiener filter [123, 124], which is the optimal filter in the mean square error sense. Their estimator assumes knowledge of the doubly selective channel statistics, a condition which is hard to fulfill in realistic scenarios where the channel is not directly observable. In order to reduce the computational

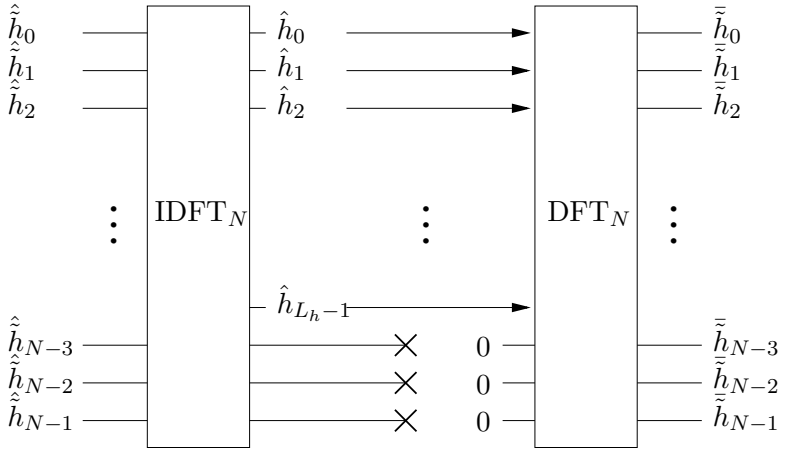

(a) Direct-cut method.

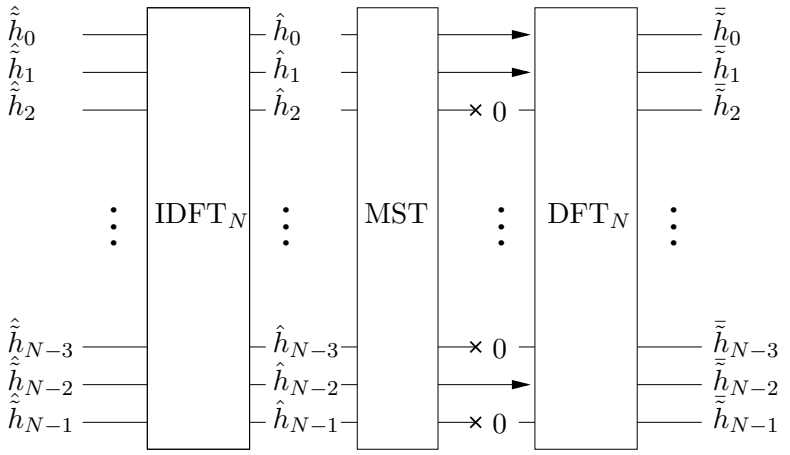

(b) Denoising with most significant tap (MST) selection.

Figure 3.1: Denoising approaches in time domain.

complexity, only a subset of pilot symbols may be processed at the time [113, ch.14] [124].

Cascaded 1D-FIR filtering allows to further reduce the complexity with almost as good performance as 2-D filtering. It relies on the assumption of separability of the channel's 2-D auto-correlation function in the time and frequency directions [162] [113, pp.493-495]. Adaptive 1-D [234] or 2-D [258] processing are other options. Edfors *et al.* propose the use of SVD-based low rank approximations [76,77,231]. Substituting unitary linear transforms by computationally less complex DFTs reduces further the complexity of both 1-D [77,271] and 2-D cascaded filtering [162]. However, the complexity reduction comes at the expense of a degradation in MSE due to leakage effects with non-sample spaced CIRs.

3.3.3 Robust designs

Optimum designs such as the 2-D Wiener filter require the knowledge of both channel statistics and signal-to-noise ratio at the receiver. However, this may not be the case in practice since the channel statistics are usually unknown. They depend on the environment and may change with time. In practice, a sub-optimal design involves choosing generic time and frequency correlation functions and thus avoid estimating the channel statistics from measurements. The correlation in frequency is governed by the power-delay profile (PDP) of the channel in time domain, whereas the correlation in time depends on the

Doppler spectrum [220, Ch.14]. In reality, both the PDP and Doppler spectrum are not known exactly. A robust interpolator should perform reliably, regardless of mismatched channel statistics [43,160,162]. The loss in performance should remain small compared to known statistics as long as the actual channel matches the maximum allowed Doppler and delay spreads.

3.3.4 Enhancing the channel estimates via DD-processing

Decision-directed channel estimation may also be employed on top of pilot-assisted channel estimation. In this case, it allows improving channel estimates because of the increased sample support and the sparsity of the pilot pattern. Indeed, channel estimation with pilot symbols alone has a limited precision. DD estimators perform usually better than the pilot-based ones at lower Doppler frequencies, whereas pilot-based methods should be preferred at higher Doppler frequencies. Decision-directed channel estimation techniques for pilot-aided SISO-OFDM were investigated for instance in [15,77,87,162,183,271,284]. DD-processing has been proposed in many different contexts to enhance channel estimation algorithms for MIMO systems as well [106,137,160,163,187,286].

3.3.5 Pilot design and placement

The geometry of the pilot pattern deserves attention as it ultimately influences the performance of channel estimation in time-frequency selective fading channels. The most commonly used pilot patterns in OFDM are presented in the following. Then, the optimal placement of pilot symbols is discussed in both the SISO and MIMO case.

Pilot patterns

Block and comb pilot structures are among the most commonly used in the literature related to OFDM as well as in practical applications. Block pilots (see Figure 3.2(a)) assume a complete block of training data is sent periodically [66,196]. The technique is appealing in slow to moderate fading, where the channel may be tracked via semi-blind or DD processing between two consecutive blocks of training. Frequency selectivity of the channel is handled at best, since all the subcarriers are used for channel estimation and thus no interpolation is needed. However, time selectivity is detrimental to block retraining, as the obtained channel estimates degrade as the channel varies over time. Consequently, the retraining rate needs to be increased. For instance, the IEEE 802.11 standard [130] for wireless LANs assumes that two complete blocks of training are sent prior to transmission of data. Data bearing blocks may also contain a few pilots for frequency synchronization purposes [119,273]. Comb pilot structures (see Figure 3.2(b)) dedicate a specific set of subcarriers to sending training data over time [20,66,71,127,144,191,196,223,245,249,260, 288]. Time-selectivity is better handled with comb pilot structure than with block pilots. On the other hand, high frequency selectivity of the channel may be an issue. It may require reducing the pilot spacing and opting for more advanced interpolation procedures. Rectangular pilot structure (see Figure 3.2(c)) includes OFDM blocks with comb-pilots, which are sent periodically and not continuously. DVB-T systems [86] use a specific pilot pattern (see Figure 3.2(d)) which combines block and rectangular structures. Blocks of pilots are meant for complete retraining, whereas comb pilots in blocks in between are used for channel tracking purposes. Hexagonal pilot designs (see Figure 3.2(e)) are optimal in the sense of sampling more efficiently the 2-D channel surface in the time-frequency plane than the rectangular pilot pattern [23,54,89–91]. About 13.4% fewer samples than

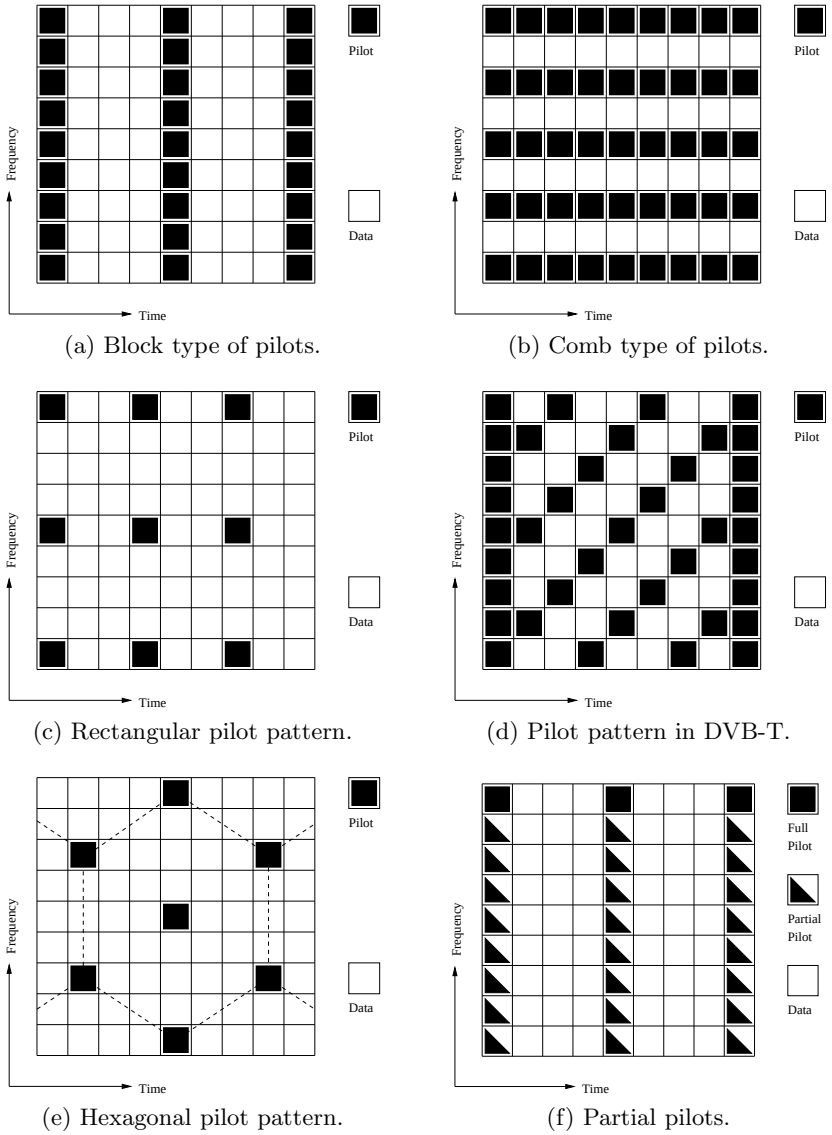

(a) Block type of pilots. (b) Comb type of pilots.

(c) Rectangular pilot pattern. (d) Pilot pattern in DVB-T.

(e) Hexagonal pilot pattern. (f) Partial pilots.

Figure 3.2: Pilot patterns in OFDM.

rectangular sampling are needed to achieve similar performance [91]. Partial pilots (see Figure 3.2(f)) were discussed already in Section 3.2.3 within the framework of semi-blind channel estimation [122, 201, 202]. The idea is to superimpose pilot to data symbols to facilitate channel estimation, without sacrificing the bandwidth efficiency while avoiding ambiguity problems [73]. Also, the set of pilot arrangements may be adaptively selected based on the prediction of the channel estimation error at the receiver [246].

Optimal placement of pilots - SISO case

The optimal placement of training symbols has been shown to enhance the overall system performance from both the estimation and information theoretical perspective [5, 6, 72, 115, 203]. Negi and Cioffi established optimality conditions for pilot placement in SISO OFDM [196]. Optimality is defined in terms of MSE of the channel estimate. The key results in [196] may be summarized as follows:

i. Time domain is preferable to frequency domain channel estimation because there are

fewer parameters in the CIR than in the CFR (L_h versus N, respectively). In such a way, variance of the estimates is also decreased.

ii. In the absence of noise, any L_h of the N available symbols may be used for training to recover the channel exactly. With less than L_h pilot symbols, the problem becomes under-determined, and there is no unique solution.

iii. In AWGN noise, the optimal pilot symbol pattern is the equispaced one. Otherwise, noise enhancement occurs. This result is also supported by information theoretical considerations [5].

iv. In a time-invariant channel, block and comb structures perform equally well provided that the number of pilots transmitted over the period of interest remains equal.

v. Intuitively, block pilot structures produce better channel estimation compared to comb pilot structures, but the quality of the estimate degrades over time as the channel changes.

vi. Comb pilot structure achieves better tracking of time-varying channels than block structure.

Also, the extra symbols required by the cyclic prefix are not that inefficient, as they allow to diagonalize the transmission in the frequency domain [180].

Optimal placement of pilots - MIMO case

Let us consider a $N_t \times N_r$ MIMO OFDM system, where L_h upper-bounds the length of the channels. Barhumi *et al.* derive optimum pilot sequences and their placement for the pilot-aided LS channel estimator [29]. As a result, optimal pilots for MIMO OFDM should fulfill the following conditions:

i. Pilot symbols must be equipowered and equispaced. The number of pilots at each transmit antenna should be chosen as $N_p \geq L_h N_t$.

ii. Under flat fading ($L_h = 1$), pilot sequences on different transmit antennas must be orthogonal.

iii. Under frequency-selective fading ($L_h \geq 1$), pilot sequences on different transmit antennas must be orthogonal and *phase shift orthogonal* in the range $\Phi \in \{-L_h + 1, \ldots, L_h - 1\}$. Phase shift orthogonality in the frequency domain corresponds in fact to circular shift orthogonality in the time domain. In other words, the pilot sequence of one antenna should not only be orthogonal to the pilot sequences of other antennas, but to circularly shifted copies of these sequences as well.

Minn and Al-Dhahir proved indeed that there exist several other optimal pilot symbol allocations [184]. The key idea is that orthogonality among training sequences at the transmit antennas must be ensured in one way or another, e.g., in either time, frequency, code domain or by combinations of those. Training over multiple OFDM symbols may be considered as well [29, 184].

3.3.6 Summary

In this section, we reviewed the ways of performing channel estimation in pilot-aided OFDM. One needs first to acquire channel estimates at pilot symbol locations. This task is usually accomplished using LS, MMSE or ML estimators. Then, CFR estimates at data subcarriers are obtained by interpolation between estimates at pilot locations. While 2-D Wiener filtering yields the optimal solution in the MSE sense, it turns out to be impractical since it assumes knowledge on both channel statistics and signal-to-noise ratio at the receiver. If complexity remains an issue with 2-D filtering, cascaded 1-D filtering offers an attractive alternative with almost negligible loss in performance. Robust estimators were introduced to avoid estimating the channel statistics [124, 160, 162]. Timing errors should also be taken into account, as they may degrade the performance of channel estimators even if channel statistics are known [20, 127]. Pilot design and placement deserve attention as well. A good choice of the pilot pattern should match the channel behavior both in time and frequency domains. In this way, the best tradeoff between channel estimator performance and transmission efficiency is found.

3.4 Concluding remarks

In this chapter, blind, semi-blind and pilot-aided channel estimation techniques for OFDM were reviewed. As blind methods are appealing due to their inherent bandwidth efficiency, they are not likely to be used alone in commercial applications and products. Indeed, they suffer from ambiguities and have high computational complexity. Moreover, some channels may not be identifiable. However, they may be used to refine pilot based estimates for each symbol, without requiring any modification of the transmitted signal structure. Blind methods remain an important topic of research since they are seminal part of any semi-blind algorithm.

Semi-blind processing incorporates a little amount of training in order to ensure better performance, improved tracking capabilities and resolve ambiguities. It offers a more feasible implementation of blind criteria to practical systems. Semi-blind methods may find an application in static scenarios (ADSL, DVB-T) as well as in ones with moderate mobility (fixed broadband wireless access, WLAN).

Pilot-aided processing is most commonly chosen in real-world systems, especially in fourth generation mobile wireless communications where mobility and high data rates are major requirements. Interleaving sufficient amount of known symbols among the transmitted data allows to track highly time-varying channels. Moreover, the quality of the channel estimates allows often choosing high-order symbol modulations, leading to increased data rates. Complexity issues may also dictate the choice of pilot-aided methods as blind or semi-blind techniques require an increased processing power and better SNR to reach similar performance targets. This issue is critical for battery operated and hence power limited mobile terminals. Finally, pilot symbols are almost always present in practical designs. They are needed for other purposes than channel estimation solely, e.g., for time and frequency synchronization. To conclude, Table 3.2 summarizes the key features in blind, semi-blind and pilot-aided channel estimation in OFDM, and allows their comparison.

	Blind	**Semi-blind**	**Pilot-aided**
Training data	None.	A single or a few pilot symbols.	Pilot symbols multiplexed with data.
Complexity	High.	Moderate to high.	Low to moderate.
Quality of the estimates	Low to moderate.	Moderate to high.	High.
Suitability to wireless channel	Freq. selective & time-invariant.	Freq. selective & slowly time-varying.	Freq. selective & time-variant.
Benefits	High effective data rates. No modification is required to transmitted signal structure.	No ambiguity. Trade-off between effective data rate and tracking capability. Large sample support. Outperforms pilot-aided estimation with the same amount of pilot information.	No ambiguity. Suitable for high mobility scenarios.
Weaknesses	Ambiguities. No channel tracking capability in general (except CM- and FA-based criteria). Some channels are not identifiable.	Less robust to abrupt change in channel condition.	Lower effective data rates. Time and frequency selectivity of the channel may be an issue depending on the amount of pilot data.

Table 3.2: Cross-comparison of blind, semi-blind and pilot-aided channel estimation for OFDM.

Chapter 4

Carrier frequency synchronization in OFDM systems

OFDM and more generally multicarrier systems are extremely sensitive to carrier frequency synchronization errors which lead to ICI and severely affect the transmission (see Section 2.3.2). Thus, estimation of the carrier frequency offset is a crucial task in OFDM-based transceivers. In this chapter, we review carrier frequency synchronization techniques specific to OFDM. Those may be classified as pre-DFT or post-DFT methods, depending on whether they operate in time or frequency domain, respectively. Coarse synchronization, i.e., estimation of the integer part of the CFO with respect to the intercarrier spacing, is typically performed in the frequency domain after the fractional part has been estimated and corrected. Fine synchronization, i.e., estimation of the fractional part with respect to the intercarrier spacing, usually takes place in the time domain. The emphasis in this review is put on the estimation of the fractional CFO, as is compromises severely the orthogonality of the transmission and leads to ICI.

In the literature on synchronization and channel estimation, algorithms are often classified as blind, semi-blind and pilot-based. However, some of the CFO estimation methods are classified as data-aided, although they do not use the explicit knowledge of the pilot symbols. Estimation techniques that rely on a repetitive structure of the OFDM symbol in time domain fall into this category [188, 190, 238]. Those are in fact null-subcarrier (NSC) based techniques, as discussed in [101] and later in this chapter. These techniques require the number of NSCs to be larger or equal to half of the total number of subcarriers. Hence, they are often referred to as data-aided, even though no data is actually transmitted on the NSCs. Sometimes, when the only null-subcarriers are the virtual subcarriers imposed by system design, the related CFO estimators are referred to as blind [167]. To avoid any confusion, we follow the classification employed in [101] which also gives an excellent review of CFO estimation techniques for OFDM systems. Thus, we will refer to NSC-based techniques in general.

First, blind maximum likelihood estimators are reviewed. Then, repetitive slots-based and nonlinear least squares estimators are presented and the correspondence between them is established. Null-subcarrier estimation is considered then and the conditions for CFO identifiability are stated. SOCS-based CFO estimation is presented next, based on either signal covariance or pseudo-covariance. Some alternative approaches for blind synchronization of OFDM transceivers are reviewed also. Those include estimators based on high-order statistics as well as on the constant modulus and finite alphabet properties. Finally, decision-directed techniques and algorithms exploiting explicitly the pilot data are presented.

The tree in Figure 4.1 provides a classification of CFO estimators and the links between them. It depicts as well the overall organization of this chapter.

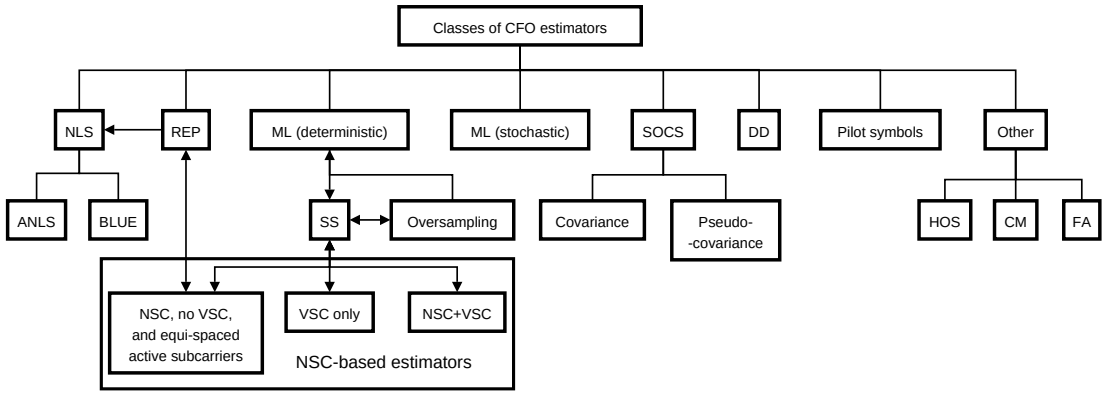

Figure 4.1: Classification of CFO estimators for OFDM. Arrows picture equivalences between estimators. ANLS: approximate nonlinear least squares, BLUE: best linear unbiased estimator, CM: constant modulus, DD: decision-directed, FA: finite alphabet HOS: high-order statistics, NLS: nonlinear least squares, REP: repetitive slots-based, SOCS: second-order cyclostationary statistics, SS: subspace estimator.

4.1 Blind maximum likelihood CFO estimation

4.1.1 ML estimators for the AWGN channel

Daffara and Chouly propose a maximum likelihood estimator of the carrier offset for the AWGN channel [69]. Estimation is performed recursively via an automatic frequency control (AFC) loop. The method is blind since the data dependence of the log-likelihood function is removed through averaging. However, local maxima arise at integer offset values, which may create false locking points for the AFC.

The seminal work by Beek *et al.* [272] describes a joint maximum likelihood timing and CFO estimator which exploits the redundancy provided by the cyclic prefix. The proposed approach stems from blind stochastic ML estimation and exploits the known correlation structure induced by the CP. The OFDM signal received through the AWGN channel is approximated as complex circular jointly Gaussian. The data dependence is removed in this way. The following likelihood function is minimized to find estimates of the timing offset $\tau \in \mathbb{N}$ and carrier frequency offset ν:

$$\Lambda(\tau,\nu) = |\gamma(\tau)| \cos\left(2\pi\nu + \arg\left\{\gamma(\tau)\right\}\right) - \rho\Phi(\tau), \tag{4.1}$$

where

$$\gamma(\tau) = \sum_{m=\tau}^{\tau+L_{\mathrm{CP}}-1} y_{\nu,\mathrm{CP},m} y^{*}_{\nu,\mathrm{CP},m+N} \tag{4.2}$$

$$\Phi(\tau) = \frac{1}{2} \sum_{m=\tau}^{\tau+L_{\mathrm{CP}}-1} |y_{\nu,\mathrm{CP},m}|^2 + |y_{\nu,\mathrm{CP},m+N}|^2, \tag{4.3}$$

where $\rho = SNR/(SNR+1)$ and $y_{\nu,\mathrm{CP},m}$ denotes the m^{th} received sample in time domain

before CP removal. The joint ML estimator of τ and ν becomes

$$\hat{\tau}_{\mathrm{ML}} = \arg\max_{\tau} \{|\gamma(\tau)| - \rho\Phi(\tau)\} \tag{4.4}$$

$$\hat{\nu}_{\mathrm{ML}} = -\frac{1}{2\pi} \arg\{\gamma(\hat{\tau}_{\mathrm{ML}})\}. \tag{4.5}$$

The estimates of τ and ν may be found from $\gamma(\tau)$. Its magnitude, which is compensated by an energy term, peaks at time instant $\hat{\tau}_{\mathrm{ML}}$, while its phase at this time instant is proportional to $\hat{\nu}_{\mathrm{ML}}$. Naturally, performance improves when increasing the CP length L_{CP} because the correlation terms add coherently at the value of the CFO while non-coherently for the noise. However, error floors are observed in multipath channels as the estimator was originally designed to deal with the AWGN case. Note that the above algorithm is suited for tracking small CFOs, as the estimation range for the normalized carrier offset is limited to $[-1/2, 1/2[$. Other approaches need to be considered for the CFO acquisition mode.

Several improved versions and variations of the above algorithm are found in the literature [128, 149, 154, 310]. For instance, the one in [128] uses smoothing algorithms (e.g., moving averages and exponentially weighted averages) to replace the sums in (4.2)-(4.3). The goal is to better mitigate multipath propagation which spreads the symbols along the time direction. The improvement introduced in [154] leads to more accurate description of the correlation features of the received signal. Moment-based and minimum variance unbiased estimators are presented as well. Finally, the technique in [149] is based on an additional data rotation scheme, and achieves 2 dB gain over [272], in the AWGN case though.

4.1.2 ML estimators for the multipath Rayleigh fading channel

Blind maximum likelihood estimation of the carrier frequency offset for OFDM under multipath Rayleigh fading was investigated in [53, 55, 165]. However, [55, 165] are based on an erroneous likelihood criteria: the received signal in (2.26) cannot be modeled as jointly Gaussian distributed due to the Rayleigh fading process which multiplies the random data. Hence, while being technically correct for the AWGN case, [55, 165] yield sub-optimal methods under multipath Rayleigh fading. For instance, error floors are observed in [55]. A valid approach under multipath Rayleigh fading is given in [53]. However, it is still a sub-optimal method. In order to remove the data dependency, the estimator relies on an approximate likelihood function.

4.2 Correlation-based CFO estimation with repetitive slots

In OFDM systems, pilot blocks are usually transmitted prior to the information frame. For instance, the IEEE 802.11 standard for WLANs [130] employs series of identical slots in time domain as a preamble. Moose's [188], Schmidl and Cox's [238] and Morelli and Mengali's [190] estimators as well as numerous variants [188, 190, 199, 238] rely on repetitive pilot structures. They are reviewed in the following.

4.2.1 Moose's estimator

Seminal work by Moose [188] proposed to use a repeated data symbol to perform CFO estimation. If an OFDM transmission block is repeated, and assuming the channel coherence time spans at least two OFDM blocks, one receives the following two $N \times 1$ vectors

in the frequency domain:

$$\tilde{\mathbf{y}}_\nu(k) = \tilde{\mathbf{r}}(k) + \tilde{\mathbf{w}}(k) \quad (4.6)$$

$$\tilde{\mathbf{y}}_\nu(k+1) = \tilde{\mathbf{r}}(k)e^{j2\pi\nu} + \tilde{\mathbf{w}}(k+1), \quad (4.7)$$

where $\tilde{\mathbf{r}}(k) = e^{j2\pi\nu k}\mathbf{F}^H\mathbf{C}(\nu)\tilde{\mathbf{H}}\mathbf{F}\mathbf{s}(k)$. Note that the guard interval is not needed anymore between the identical blocks, and it is omitted from the model in (2.28). In the noise-free case, there exists a phase shift of $2\pi\nu$ between the components of $\tilde{\mathbf{y}}_\nu(k+1)$ and $\tilde{\mathbf{y}}_\nu(k)$. This intuitively leads us to the following estimator:

$$\hat{\nu} = \frac{1}{2\pi}\arg\left\{\tilde{\mathbf{y}}_\nu^H(k)\tilde{\mathbf{y}}_\nu(k+1)\right\}. \quad (4.8)$$

The above estimator resolves the normalized carrier frequency offset without any ambiguity in the range $[-1/2, +1/2[$, i.e., half of the subcarrier spacing of the repeated symbol. Otherwise, ambiguities are encountered by the $\arg\{\}$ function when the phase shift exceeds $\pm\pi$. A basic strategy to enlarge the estimation range for CFO acquisition is to shorten the DFTs and use larger intercarrier spacings for the repeated data block [188].

The estimator in (4.8) proves to be ML [188]. Notice that it is unaffected by multipath propagation, unlike the estimator by Beek *et al.* [272]. Furthermore, both signal and ICI components differ only up to a phase shift proportional to the CFO. Thus, the frequency offset may be estimated even though it is too large to guarantee satisfactory data demodulation.

4.2.2 Schmidl and Cox's estimator

Instead of two consecutive identical blocks, Schmidl and Cox's algorithm (SCA) [238] considers a training block with two identical halves in time domain. The latter is generated by transmitting a PN sequence on the even subcarriers, while the odd ones are set to zero. Let Q be the number of samples in the first half of the training symbol, excluding the cyclic prefix. Denoting by $y_{\nu,\mathrm{CP},m}$ the m^{th} received sample in time domain before CP removal, we define the two quantities

$$p_{\mathrm{SCA}}(\tau) = \sum_{m=0}^{Q-1} y^*_{\nu,\mathrm{CP},\tau+m} y_{\nu,\mathrm{CP},\tau+m+Q}, \quad r_{\mathrm{SCA}}(\tau) = \sum_{m=0}^{Q-1} |y_{\nu,\mathrm{CP},\tau+m+Q}|^2, \quad (4.9)$$

where $\tau \in \mathbb{N}$ is the time index corresponding to the first sample in a window of $2Q$ samples. This window slides over time as the receiver searches for the training block by looking for the two identical halves in time domain. The method proceeds in two steps. The timing offset is first estimated as

$$\tau_0 = \arg\max_\tau m_{\mathrm{SCA}}(\tau), \quad m_{\mathrm{SCA}}(\tau) = \frac{|p_{\mathrm{SCA}}(\tau)|^2}{(r_{\mathrm{SCA}}(\tau))^2}, \quad (4.10)$$

where $m_{\mathrm{SCA}}(\tau)$ is the timing criterion. Then, assuming the timing offset τ_0 has been correctly estimated, there exists a phase difference of $\pi\nu$ between the two symbol halves. Consequently, the CFO is estimated as

$$\hat{\nu} = \frac{1}{\pi}\arg\left\{p_{\mathrm{SCA}}(\tau_0)\right\}. \quad (4.11)$$

Symbol timing and carrier frequency synchronization are often performed jointly in the literature. With repetitive slots (REP) based estimation, the CFO is usually obtained as the argument of the timing criterion taken at the optimal timing instant. The estimation range of the SCA is within the interval $[-1, +1[$ of intercarrier spacing. The range is hence doubled compared to Moose's algorithm, and allows estimating the fractional CFO.

However, there might remain an uncompensated frequency shift of $2z/T_s$ [Hz], where z is an integer. To resolve the integer shift $k_\nu = 2z$, another training block is required by [238]. First, the fractional CFO is corrected for both blocks using the estimate from (4.11), and ICI is hence avoided. Second, it is assumed that the pairs of subcarriers from one block to the other are differentially modulated with phase differences given by the sequence v_n, $n \in \mathcal{N}_\text{A}$, where $\mathcal{N}_\text{A}$ is the set of modulated (even) subcarriers. Since the CFO-induced phase shift is similar for each pair of frequencies, a criterion similar to the one in (4.10) may be used to estimate k_ν as

$$\hat{k}_\nu = 2 \arg\max_{g \in \mathbb{N}} \{b_\text{SCA}(g)\}, \quad b_\text{SCA}(g) = \frac{|\sum_{n \in \mathcal{N}_\text{A}} \tilde{y}^*_{1,n+2g} v^*_n \tilde{y}^*_{2,n+2g}|^2}{2\left(\sum_{n \in \mathcal{N}_\text{A}} |\tilde{y}_{2,n}|^2\right)^2}, \tag{4.12}$$

where $\tilde{y}_{k,n}$, $k = 1, 2$ denotes the n^{th} received sample of the k^{th} block in frequency domain. Finally, by combining the fractional and integer offset estimates from (4.11) and (4.12), respectively, the final CFO estimate is obtained by $\hat{\nu} = \hat{k}_\nu + \hat{\epsilon}$.

4.2.3 BLUE estimator

Morelli and Mengali [190] proposed an extension of the Schmidl and Cox's algorithm with a training block composed of $J > 2$ identical parts in time domain. In the sequel, it is referred to as the extended SCA (ESCA). The main benefit over the conventional SCA is an increase of the estimation range which becomes $[-J/2, +J/2[$. The proposed estimator exploits the correlations between identical slots of the training block in time domain as

$$r_\text{ESCA}(m) = \frac{1}{N - mQ} \sum_{n=mQ}^{N-1} y_{\nu,n} y^*_{\nu,n-mQ}, \quad 0 \le m \le H, \tag{4.13}$$

where $Q = N/J$ is the length in sampling intervals of each section of the training block and $H \in \mathbb{N}$ is a design parameter. By considering the phase differences

$$\varphi(m) = [\arg\{r_\text{ESCA}(m)\} - \arg\{r_\text{ESCA}(m-1)\}] \mod 2\pi, \quad 1 \le m \le H, \tag{4.14}$$

the best linear unbiased estimator (BLUE) of the CFO is expressed as [190]

$$\hat{\nu}_\text{ESCA} = \frac{J}{2\pi} \sum_{m=1}^{H} \omega_\text{ESCA}(m) \varphi(m), \tag{4.15}$$

where the weighting coefficients $\omega_\text{ESCA}(m)$ are given by

$$\omega_\text{ESCA}(m) = 3 \frac{(J-m)(J-m+1) - H(J-H)}{H(4H^2 - 6HJ + 3J^2 - 1)}. \tag{4.16}$$

The weights in (4.16) are channel independent. Thus the ESCA is the BLUE for any channel. It was shown in [190] that the variance of the ESCA estimator achieves its minimum when $H = J/2$. It is interesting to notice that (4.15) reduces to the SCA for

$J = 2$ and $H = 1$. The ESCA estimates have otherwise slightly lower variance than those of SCA [190]. The price to be paid is an increase in computational complexity, as H angles have to be computed in (4.14) instead of one for the SCA.

4.2.4 Multi-stage approach

The multistage estimator from [248] trades off between estimation range and estimation variance. The lowest variance is achieved at the expense of a smaller range, and vice-versa. The method assumes a preamble composed of $J = 2^{K_S}$ repetitive slots in time domain, $K_S \in \mathbb{N}$. At the i^{th} stage, $J/2^i$ base sub-blocks are bundled together to obtain 2^i new sub-blocks $i = 1, \ldots, K_S$ (see Figure 4.2). Thus, K_S stages are considered in total. The idea of partitioning the sub-blocks is also found in [186]. The CFO estimate for the i^{th} stage is estimated by correlating the adjacent i^{th} stage sub-blocks as

$$\hat{\nu}_i = \frac{2^i}{2\pi} \arg \left\{ \sum_{n=0}^{N/2^i-1} y^*_{\nu,n} y_{\nu,N/2^i+n} \right\}, \quad i = 1, \ldots, K_S. \tag{4.17}$$

The first stage is equivalent to the SCA [238], while upper stages are equivalent to Morelli and Mengali's technique [190]. As the size of the sub-block decreases, the estimation range increases. At the i^{th} stage, the range yields $|\hat{\nu}_i| < 2^{i-1}$. After all estimated values $\hat{\nu}_i$ ($i = 1, \ldots, K_S$) have been obtained, ambiguities induced by multiple estimation intervals have to be resolved. This leads to a phase unwrapping problem.

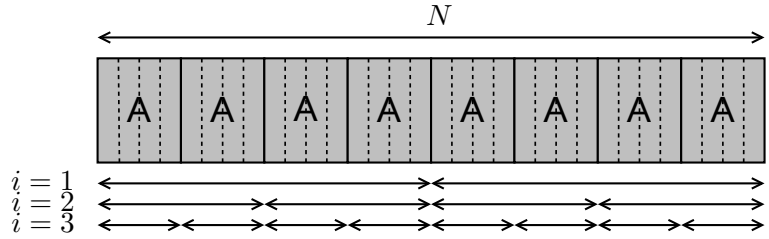

Figure 4.2: Time domain representation of an OFDM preamble with a repetitive structure **A**. The cyclic prefix is omitted. The multi-level structure allows multi-stage processing.

4.2.5 Improvements and coarse synchronization

Several variants of the repetitive slots-based methods [188, 190, 199, 238] may be found in the literature. The work in [186] improves the structure of repetitive training by maximizing sign inversions within the slots. The latter ensures the robustness of the timing synchronization against frequency offsets, as the CFO estimate is often obtained as the argument of the timing criterion at the correct timing instant [238, 272]. Some further refinements for coarse timing delay and CFO acquisition are proposed in [139].

There exist a lot of references on coarse carrier offset acquisition, i.e., estimation of the integer part of the CFO [159, 189, 238, 304, 308]. Estimation usually takes places in the frequency domain, after the fractional part has been estimated and compensated for. In IEEE 802.11 WLANs systems [130, 159], the last two short OFDM symbols are intended for coarse CFO estimation. Two algorithms for estimating the integer part of the CFO are proposed in [189], both based on the ML principle and on the observation of two consecutive OFDM symbols. Note that fully blind estimation of the integer part of the

CFO can not be achieved without some side information such as, e.g., differential encoding [304] or additional correlation between the data symbols or blocks [189]. Otherwise, the integer CFO shifts the carriers cyclically, without any means to identify their original position.

4.3 Nonlinear least squares CFO estimation

In this section, we establish the link between nonlinear least squares (NLS)-based and correlation-based CFO estimation. For this purpose, we follow the derivation and unified framework proposed by Ghogho and Swami [100, 101]. The approximate NLS approach [100] is reviewed as well.

4.3.1 NLS algorithm

Let us consider a single OFDM block, for simplicity. Let us then assume it is made of identical sub-blocks of length $Q = N/J$ each in time domain, i.e., $\tilde{x}_{q+lQ} = \tilde{x}_q$, $q = 0, \ldots, Q-1$ and $l = 0, \ldots, J-1$. Nonlinear least squares estimation of the carrier frequency offset was proposed in [159] in the context of OFDM-based WLANs. Further improvement of the NLS estimator at low SNR regime may be achieved [175]. Assuming a repetitive preamble structure in time domain, the NLS estimate of the CFO ν is obtained as [100]:

$$\hat{\nu}_{\text{NLS}} = \arg\max_{\tilde{\nu}} \sum_{q=0}^{Q-1} \frac{1}{J} \left| \sum_{l=0}^{J-1} e^{-j\frac{2\pi l\tilde{\nu}}{J}} y_{\nu,q+lQ} \right|^2, \tag{4.18}$$

where $y_{\nu,q+lQ}$ are the received signal samples in time domain after CP removal.

4.3.2 Relationship between correlation-based techniques and NLS estimators

It is shown in [100, 101] that the NLS estimator may also be expressed as

$$\hat{\nu}_{\text{NLS}} = \arg\max_{\tilde{\nu}} \sum_{l=1}^{J-1} \text{Re}\left\{ r(lQ) e^{-j\frac{2\pi l\tilde{\nu}}{J}} \right\}, \tag{4.19}$$

where $r(\tau)$ is the correlation at lag τ defined by

$$r(\tau) = \sum_{n=0}^{N-1-\tau} y^*_{\nu,n} y_{\nu,n+\tau}, \quad \tau \in \mathbb{N}. \tag{4.20}$$

Clearly, (4.18) and (4.19) establish relationship between NLS and correlation-based estimators in the case of repetitive preambles. Indeed, the term $r(lQ)$ in (4.19) is the correlation at lag $\tau = lQ$ between the received samples corrupted by CFO and Q is precisely the repetitive slot period. For $J = 2$, the estimator in (4.19) may be expressed in a closed-form as

$$\hat{\nu}_{\text{NLS}} = \frac{1}{\pi} \arg\left\{ r\left(\frac{N}{2}\right) \right\}, \tag{4.21}$$

which is equivalent to the SCA [238]. No closed-form solution is available for solving (4.19) when $J > 2$ [100, 101].

4.3.3 Low complexity approaches

Let us define $\mathbf{z} = [z_0, \ldots, z_{Q-1}]^T$ with $z_q = \exp(j2\pi\nu(q+L_{\mathrm{CP}})/N)\tilde{\mathbf{H}}_{\{q,:\}}\tilde{\mathbf{x}}$, $q = 0, \ldots, Q-1$. The expected value of $r(lQ)$ conditioned on $\mathbf{z}$ in (4.20) is then given by [100, 101]

$$\mathrm{E}\left[r(lQ)|\mathbf{z}\right] = (J-l)\|\mathbf{z}\|^2 e^{j\frac{2\pi l\nu}{J}}, \quad l = 1, \ldots, J-1, \tag{4.22}$$

where $\|\mathbf{z}\| = \sqrt{\mathbf{z}^H\mathbf{z}}$. Therefore, information on the frequency offset is present at every correlation lag, except for $l = 0$. This implies that the SCA estimator in (4.21) may still be used for $J > 2$, though it is sub-optimal in this case.

Lower estimation variance may be achieved by efficiently combining the phases of correlation values at different lags lQ, $l = 1, \ldots, J-1$. The previously described BLUE estimator [190] provides one way of combining. The BLUE approach is followed in [308] as well, with similar results. Multiple correlation values are also exploited in [307, 308]. A more specific repetitive structure in the time domain is generated in [309] by nulling odd-numbered subcarriers in the frequency domain. By doing so, the estimation range is increased up to a half of the total bandwidth, i.e., $[-N/4, N/4[$. The drawback is that only pairs of samples are correlated together in time domain, which may lead to high variance of the estimates. Finally, the multi-stage estimator [248] exploits the correlation lags in a sequential way.

Ghogho and Swami derive an approximate NLS estimator (ANLS) [100]. Let ϕ_l denote the unwrapped phase of the correlation estimate $r(lQ)$. Under the small error assumption, the approximation $\sin(\phi_l - 2\pi l\nu/J) \approx (\phi_l - 2\pi l\nu/J)$ holds and the NLS estimator in (4.19) may be approximated in a closed-form by [100]:

$$\hat{\nu}_{\mathrm{ANLS}} = \frac{J}{2\pi}\frac{\sum_{l=1}^{J-1} l|r(lQ)|\phi_l}{\sum_{l=1}^{J-1} l^2|r(lQ)|}. \tag{4.23}$$

Unlike the BLUE estimator in [190] or the estimator in [248], the above approach does require phase unwrapping. However, phase unwrapping is not a serious problem in (4.23), as only a few correlation values largely spaced apart are needed.

4.4 CFO estimation based on null-subcarriers

In this section, we first review the class of NSC-based CFO estimators originally introduced by Tureli et al. [167,266–268] and further developed in [28,45,100,102,174]. Computationally efficient implementations are also presented. Then, the link between subspace-based, ML and repetitive slots-based estimation is established. Finally, the identifiability conditions for NSC-based estimators are stated.

4.4.1 Algorithms

Let us consider the OFDM signal model with null-subcarriers obtained by combining (2.27) and (2.31):

$$\mathbf{y}_\nu(k) \;=\; \beta_k e^{j2\pi\nu(kP+L_{\mathrm{CP}})/N}\mathbf{C}(\nu)\mathbf{F}_{\{:,\mathcal{N}_{\mathrm{A}}\}}\mathbf{D}_{\tilde{\mathbf{h}},\{\mathcal{N}_{\mathrm{A}},\mathcal{N}_{\mathrm{A}}\}}(k)\mathbf{a}(k) + \mathbf{w}(k), \tag{4.24}$$

where $\mathbf{D}_{\tilde{\mathbf{h}},\{\mathcal{N}_{\mathrm{A}},\mathcal{N}_{\mathrm{A}}\}}(k) = \mathrm{diag}\{\tilde{\mathbf{h}}^T(k)\mathbf{V}_{\mathrm{NSC}}(k)\}$ is a $N_a \times N_a$ diagonal matrix containing the CFR values in $\tilde{\mathbf{h}}(k)$ at active subcarriers only. The $N \times N_a$ matrix $\mathbf{F}_{\{:,\mathcal{N}_{\mathrm{A}}\}}$ denotes the IDFT matrix truncated to the columns modulating the set of active subcarriers.

In the noiseless and CFO-free case, there is no received energy after demodulation at null-subcarrier locations. This translates mathematically into

$$\begin{aligned} \mathbf{f}_n^H \mathbf{y}_0(k) &= \beta_k \mathbf{f}_n^H \mathbf{F}_{\{:,\mathcal{N}_\mathrm{A}\}} \mathbf{D}_{\tilde{\mathbf{h}},\{\mathcal{N}_\mathrm{A},\mathcal{N}_\mathrm{A}\}}(k) \mathbf{a}(k) && (4.25) \\ &= 0, \quad \forall\, n \notin \mathcal{N}_\mathrm{A}, && (4.26) \end{aligned}$$

where $\mathbf{f}_n$ denotes the n^{th} column vector of the IDFT matrix $\mathbf{F}$.

The following cost function was originally proposed by Liu and Tureli in [167], given a finite number of K vector observations:

$$\begin{aligned} p(z) &= \sum_{n \notin \mathcal{N}_\mathrm{A}} \sum_{k=1}^{K} \left| \mathbf{f}_n^H \mathbf{Z}^{-1} \mathbf{y}_\nu(k) \right|^2 && (4.27) \\ &= \sum_{n \notin \mathcal{N}_\mathrm{A}} K\, \mathbf{f}_n^H \mathbf{Z}^{-1} \hat{\mathbf{R}}_{\mathbf{y}_\nu \mathbf{y}_\nu} \mathbf{Z} \mathbf{f}_n, && (4.28) \end{aligned}$$

with $\mathbf{Z} = \mathrm{diag}\{1, z, z^2, \ldots, z^{N-1}\}$ and $\hat{\mathbf{R}}_{\mathbf{y}_\nu \mathbf{y}_\nu} = (1/K) \sum_{k=0}^{K-1} \mathbf{y}_\nu(k) \mathbf{y}_\nu^H(k)$. In the noise-free case, $p(\exp(j2\pi\nu/N)) = 0$. Clearly, the cost function $p(z)$ evaluated at $z = \exp(j2\pi\tilde{\nu}/N)$ equals the total received energy at NSC locations, for a given frequency offset compensation value $\tilde{\nu}$. Consequently, the CFO is found as

$$\hat{\nu}_\mathrm{NSC} = \arg\min_{\tilde{\nu}} p\left(e^{j\frac{2\pi\tilde{\nu}}{N}} \right). \tag{4.29}$$

A first order perturbation analysis of the estimator in (4.29) is performed in [267]. Equivalently, the frequency offset estimate may be obtained by maximizing the received energy over the set of active subcarriers. Hence, one may find the carrier offset by finding the roots of $p(z)$ on the unit circle similarly to the root-MUSIC algorithm in array signal processing [27].

A multi-antenna generalization of the cost function in (4.28) is found in [266] for OFDM with receiver diversity. The proposed approach stems from the nonlinear least squares method. In the derivation, the covariance matrix $\hat{\mathbf{R}}_{\mathbf{y}_\nu \mathbf{y}_\nu} = (1/KN_r) \sum_{k=0}^{K-1} \sum_{r=1}^{N_r} |\gamma_r|^2 \mathbf{y}_{\nu,r}(k) \mathbf{y}_{\nu,r}^H(k)$ is now evaluated across the N_r received signal blocks $\mathbf{y}_{\nu,r}(k)$ at the receiver antenna array, and substituted in (4.28). If selected proportional to the branch SNR, the branch weighting coefficients $|\gamma_r|$ $(r = 1, \ldots, N_r)$ allow providing diversity gains. Diversity turns out to improve CFO identifiability in the case of deep channel fades, when zeros of the cost function get close to the DFT grid. Furthermore, the NLS-based criterion offers robustness against correlation among diversity branches.

4.4.2 Computationally efficient implementations

First, notice that for a large number of null-subcarriers $N_z > N_a$, from computational complexity point of view it is preferable to maximize the energy over the set of active carriers. A line search is required to find out the CFO in (4.29), which adds to the complexity if high precision is needed. However, a priori knowledge or coarse estimation may reduce the range of the line search. One may also choose adaptive estimation via least-mean squares (LMS) or gradient-based approaches [173].

Another option is to obtain the CFO via polynomial rooting, as $p(z)$ forms a polynomial of order $2(N-1)$ in z. Then, the CFO estimate is taken as the phase of the root which is the closest to the unit circle [167]. Another way to estimate the carrier offset is to exploit

a shift-invariant structure in the received signal that allows deriving an ESPRIT type of algorithm [268]. The benefit is that the CFO is obtained in a closed-form, and improved resolution is achieved over the MUSIC-like search in [167]. Moreover, the method possesses good small sample performance, e.g., $K = 10$ received blocks are enough in practice.

By considering truncated Taylor series of order Q_o for $\mathbf{Z}^{-1}$ in (4.27) ($Q_o \geq |\tilde{\nu}|(N-1)/2$), the complexity involved in solving (4.29) may be further brought down without sacrificing much the performance [21]. In this case, CFO estimation requires rooting a polynomial of degree Q_o, which is typically much smaller than the degree of the original polynomial $2(N-1)$. However, the truncated Taylor series approximation holds for small carrier offsets only ($|\nu| \ll 1$).

4.4.3 Link between subspace and ML estimation

Ghogho *et al.* [102] proved the equivalence between Tureli's estimator [167, 268] and the deterministic maximum likelihood approach. The derivation is briefly presented here. Let us assume that both the channel frequency response and the data symbols in equation (4.24) are deterministic unknown quantities. Let us denote by

$$\boldsymbol{\alpha}(k) = e^{j2\pi\nu(kP+L_{\mathrm{CP}})/N}\mathbf{D}_{\tilde{\mathbf{h}},\{\mathcal{N}_{\mathrm{A}},\mathcal{N}_{\mathrm{A}}\}}(k)\mathbf{a}(k) \tag{4.30}$$

the k^{th} block affected by channel fading and the CFO-induced rotation. Assuming complex circular white Gaussian noise, the maximum likelihood estimates of ν and $\boldsymbol{\alpha} = [\boldsymbol{\alpha}^T(0), \ldots, \boldsymbol{\alpha}^T(K-1)]^T$ based on (4.24) are found as

$$(\hat{\nu}, \hat{\boldsymbol{\alpha}}) = \arg\min_{\tilde{\nu},\boldsymbol{\alpha}} \sum_{k=0}^{K-1} \left\|\mathbf{y}_\nu(k) - \beta_k \mathbf{C}(\tilde{\nu})\mathbf{F}_{\{:,\mathcal{N}_{\mathrm{A}}\}}\boldsymbol{\alpha}(k)\right\|^2. \tag{4.31}$$

The ML estimate of $\boldsymbol{\alpha}(k)$, for known $\tilde{\nu}$, is given by

$$\hat{\boldsymbol{\alpha}}(k) = \frac{1}{\beta_k}\left[\mathbf{F}_{\{:,\mathcal{N}_{\mathrm{A}}\}}\right]^H \mathbf{C}^*(\tilde{\nu})\mathbf{y}_\nu(k). \tag{4.32}$$

Substituting (4.32) into (4.31) and simplifying, the ML estimate of the CFO is obtained as

$$\hat{\nu} \;=\; \arg\min_{\tilde{\nu}} \sum_{k=0}^{K-1} \left\|\boldsymbol{\Pi}_{\mathrm{NSC}}\mathbf{C}^*(\tilde{\nu})\mathbf{y}_\nu(k)\right\|^2, \quad \boldsymbol{\Pi}_{\mathrm{NSC}} = \mathbf{F}_{\{:,\mathcal{N}_{\mathrm{NSC}}\}}\left[\mathbf{F}_{\{:,\mathcal{N}_{\mathrm{NSC}}\}}\right]^H. \tag{4.33}$$

Notice that $\boldsymbol{\Pi}_{\mathrm{NSC}}$ above is the projection matrix to the subspace orthogonal to the signal subspace, which yields the space of null-subcarriers. Thus, the CFO is estimated in (4.33) as the value of $\tilde{\nu}$ minimizing the projection of the compensated vector $\mathbf{C}^*(\tilde{\nu})\mathbf{y}_\nu(k)$ to the subspace of NSCs. Equivalently, one may maximize the projection in the signal space using the projection matrix $\boldsymbol{\Pi}_{\mathrm{A}} = \mathbf{I}_N - \boldsymbol{\Pi}_{\mathrm{NSC}} = \mathbf{F}_{\{:,\mathcal{N}_{\mathrm{A}}\}}[\mathbf{F}_{\{:,\mathcal{N}_{\mathrm{A}}\}}]^H$ instead, where $\mathcal{N}_{\mathrm{A}}$ is the set of active subcarrier indices. Hence, the link with subspace-based estimation is clear, as well as the geometrical projection argument [45, 93, 296]. Note that [93] belongs as well to the class of NSC-based deterministic ML estimators.

Let us now establish the correspondence with the estimator in [167] by rewriting (4.33)

as

$$\hat{\nu} = \arg\min_{\tilde{\nu}} \sum_{k=0}^{K-1} \left| \mathbf{y}_{\nu}^{H}(k)\mathbf{C}(\tilde{\nu})\mathbf{F}_{\{:,\mathcal{N}_{\mathrm{NSC}}\}} \left[\mathbf{F}_{\{:,\mathcal{N}_{\mathrm{NSC}}\}}\right]^{H} \mathbf{C}^{*}(\tilde{\nu})\mathbf{y}_{\nu}(k) \right|^{2} \tag{4.34}$$

$$= \arg\min_{\tilde{\nu}} \sum_{n\notin\mathcal{N}_{\mathrm{A}}} \sum_{k=0}^{K-1} \left| \mathbf{f}_{n}^{H}\mathbf{C}^{*}(\tilde{\nu})\mathbf{y}_{\nu}(k) \right|^{2} \equiv \hat{\nu}_{\mathrm{NSC}}. \tag{4.35}$$

Thus, deterministic ML estimation is equivalent to Tureli's NSC-based algorithm, and the estimators developed in [167, 174] are thus ML as well.

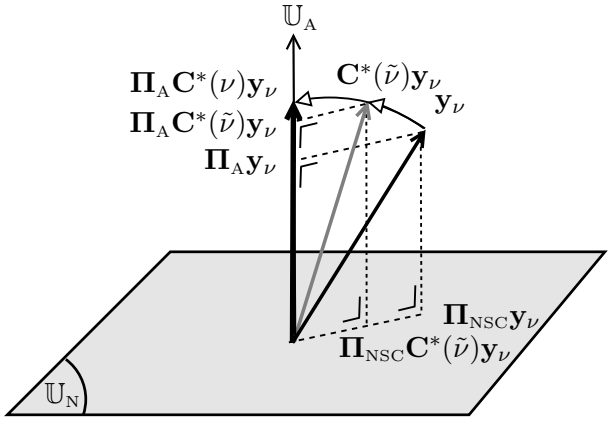

Figure 4.3: Geometrical description for NSC-based CFO estimators (noise-free case). Projection to signal space $\mathbb{U}_{\mathrm{A}} = \mathrm{span}\left(\mathbf{F}_{\{:,\mathcal{N}_{\mathrm{A}}\}}\left[\mathbf{F}_{\{:,\mathcal{N}_{\mathrm{A}}\}}\right]^{H}\right)$ is maximized or, equivalently, projection to null-subcarrier space $\mathbb{U}_{\mathrm{N}} = \mathrm{span}\left(\mathbf{F}_{\{:,\mathcal{N}_{\mathrm{NSC}}\}}\left[\mathbf{F}_{\{:,\mathcal{N}_{\mathrm{NSC}}\}}\right]^{H}\right)$ is minimized.

4.4.4 Relationship to repetitive slots-based estimators

Let us consider a single block ($K = 1$) for simplicity. Active subcarrier frequencies are assumed to lie at multiples of $J > 2$ and to be equi-spaced. Null-subcarriers are placed elsewhere. Such a placement leads to a repetitive structure with J identical sub-blocks in time domain. Therefore, repetitive slots-based estimators rely implicitly on NSCs [101]. Similarly two identical consecutive OFDM blocks [188] may be seen as two half blocks of a $2N$-point DFT [101]. No CP is needed in such case.

Now, it is instructive to rewrite the estimator in (4.33) in terms of the time domain correlation function as [102]:

$$\hat{\nu}_{\mathrm{NSC}} = \arg\max_{\tilde{\nu}} \sum_{\tau=1}^{N-1} \mathrm{Re}\left\{ \sum_{k=0}^{K-1} \left[r_{k}(\tau)\psi_{\mathcal{N}_{\mathrm{A}}}^{*}(\tau)\right] e^{-j\frac{2\pi\tau\tilde{\nu}}{N}} \right\}, \tag{4.36}$$

with

$$\psi_{\mathcal{N}_\mathrm{A}}(\tau) = \frac{1}{N}\sum_{n\in\mathcal{N}_\mathrm{A}} e^{j\frac{2\pi n\tau}{N}} \tag{4.37}$$

$$r_k(\tau) = \sum_{n=0}^{N-1-\tau} y^*_{\nu,n}(k)y_{\nu,n+\tau}(k), \tag{4.38}$$

where $y_{\nu,n}(k)$ is defined as the n^{th} element of $\mathbf{y}_\nu(k)$. According to the analysis in [100–102], the two following cases may be distinguished:

1. ***Equi-spaced active subcarriers and no virtual subcarrier:*** In this case, $\psi_{\mathcal{N}_\mathrm{A}}(\tau)$ is non-zero at multiples of $Q = N/J$ only. Then, the NSC estimator in (4.36) reduces to the repetitive slots-based method in (4.19). Consequently the latter is ML as well.

2. ***Equi-spaced active subcarriers together with virtual subcarriers***: If VSCs are present at the edges of the OFDM block, the function $\psi_{\mathcal{N}_\mathrm{A}}(\tau)$ is generally non-zero at any correlation lag. Thus, most of the correlation lags contribute to the ML estimator in (4.36). Hence, the latter differs from the REP estimator in (4.19) which employs correlation lags multiples of Q only (the $J-1$ correlation peaks in fact). In general, most of the proposals based on repetitive slots do not use all the correlation lags. Hence, REP estimators are not ML but are still consistent [100, 296].

The equivalences established so far between the different classes of CFO estimators are also depicted in Figure 4.1 at the beginning of this chapter. The link between NLS [100,159] and REP [190,238] estimators was stated in Section 4.3.2. SS techniques [45], deterministic ML estimation [45, 102] and NSC-based estimators [167, 266–268] were bridged together in Section 4.4.3. Finally, the link to REP estimators was explained above.

4.4.5 Identifiability conditions

The two following issues may contribute to the loss of identifiability of the CFO for NSC-based methods: *i) the number and the placement of null-subcarriers, ii) the location of channel zeros in the frequency domain.*

In this section, the identifiability conditions of the CFO are briefly stated, based on the work by Ghogho *et al.* [98, 102]. Necessary and sufficient conditions for identifiability are given in the case of a single OFDM symbol ($K = 1$). Rules remain unchanged for arbitrary K as long as the locations of NSCs stay the same across the symbols. Theorem 2 [102] states a joint placement rule for NSCs and VSCs providing a full acquisition range. Finally, null-subcarrier hopping schemes are investigated, as well as optimal design rules for the MIMO case.

Necessary conditions

With $\boldsymbol{\alpha} = \exp(j2\pi\nu(kP + L_\mathrm{CP})/N)\mathbf{D}_{\tilde{\mathbf{h}},\{\mathcal{N}_\mathrm{A},\mathcal{N}_\mathrm{A}\}}\mathbf{a}$ from (4.30), a necessary condition for identifiability is that $\boldsymbol{\alpha} \neq \mathbf{0}_{N_a\times 1}$, or equivalently, $\boldsymbol{\alpha}^H\boldsymbol{\alpha} \neq 0$, i.e., the useful signal energy is non-zero. Otherwise, the received signal in (4.24) does not contain any information on the CFO. Given that any FIR channel of order L'_h (i.e., with $L_h + 1$ non-zero taps in the time domain) may possess at most L'_h nulls in the frequency domain, it may null L'_h subcarriers frequencies in the worst case. Hence, one way to fulfill the condition $\boldsymbol{\alpha} \neq \mathbf{0}_{N_a\times 1}$

is to require at least $N_a = L'_h + 1$ active subcarriers, i.e., $N_a > L'_h$. The latter condition guarantees that a CFO estimate maximizes the criterion in (4.33) but does not guarantee its uniqueness.

Sufficient conditions

Let $P_{\mathcal{N}_\mathrm{A}}(m)$ be defined as in [102] and denote the number of active subcarriers that do not have an active neighbor at distance m (cyclically), $m \in \mathbb{N}$. Thus, $P_{\mathcal{N}_\mathrm{A}}$ depends on both the number of NSCs and their placement. Then, Theorem 1 introduced in [102] states sufficient conditions for identifiability.

Theorem 1 (cf. [102]) *The CFO in equation (4.24) is uniquely identifiable in* $[-R/2, R/2[$, $R \in \mathbb{N}$, *for any FIR channel of order* L'_h *if and only if the two following conditions are fulfilled:*

1. $N_a > L'_h$,
2. $P_{\mathcal{N}_A}(m) > L'_h$, $m = 1, \ldots, \lfloor R/2 \rfloor$.

In words, Theorem 1 says that at least L'_h+1 active subcarriers must have nearest neighbors no closer than $\lfloor R/2 \rfloor$ in order to ensure identifiability in $[-R/2, R/2[$ [101]. Note that from the theorem, it suffices to have $N_a > L'_h$ active subcarriers in order to ensure uniqueness in the range $[-1/2, 1/2[$ $(R = 1)$.

As a consequence of Theorem 1 and based upon the argumentation in [102], equi-spaced NSCs provide the most robust placement to the presence of channel zeros. Consequently, a longer delay spread ($L'_h < N_z$) may be tolerated for a fixed number of NSCs. On the other hand, consecutive NSCs only [167] (e.g., VSCs imposed by system design) yield the most sensitive scenario: identifiability is guaranteed for the AWGN channel only, but a full acquisition range of $[-N/2, N/2[$ is provided in this case. Distinct spacing of null-subcarriers was investigated in [174]. It guarantees ambiguity-free full range CFO estimation. However, the requirement $N_z > L'_h+1$ makes this scheme slightly less robust to channel zeros compared to equi-spaced NSC schemes. Another restriction is the maximum number $\sqrt{2N}$ of NSCs with distinct spacing.

Null-subcarrier hopping

It is shown in [28, 174] that the location of channel zeros does not affect identifiability of the CFO if the placement of consecutive NSCs is changed from one OFDM block to another. In this case, one refers to null-subcarrier hopping. Hopping guarantees a unique minimum in $[-N/2, N/2[$ for the criterion in (4.33) and hence identifiability. Intuitively, NSC-hopping randomizes the channel over frequency just as frequency hopping in spread spectrum systems. As a result, the identifiability of the CFO is restored [28].

Optimal placement of NSCs and VSCs - SISO case

An optimum design in the sense of mimimum conditional Cramér-Rao bound (CCRB) requires the active subcarriers to be equi-spaced when $N_a \leq N/2$ or the null-subcarriers to be equi-spaced when $N_a > N/2$ [98, 102]. Furthermore, the CCRB improves with an increasing number of NSCs. The CCRB is established assuming that both the channel and data parameters are deterministic quantities. Hence, the obtained bound is specific to a given set of data and channel conditions. Then, Theorem 2 [102] shows that a proper combining of consecutive NSCs (i.e, VSCs) and equi-spaced NSCs leads to a full range

estimator, which guarantees identifiability of the CFO regardless of the channel zeros. The null-subcarrier placement described is Theorem 2 is represented schematically in Figure 4.4 [102].

Theorem 2 (cf. [102]) *Let assume a total number N_z of NSCs. If the number of consecutive NSCs (i.e., VSCs), $N_v > L'_h$, the number of equi-spaced NSCs, $N_n = N_z - N_v > L'_h$, and the spacing between the equi-spaced NSCs is $M > L'_h$, then the CFO in equation (4.24) is uniquely identifiable in the entire acquisition range $[-N/2, N/2[$ regardless of channel zeros.*

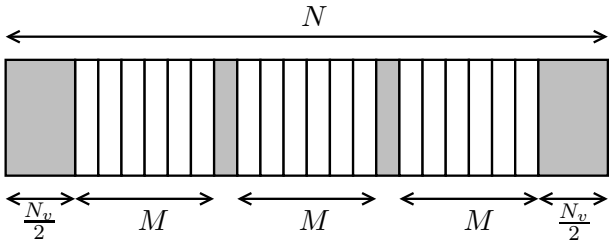

Figure 4.4: Null-subcarrier placement in frequency domain leading to full estimation range $[-N/2, N/2[$ according to Theorem 2 [98, 102]. Gray regions represent null-subcarriers.

To conclude, CFO identifiability is a tradeoff between the estimation range and the number and placement of active (respectively null-) subcarriers. Table 4.1 summarizes the different NSC/VSC placement approaches discussed so far and states their maximum allowed estimation ranges.

NSC/VSC placement scheme	**Minimum required number of NSC/VSCs**	**Estimation range**
N_v consecutive NSCs (VSCs only)	$L'_h < 1$ (AWGN channel)	$\left[-\frac{N}{2}, \frac{N}{2}\right[$
N_z equi-spaced NSCs	$L'_h < N_z < N - L'_h$	$\left[-\frac{N}{2N_z}, \frac{N}{2N_z}\right[$
N_a equi-spaced active subcarriers	$L'_h < N_a$	$\left[-\frac{N}{2N_a}, \frac{N}{2N_a}\right[$
N_z NSCs with distinct spacing	$L'_h+1 < N_z < N-L'_h,\ N_z < \sqrt{2N}$	$\left[-\frac{N}{2}, \frac{N}{2}\right[$
$N_n = N_z - N_v$ equi-spaced NSCs with spacing M and N_v VSCs	$L'_h < N_n,\ L'_h < M,\ L'_h < N_v$	$\left[-\frac{N}{2}, \frac{N}{2}\right[$
Consecutive NSC hopping scheme	$L'_h < N_a$	$\left[-\frac{N}{2}, \frac{N}{2}\right[$

Table 4.1: Identifiability conditions and estimation range as a function of the placement of NSC/VSCs according to [102, 173]. In the table, L'_h refers to the channel order and N it the total number of subcarriers. N_a, N_v, N_z are the number of active, virtual and null-subcarriers, respectively. N_n denotes the number of NSCs that are not VSCs.

Placement of NSCs, VSCs and pilots symbols - MIMO case

Ma *et al.* investigate optimal training symbol designs for channel and CFO estimation in MIMO OFDM [173]. They propose the following rules:

1. Insert N_t training symbols in the information blocks corresponding to the N_t transmit antennas.

2. Insert one zero subcarrier per block, whose position hops from block to block with hop-step $N/(L'_h+1)$. Null-subcarrier hopping ensures CFO identifiability regardless of channel nulls [28, 174]. Then, insert additional null-subcarriers in each block. Perform the standard OFDM operations of IFFT and CP insertion per transmit antenna.

3. At the receiver, remove first the CP from the received blocks. Then, estimate the carrier offset via the standard NSC based method [167,174], taking into account the NSC hopping pattern.

4. Compensate for the CFO in time domain, perform DFT and remove NSCs.

5. Collect L'_h+1 blocks and estimate the channel from the training data.

6. Perform phase estimation using the training data in order to find out the residual CFO. Remove the latter prior to symbol detection.

Uniqueness of the CFO estimate is guaranteed in $[-N/2, N/2[$, i.e., the estimator is full range. The interesting point is that channel and CFO estimation almost decouple. Decoupling may not be perfect at stage 4 because of the residual CFO. However, the latter is estimated and canceled out at stage 6 by exploiting the non-zero pilot data. This improves significantly the performance of the MIMO OFDM transmission [173].

4.5 CFO estimation using second-order cyclostationarity

4.5.1 Algorithms based on second-order cyclostationary covariances

Bölcskei proposed a SOCS-based blind symbol timing and carrier offset estimator [35] in the line of the blind channel estimators [36, 37] reviewed in Section 3.1.1. Pulse-shaping, subcarrier weighting or periodic precoding (e.g., using a CP) introduce second-order cyclostationarity in the OFDM signal [35]. In this case, the synchronization parameters, i.e., timing error and CFO, may be extracted from the second-order statistics [35].

The estimator in [35] is asymptotically unbiased and consistent. Performance is comparable to [272], while being slightly better at low SNR and worse in the high SNR regime. The method in [205] is SOCS-based as well. Together with CP, subcarrier weighting [35, 176] yields more cross-correlation samples containing information on the synchronization parameters, thus reducing the estimation error. With CP only, timing and carrier offset information is present at cross-correlation lags $\pm N$ only. However, SOCS-based estimators [35, 68] are typically characterized by slow acquisition times ranging from a few tens to a hundred of OFDM blocks.

4.5.2 Exploiting cyclostationary pseudo-covariances

A non-circular complex-valued signal is characterized statistically different real and imaginary parts. This property may be exploited for synchronization purposes [60, 62, 63, 259]. Non-circularity is usually introduced for instance by using real-valued modulations. It is also experienced in OFDM/OQAM [36, 61], or more generally in systems suffering from I/Q imbalance [270].

As already noted in Section 3.1.1, the cyclic prefix makes the received signal cyclostationary with cyclic frequencies $\{p/P,\ 0 \leq p \leq P-1\}$, where P is the total OFDM block length. Consequently, with non-circular signals, cyclo-stationarity is observed in the

pseudo-correlation coefficients $r_c(n,\tau) = \mathrm{E}\left[y_{\nu,\mathrm{CP},n+\tau}\, y_{\nu,\mathrm{CP},n}\right]$. We denote the n^{th} received sample in time domain before CP removal by $y_{\nu,\mathrm{CP},n}$, taken serially and thus not limited by the block boundaries. Note that the pseudo-correlation function is identically zero for circular signals. Now, the CFO tends to induce circularity to the transmission, acting like a rotating phase term changing from sample to sample. Intuitively, the estimator in [63] aims at restoring the initial non-circularity.

Let $\mathcal{A}_0$ be a compact set included in $[0, \min(1/2, 1/P)[$. Assuming real-valued modulations, the estimator in [63] is expressed as

$$\hat{\nu} = \arg\max_{\alpha\in\mathcal{A}_0} \mathcal{J}_{N_s}(\alpha), \quad \mathcal{J}_{N_s}(\alpha) = \sum_{p=0}^{P-1} \left\| \hat{\mathbf{r}}_{c,N_s}^{(\alpha+p/P)} \right\|_{\mathbf{W}_p}^2, \tag{4.39}$$

where $\|\mathbf{x}\|_{\mathbf{W}_p}^2 = \mathbf{x}^H \mathbf{W}_p \mathbf{x}$, given the positive Hermitian weighting matrix $\mathbf{W}_p$, $p = 0, \ldots, P-1$, and

$$\hat{\mathbf{r}}_{c,N_s}^{(\alpha)} = \left[\hat{r}_{c,N_s}^{(\alpha)}(-T), \ldots, \hat{r}_{c,N_s}^{(\alpha)}(T)\right]^T \tag{4.40}$$

$$\hat{r}_{c,N_s}^{(\alpha)}(\tau) = \frac{1}{N_s} \sum_{n=0}^{N_s-1} y_{\nu,\mathrm{CP},n+\tau} y_{\nu,\mathrm{CP},n} e^{-j\frac{4\pi\alpha n}{N}}. \tag{4.41}$$

A total number of N_s observations is assumed (i.e., $K = N_s/P$ blocks) for the computation of the sample pseudo-correlation in (4.41), as well as $2T+1$ lags. The estimator in (4.39) is less sensitive to circular noise than algorithms based on cyclostationary covariances. It also requires smaller sample support to achieve similar performance. A few tens of blocks are sufficient in practice [63]. However, the estimation range $[0, \min(1/2, 1/P)[$ is small, especially for large block lengths P. For this reason, this estimator is more suited for refinement than for acquisition purposes. Computational complexity may also be an issue as high resolution is needed to detect the pseudo-correlation peaks if an initial estimate is not available.

4.6 Other approaches for blind carrier offset estimation

In this section, we briefly review miscellaneous alternatives for carrier synchronization proposed in the literature.

Joint modeling of CFO and PHN is proposed in [197]. Then, estimators based on fourth-order statistics may be found in [170, 182, 293]. A fourth-order nonlinearity may be used to cancel out the effect of QPSK modulation prior to CFO estimation [170, 182]. The sample kurtosis may be exploited for carrier frequency synchronization in SISO, MIMO and multi-user OFDM systems [293]. The kurtosis is a measure of signal non-gaussianity. The estimator in [293] relies on the idea that the received signal is closer to Gaussian when corrupted by CFO than in the CFO-free case. Small sample support (about 10 blocks) is needed, but the estimation range is limited to $[-1/2, 1/2[$.

Blind estimation of the carrier offset via oversampling was proposed in [46, 62]. The method in [62] exploits the intrinsic phase shift of neighboring sample points induced by CFO. NSCs are not necessarily needed because the low rank model is guaranteed by the oversampling itself. The approach belongs to the class of deterministic subspace-based ML estimators [45, 102]. However, noise correlation in the oversampled signal is neglected by [62] and may degrade the performance in practice.

Estimation via the finite alphabet property was investigated for PSK [95] and QAM [96]

constellations as well as differentially coded OFDM transmission [169]. Finally, highly reliable CFO estimation may be achieved by exploiting the constant modulus property. See Publications VI and VII, as well as [97]. The related work is reviewed in detail in Chapter 6.

4.7 Pilot-based CFO estimation

NSC and repetitive slots-based algorithms presented so far make an implicit use of pilot symbols. Indeed, they obtain the CFO as the phase shift between identical structures in time domain [188, 190, 238], or as the value minimizing the projection to the space of null-subcarriers [45, 102, 167], respectively. While assuming pilot structures either in time or frequency domain, those estimators do not explicitly use pilot symbols as it is usually the case in channel estimation, for instance (see Chapter 3). There are mainly two reasons for this. First, the unknown wireless transmission channel impairs the received data in time domain. In addition, CFO leads to nonlinear distortion. It translates into ICI in frequency domain, where pilots symbols are affected by unknown and data dependent interference from adjacent subcarriers. The separation between pilot and information-bearing symbols is challenging because of the CFO [173]. Channel and CFO estimation have to be performed jointly in this case, at the price of a higher computational complexity. Another option is to design training in such a way that estimation tasks decouple [173]. Also, since carrier frequency synchronization is among the first tasks performed at the receiver prior to channel estimation, channel independent estimators are highly desirable.

A few estimators in the literature employ pilot data explicitly [67, 88, 156, 171, 173, 189, 264, 296]. The approach in [156] combines distinctively spaced pilot tones and VSCs and NSCs within a preamble: the whole OFDM block is devoted to either null or pilot symbols in this case. The CFO estimate is obtained via deterministic ML estimation similarly to [45, 102]. Consistency is guaranteed in $[-N/2, N/2[$ provided that at least two pilot tones are not occupied by channel nulls. A parallel is made between the CFO estimator and the periodogram of the preamble, as also noted in [102]. An iterative MIMO OFDM receiver exploiting both pilots and NSCs is proposed in [257]. It provides ML estimates of both channel coefficients and carrier offset using the EM algorithm. Pilot symbols (e.g., dedicated synchronization blocks) may be used for coarse CFO estimation purposes [171]. The tracking mode/loop may be engaged once an initial estimate is available. During CFO tracking, the residual error on the CFO is assumed to be small. Algorithms with a smaller estimation range but lower variance may be used to refine the estimate.

Differentially encoded pilots are interleaved with data symbols in [264] without the need for NSCs. The proposed weighted least squares (WLS) algorithm derives its estimates based on phase differences between two consecutive pilot symbols. Optimal weights are channel dependent. With approximate and hence sub-optimal weights, WLS offers still gain over the conventional LS [264] provided that the fractional CFO is small. However, phase variations of the CFR between adjacent subcarriers are neglected in [264], which would certainly be an issue in highly frequency selective channels.

Ma *et al.* propose the pilot design described in Section 4.4.5 for CFO and MIMO channel estimation [173]. Pilots and null subcarriers are placed such that the CFO and channel estimation tasks decouple. Since pilot symbols are affected by ICI, the CFO needs to be acquired first and the channel may be estimated after that. CFO acquisition is based on NSCs solely. The non-zero pilot data is exploited for refinement purposes only, in order to cancel out the residual CFO.

Decision-directed CFO estimation is another option [88, 152, 242]. Joint estimation of

CFO and sampling frequency offset (SFO) by exploiting hard symbol decisions is studied in [242], assuming coarse synchronization has been performed. The approach in [152] features a dual loop tracking structure in both time and frequency domains. Convergence is achieved relatively fast in about ten blocks, thanks to the dual loop structure. However, an acquisition stage is still needed. Loop parameters have to be properly set and ICI is neglected as the method accounts only for the CFO-induced phase rotation between adjacent subcarriers. Again, the variations of the channel phase are neglected.

Finally, CFO estimators stemming from extended Kalman filtering are considered in this thesis. The related literature as well as the algorithms proposed in Publications II-III are reviewed in depth next chapter. The use of particle filters for carrier frequency synchronization was also investigated [200].

4.8 Concluding remarks

In this chapter, we reviewed carrier frequency synchronization techniques specific to OFDM systems. Most of the concepts and analysis apply to multicarrier communications in general, e.g. MC-CDMA. Estimation of the carrier frequency offset is a crucial task in multicarrier transceivers. Hence, it must be accomplished with high fidelity, especially when high data rates are targeted and thus very narrow subcarrier spacings are used.

In general, CFO estimation in OFDM may be considered as a harmonic retrieval problem in multiplicative and additive noise [58, 59]. Therefore, one may essentially use any algorithm which can retrieve the spectral line corresponding to the CFO [101]. However, solving the HR problem only does not take advantage of the structure of the OFDM transmission model (finite symbol alphabet, NSCs, pilots symbols). A more efficient way is to establish a relation to direction of arrival (DOA) estimation [239] and subspace techniques in general. Hence, the MUSIC and ESPRIT type of subspace algorithms for carrier frequency synchronization purposes in multicarrier transmissions are of interest [34, 167, 174, 268].

Table 4.2 presents a summary and comparison of the various classes of CFO estimators presented in this chapter. Algorithms are compared considering *bandwidth efficiency*, *computational complexity*, *variance of the estimates* and *speed of convergence*. The following conclusions may be drawn based on the table. First, separation between pilot and information-bearing symbols is difficult due to nonlinear distortions created by CFO. This explains the small number of estimators relying solely on non-zero pilot data. Decision-directed [200, 225] (see also Publications II and III) or pilot-based estimation are more suited for tracking and refinement purposes than for acquisition. If the CFO is too large, the ICI may lead to incorrect symbol decisions or pilot symbol extraction. Hence, it is important to design channel and data independent estimators. Zero type of pilots (i.e., NSCs and/or VSCs) together with properly designed algorithms allow efficiently decoupling the carrier frequency synchronization from both channel estimation and data detection. Those tasks may then be performed as subsequent steps.

In OFDM systems, pilot blocks are usually transmitted prior to the information frame in sequence of identical slots in time domain (see, e.g., IEEE 802.11 standard [130]). Hence, repetitive-slots based estimators are considered. They do not exploit the pilot information explicitly but look instead for the CFO-induced phase shift between the repeated blocks. Repetitive-slots based estimators have low computational complexity. Equivalence to ML estimation holds only when virtual subcarriers are not present. Otherwise, correlation-based methods provide consistent estimates of the CFO regardless of multipath fading. The approximate ANLS [102] and BLUE [190] estimators have a closed-form solution which

is a major advantage. Moreover, they are computationally simpler, while not sacrificing the performance significantly.

The unified framework in [101] establishes links between most of the existing CFO estimation algorithms in the literature. Most of them rely explicitly or implicitly on the presence of null- and/or virtual subcarriers. NSC- and VSC-based estimators stem directly from maximum likelihood estimation. They are also equivalent to subspace methods which find the CFO by minimizing the projection to the subspace of null-subcarriers [45]. NSC-based techniques are in general appealing due to their low variance and fast convergence [102, 167, 174, 268]. Estimation using a single or a few received blocks may be achieved. This is obviously a significant advantage in the case of time-varying channels and carrier frequency offsets. The computational complexity involved by the line search may be reduced drastically by choosing polynomial rooting algorithms [21, 268].

Exploiting the finite alphabet property is another way to retrieve the CFO [95, 96]. Differential encoding allows improving the performance of FA-based estimators [169]. If constant modulus constellations are used, the estimation error may be further lowered. See Publications VI and VII, as well as [97]. Moreover, NSCs are not necessarily needed anymore in this case.

SOCS type of estimators usually suffer from low convergence speeds. Hence, their practical use is limited to time-invariant channels and continuous type of transmissions. However, bandwidth efficiency is high, as no NSC is needed. Cyclostationarity needs to be introduced in some way, but is generally present in most of the OFDM systems because of the CP. In the case of real-valued modulations schemes, pseudo-covariances may be used in place of covariances [63, 259]. Low variance is obtained for the estimates and much smaller sample support is required. High-order statistics may also be useful for carrier frequency synchronization [170, 182, 293]. Usually, the related algorithms are characterized by low convergence speeds and large variance. However, the sample Kurtosis function allows reliable estimation of small CFOs with relatively low sample size [293].

The estimation of a single shift in the carrier frequency was studied so far. A time-varying channel may cause a spread of frequency shifts known as the Doppler spread. In the presence of a severe Doppler spread, ICI cancellation strategies [18, 241, 312] have to be pursued for successful OFDM transmission.

Algorithms	**References**	**BW. efficiency**	**Compl.**	**Var.**	**Convergence speed**
Pilot-aided	[67, 88, 156] [171, 264] [296]	$*$	$*$	$**$	$***$ (1 block)
DD	[152, 242]	$**$	$**$	$**$	$**$ (5 to 10 blocks)
EKF	II, III, [225]	$**$	$**$	$**$	$**$ (5 to 10 blocks)
PF	[200]	$**$	$***$	$**$	$**$ (5 to 10 blocks)
Blind: SOCS (correlation)	[35]	$***$	$**$	$***$	$*$ ($>$ 100 blocks)
SOCS (pseudo-correlation)	[61, 63, 259]	$***$	$**$	$*$	$**$ (10 to 50 blocks)
REP	[188, 190] [238]	$*$	$*$	$**$	$**$ (1 block)
NLS	[100]	$*$	$**$	$**$	$***$ (1 block)
ANLS	[100]	$*$	$*$	$**$	$***$ (1 to 10 blocks)
BLUE	[190]	$*$	$*$	$**$	$***$ (1 to 10 blocks)
NSC, VSC	[167, 268]	$**$	$**$	$*$	$***$ (1 to 5 blocks)
HOS (in general)	[170, 182]	$***$	$***$	$***$	$*$ ($>$ 100 blocks)
HOS (Kurtosis)	[293]	$***$	$**$	$**$	$**$ (1 to 10 blocks)
ML (stochastic)	[53]	$***$	$***$	$**$	$***$ (1 to 5 blocks)
ML (deterministic)	[272]	$**$	$**$	$*$	$***$ (1 block)
SS	[45, 93]	$**$	$**$	$*$	$***$ (1 to 5 blocks)
CM	VI, VII, [97]	$***$	$**$	$*$	$***$ (1 block)
FA	[95, 96]	$***$	$**$	$***$	$*$ (10 to 100 blocks)
FA (differential encoding)	[169]	$***$	$**$	$**$	$**$ (2 blocks)

Table 4.2: Comparative chart of CFO estimators for OFDM ($*$: low, $**$: medium, $***$: high). BW. efficiency: bandwidth efficiency; Compl.: computational complexity; Var.: variance of the estimates.

Chapter 5

Joint channel estimation and frequency synchronization for MIMO OFDM

The theoretical benefits of high spectral efficiency, improved link quality and simple equalization may not be fully achieved in mobile MIMO OFDM transmissions because the wireless channels are both time and frequency selective. Furthermore, Doppler shifts caused by mobility in addition to oscillator inaccuracies give rise to carrier frequency offsets, which significantly degrade the system performance. Hence, channel estimation and CFO compensation are both essential in OFDM receivers. In high speed mobile scenarios, the task is not only to estimate the channel coefficients and CFO parameters reliably, but to track them over time as well. In this way, equalizer coefficients may be updated periodically and symbol error rates are kept at low levels. Complexity is also lower with sequential estimation.

In this chapter, joint channel and CFO estimation and tracking algorithms for SISO and MIMO OFDM systems are introduced. A time domain estimation and tracking stage stemming from extended Kalman filtering is a key component of the proposed technique. Kalman filtering algorithms [218, Ch.V.B] offer a good tradeoff between complexity and performance. They have been successfully used to solve various signal processing problems in wireless communications [7, 40, 50, 132, 151, 225, 226].

The proposed algorithms are derived under the following general assumptions:

i. A $N_t \times N_r$ MIMO OFDM system with multiple carrier frequency offsets as described in Section 2.2 is considered. One CFO parameter is assumed for each MIMO branch, similarly to [32].

ii. The individual MIMO channels are assumed to be time and frequency selective. Block fading model is assumed. MIMO branches are chosen uncorrelated in simulations. Nevertheless, tracking of correlated MIMO channels is feasible. However, in this case, the overall system performance decreases.

iii. The carrier frequency offsets may be time-varying.

iv. Perfect time synchronization is assumed.

v. The transmitted data is uncoded and QPSK-modulated, but the method extends to other modulation schemes.

vi. A few training blocks are sent at the beginning of the transmission in order to acquire initial estimates of the channel coefficients and CFO parameters.

vii. The additive noise is i.i.d. complex circular Gaussian with zero-mean and known variance.

A common state-space model is introduced, and is used in Publications I-III as well as in the derivations in [225,226]. It allows channel and CFO estimation and tracking in MIMO OFDM using the extended Kalman filter [57, Ch.8]. Channel estimation and tracking in MIMO OFDM may be performed via conventional Kalman filter as a special case.

5.1 State-space model for MIMO OFDM transmission with carrier frequency offsets

In this section, a state-space framework is established. It is employed in time domain estimation of channel coefficients and carrier frequency offsets in mobile SISO and MIMO OFDM systems.

5.1.1 State equation

Let us write the state-variable model. The state vector at time instance k is comprised of the MIMO channel coefficients $\mathbf{h}(k)$ from (2.4) and the vector of frequency offsets $\boldsymbol{\nu}(k)$ from (2.5):

$$\boldsymbol{\mathfrak{s}}(k) = \left[\begin{array}{cc} \mathbf{h}^T(k), & \boldsymbol{\nu}^T(k) \end{array} \right]^T. \tag{5.1}$$

There are $N_t N_r L_h$ channel taps and $N_t N_r$ frequency offset values in the state vector of dimension $N_t N_r (L_h + 1) \times 1$. Then, the linear state equation may be written as follows:

$$\boldsymbol{\mathfrak{s}}(k) = \mathbf{A}_{\boldsymbol{\mathfrak{s}}} \, \boldsymbol{\mathfrak{s}}(k-1) + \mathbf{v}(k). \tag{5.2}$$

The $N_t N_r (L_h + 1) \times 1$ state noise vector $\mathbf{v}$ is assumed to be zero-mean complex circular Gaussian. The state noise covariance matrix $\mathbf{Q}_{\mathbf{v}}$ has the following structure:

$$\mathbf{Q}_{\mathbf{v}} = \left[\begin{array}{cc} \mathbf{Q}_{\mathbf{h}} & \mathbf{0}_{N_t N_r L_h \times N_t N_r} \\ \mathbf{0}_{N_t N_r L_h \times N_t N_r} & \mathbf{Q}_{\boldsymbol{\nu}} \end{array} \right]_{N_t N_r (L_h+1) \times N_t N_r (L_h+1)}, \tag{5.3}$$

where $\mathbf{Q}_{\mathbf{h}} = \sigma_h^2 \mathbf{I}_{N_t N_r L_h}$ and σ_h^2 is the variance of the state noise associated with channel coefficients. $\mathbf{Q}_{\boldsymbol{\nu}} = \sigma_\nu^2 \mathbf{I}_{N_t N_r}$ and σ_ν^2 is the variance of the state noise associated with carrier frequency offsets.

The state transition matrix $\mathbf{A}_{\boldsymbol{\mathfrak{s}}}$ is of size $N_t N_r (L_h+1) \times N_t N_r (L_h+1)$. In this chapter $\mathbf{A}_{\boldsymbol{\mathfrak{s}}}$ is considered to be close to the identity matrix ($\mathbf{A}_{\boldsymbol{\mathfrak{s}}} = a \, \mathbf{I}_{N_t N_r (L_h+1)}$, $a = 0.99$). A necessary condition for stability of the state equation is that the spectral radius of $\mathbf{A}_{\boldsymbol{\mathfrak{s}}}$, i.e., its maximum eigenvalue, should be strictly less than 1. The state transition matrix describes the dynamics of the state vector, i.e., its time auto-correlation properties. Since the channel auto-correlation in time and the Doppler spectrum are related to each other by Fourier transform, the elements of $\mathbf{A}_{\boldsymbol{\mathfrak{s}}}$ are directly related to the Doppler frequency [117, 132]. Assuming Jakes' model [134], the parameter a above is directly given by $J_0(2\pi f_D T_s)$, where J_0 is the first-order Bessel function [117]. The Doppler frequency determines the order of the auto-regressive (AR) model as well. Low-order AR models are widely used in the literature [72, 73, 117, 132, 265]. The part of the state vector containing the channel coefficients may also be augmented to model an AR process of order p [151, 265]. The

AR model order is closely related to the number of peaks in the Doppler spectrum [253]. Intuitively, one would expect that the greater the AR model order, the more precise the model would be [151, Fig.1]. However, this may lead to over-fitting and result in degraded performance [117]. Information theoretic considerations suggest that a first-order Markovian model is a reasonable assumption for Rayleigh distributed channel coefficients under low to moderate channel spreads ($f_D T_s \in [0.001, 0.004[$) [277].

In the following, the state transition matrix as well as the statistics of state and measurement noise are assumed to be known. The parameters $\mathbf{A}_{\mathfrak{s}}$, $\mathbf{Q}_{\mathbf{v}}$ and $\mathbf{R}_{\mathbf{w}}$ can, however, be reliably estimated from the received data, see e.g. [79].

5.1.2 Measurement equation

Let us now establish the measurement equation. For this purpose, let us recall the expression in (2.11) for the received signal at the r^{th} receive antenna. One may now reformulate the corresponding CFO corrupted signal as

$$\mathbf{y}_r(k) = \sum_{t=1}^{N_t} \tilde{\mathbf{X}}_{tr}^{(\nu)}(k)\mathbf{h}_{tr}(k) + \mathbf{w}_r(k), \quad r = 1, \ldots, N_r, \tag{5.4}$$

with

$$\tilde{\mathbf{X}}_{tr}^{(\nu)}(k) = e^{j2\pi(kP+L_{\mathrm{CP}})\nu_{tr}(k)/N}\mathbf{C}(\nu_{tr}(k))\tilde{\mathbf{X}}_t(k). \tag{5.5}$$

The matrix $\tilde{\mathbf{X}}_t(k)$ in (5.5) implements the circular convolution between the modulated symbol vector $\tilde{\mathbf{x}}_t(k)$ at the t^{th} transmit antenna and the MIMO branch CIR vector $\mathbf{h}_{tr}(k)$. Hence, it is a circulant matrix of size $N \times L_h$ with the vector $\tilde{\mathbf{x}}_t(k)$ as first column.

The set of N_r equations in (5.4) may be written in more compact matrix vector form as

$$\mathbf{y}(k) = \tilde{\mathbf{X}}^{(\nu)}(k)\mathbf{h}(k) + \mathbf{w}(k), \tag{5.6}$$

where $\mathbf{y}(k) = [\mathbf{y}_1^T(k), \ldots, \mathbf{y}_{N_r}^T(k)]^T$ is the k^{th} received block of size $N_r \times 1$ at the N_r receive antennas, and $\mathbf{w}(k) = [\mathbf{w}_1^T(k), \ldots, \mathbf{w}_{N_r}^T(k)]^T$ is the zero-mean complex circular Gaussian noise vector with covariance matrix $\mathbf{R}_{\mathbf{w}} = \sigma^2\mathbf{I}_{N_rN}$. The vector $\mathbf{h}(k)$ of MIMO channel coefficients is defined as in (2.4), whereas the modulated data and the frequency offsets are embedded in the matrix $\tilde{\mathbf{X}}^{(\nu)}(k)$ of size $N_rN \times N_tN_rL_h$ defined as

$$\tilde{\mathbf{X}}^{(\nu)}(k) = \begin{bmatrix} \tilde{\mathbf{X}}_{11}^{(\nu)}(k) & \ldots & \tilde{\mathbf{X}}_{N_t1}^{(\nu)}(k) & \mathbf{0}_{N\times L_h} & \ldots & & & \ldots & \mathbf{0}_{N\times L_h} \\ \vdots & & & \tilde{\mathbf{X}}_{1r}^{(\nu)}(k) & \ldots & \tilde{\mathbf{X}}_{N_tr}^{(\nu)}(k) & & & \vdots \\ \mathbf{0}_{N\times L_h} & & & & \ldots & \mathbf{0}_{N\times L_h} & \tilde{\mathbf{X}}_{1N_r}^{(\nu)}(k) & \ldots & \tilde{\mathbf{X}}_{N_tN_r}^{(\nu)}(k) \end{bmatrix}. \tag{5.7}$$

Notice that the observations in (5.6) are linear in the channel coefficients, while being nonlinear functions of the carrier frequency offsets. Equation (5.6) is referred to as measurement equation and forms together with (5.2) the state-space model for MIMO OFDM transmission impaired by multiple CFOs.

5.2 Joint time domain estimation and tracking of channels and frequency offsets in MIMO OFDM

In this section, we present an algorithm which performs the joint estimation and tracking of MIMO channel coefficients and carrier frequency offsets. It is described in Publications

II-III and [225]. The proposed method stems from extended Kalman filtering and uses the previously introduced state-space model. Tracking takes place in the time domain, whereas equalization is performed in the frequency domain. In the following, we provide an overview of the proposed algorithm.

5.2.1 State-space model

Let the state vector $\boldsymbol{\mathfrak{s}}$ be defined as in (5.1), i.e., it is comprised of both the MIMO channel coefficients and the values of the CFOs. Assuming multiple CFOs in MIMO system as discussed in Section 2.2.2, the state-space description of equations (5.2) and (5.6) may be reformulated as

$$\begin{aligned} \boldsymbol{\mathfrak{s}}(k) &= \mathbf{A}_{\boldsymbol{\mathfrak{s}}}\, \boldsymbol{\mathfrak{s}}(k-1) + \mathbf{v}(k) && (5.8)\\ \mathbf{y}(k) &= \mathbf{g}\left(\boldsymbol{\mathfrak{s}}(k)\right) + \mathbf{w}(k), && (5.9) \end{aligned}$$

where the nonlinear function $\mathbf{g} : \mathbb{C}_{N_t N_r (L_h+1)} \rightarrow \mathbb{C}_{N_r N}$ of the state vector $\boldsymbol{\mathfrak{s}}$ is defined as $\mathbf{g}$:

$$\boldsymbol{\mathfrak{s}}(k) \;\mapsto\; \mathbf{g}\left(\boldsymbol{\mathfrak{s}}(k)\right) = \tilde{\mathbf{X}}^{(\nu)}(k)\mathbf{h}(k). \tag{5.10}$$

Nonlinearity of the measurement equation (5.9) is caused by CFOs. The channel coefficients are still linearly related to observations. A common assumption for applying Kalman filter [116] to the above state-space model is that the state variables $\boldsymbol{\mathfrak{s}}(k)$ are Gauss-Markov random processes. This is nearly satisfied in many practical applications for which the channel coefficients may be described as Rayleigh distributed with uncorrelated scattering [132, 277].

Given the linear state and nonlinear measurement equations, we need to define the Jacobian matrix $\partial \mathbf{g}/\partial \boldsymbol{\mathfrak{s}}^T$ in order to apply EKF. The Jacobian matrix $\mathbf{G}_{\boldsymbol{\mathfrak{s}}}$ of $\mathbf{g}(\boldsymbol{\mathfrak{s}})$ with respect to $\boldsymbol{\mathfrak{s}}$ is defined as:

$$\mathbf{G}_{\boldsymbol{\mathfrak{s}}(k)} \triangleq \left.\frac{\partial \mathbf{g}}{\partial \boldsymbol{\mathfrak{s}}^T}\right|_{\boldsymbol{\mathfrak{s}}=\boldsymbol{\mathfrak{s}}(k)} = \left[\left.\frac{\partial \mathbf{g}}{\partial \mathbf{h}^T}\right|_{\boldsymbol{\mathfrak{s}}=\boldsymbol{\mathfrak{s}}(k)}, \left.\frac{\partial \mathbf{g}}{\partial \boldsymbol{\nu}^T}\right|_{\boldsymbol{\mathfrak{s}}=\boldsymbol{\mathfrak{s}}(k)}\right]_{N_r N \times N_t N_r (L_h+1)}. \tag{5.11}$$

Hence $\partial \mathbf{g}/\partial \boldsymbol{\mathfrak{s}}^T$ can be split into two parts, based on the derivative with respect to $\mathbf{h}$ and $\boldsymbol{\nu}$. Expressions for these two quantities are derived in Publication III.

5.2.2 Extended Kalman filter equations

By using the expression for the Jacobian matrix in (5.11), extended Kalman filter [57, Ch.8], [116] may be applied to estimate and track the state vector $\boldsymbol{\mathfrak{s}}$ over time as

$$\begin{aligned} \boldsymbol{\mathfrak{s}}_{(k|k-1)} &= \mathbf{A}_{\boldsymbol{\mathfrak{s}}}\, \boldsymbol{\mathfrak{s}}_{(k-1|k-1)} && (5.12)\\ \mathbf{P}_{(k|k-1)} &= \mathbf{A}_{\boldsymbol{\mathfrak{s}}}\, \mathbf{P}_{(k-1|k-1)}\, \mathbf{A}_{\boldsymbol{\mathfrak{s}}}^T + \mathbf{Q}_{\mathbf{v}} && (5.13)\\ \mathbf{K}_{(k)} &= \mathbf{P}_{(k|k-1)} \mathbf{G}^H_{\boldsymbol{\mathfrak{s}}(k|k-1)} \left[\mathbf{G}_{\boldsymbol{\mathfrak{s}}(k|k-1)} \mathbf{P}_{(k|k-1)} \mathbf{G}^H_{\boldsymbol{\mathfrak{s}}(k|k-1)} + \mathbf{R}_{\mathbf{w}}\right]^{-1} && (5.14)\\ \mathbf{P}_{(k|k)} &= \left[\mathbf{I}_{N_t N_r (L_h+1)} - \mathbf{K}_{(k)} \mathbf{G}_{\boldsymbol{\mathfrak{s}}(k|k-1)}\right] \mathbf{P}_{(k|k-1)} && (5.15)\\ \boldsymbol{\mathfrak{s}}_{(k|k)} &= \boldsymbol{\mathfrak{s}}_{(k|k-1)} + \mathbf{K}_{(k)} \left[\mathbf{y}(k) - \mathbf{g}\left(\boldsymbol{\mathfrak{s}}_{(k|k-1)}\right)\right]. && (5.16) \end{aligned}$$

The matrix $\mathbf{K}_{(k)}$ is known as the Kalman gain. Matrices $\mathbf{P}_{(k|k-1)}$ and $\mathbf{P}_{(k|k)}$ are the covariance matrices of the prediction and filtering error, respectively. The notation $(k|k-1)$

refers to the predicted value at time instance k, given the filtered estimate at time instance $k-1$ with subscript $(k-1|k-1)$. In fact, the extended Kalman filter is equivalent to the conventional Kalman filter [116] applied to the linearized state-space model.

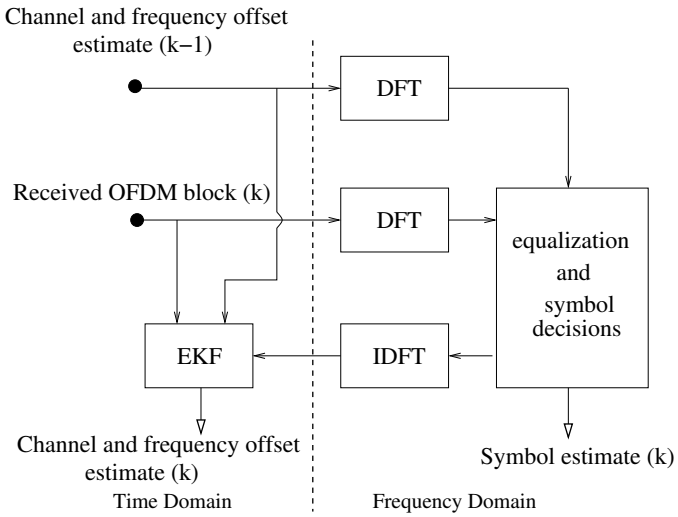

Figure 5.1: Time domain channel and frequency offset estimation and tracking followed by frequency domain equalization.

5.2.3 Proposed receiver algorithm

The proposed algorithm works as follows. Upon reception, the k^{th} OFDM block is passed through the MMSE equalizer in (2.25). The equalizer coefficients are computed using the previous filtered estimates of the MIMO channel coefficients and the CFOs, i.e., $\mathbf{h}(k-1|k-1)$ and $\boldsymbol{\nu}(k-1|k-1)$, respectively. Once symbol detection has been performed, the estimated data is re-modulated. Finally, an extended Kalman filter stage operating in the time domain generates the filtered estimate of the state vector at time instance k.

At this point one may refine the estimates by re-decoding the symbol vector using the filtered estimates $\mathbf{h}(k|k)$ and $\boldsymbol{\nu}(k|k)$. Re-decoding allows decreasing the symbol error rates substantially, while running the EKF-stage one more time lowers the channel and CFO estimation error. Moreover, improved tracking capability over time is achieved, especially in fast fading environments.

Except for the first few OFDM blocks, the algorithm works in a decision-directed mode. The initialization phase requires a few symbols. Typically a number of symbols equal to about half the dimension of the state vector is sufficient. Time domain LS or MMSE estimates are a simple and robust way to initialize the state parameters [50]. Without any a priori information on the channel and noise statistics, the LS scheme is a reasonable choice. Provided that coarse CFO acquisition is performed correctly, the estimation range of the proposed algorithm is not necessarily limited to the intercarrier spacing. The track may be lost in certain circumstances such as deep channel fades or abrupt time variations of the CFOs. Error accumulation in decision-directed processing, a misspecified order for the AR parameters as well the nonlinear nature of the measurement equation with respect to the CFOs may cause divergence of the extended Kalman filter.

Training symbols are sent periodically in order to avoid loosing the track. No special block structure has been considered for training, assuming that the whole OFDM symbol

is known to the receiver. Optimality considerations of the training schemes are beyond the scope of this thesis, and hence are not considered any further. Simulation studies in Publications I-III demonstrate that training every 50 to 100 blocks offers reliable tracking performance in scenarios with low to moderate mobility (3-60 [km/h], channel spread $f_D T_s \in [7.1 \cdot 10^{-4}, 1.4 \cdot 10^{-2}]$). At the same time, the training overhead is kept at low levels (1-2%). Thus, high spectral efficiency is obtained compared to mobile wireless communications systems which typically require 15-25% of pilot symbols. In the case of highly time-variant channel and CFO parameters, pilot symbols need to be included in every OFDM block. The overall structure of the receiver is illustrated in Figure 5.1 and the pseudo-code of the proposed algorithm is given in Table 5.1.

1. Decode	Decode the received vector $\mathbf{y}(k)$ and find the symbol estimate $\hat{\mathbf{s}}(k)$, using $\mathfrak{s}(k-1\|k-1)$, i.e., the filtered estimate of the state vector at time instance $k-1$.
2. Re-modulate	Re-modulate $\hat{\mathbf{s}}_t(k)$: $\hat{\tilde{\mathbf{x}}}_t(k) = \mathbf{F}\hat{\mathbf{s}}_t(k),\ t = 1, \ldots, N_t$.
3. Build estimates	Using $\hat{\tilde{\mathbf{x}}}(k) = [\hat{\tilde{\mathbf{x}}}_1^T(k), \ldots \hat{\tilde{\mathbf{x}}}_{N_t}^T(k)]^T$ and the predicted state vector $\mathfrak{s}(k\|k-1)$, build the estimate of $\tilde{\mathbf{X}}^{(\nu)}(k)$ and compute the Jacobian matrix $\mathbf{G}_{\mathfrak{s}(k\|k-1)}$.
4. Run EKF	Given the vector $\mathbf{y}(k)$ of observations, run the extended Kalman filter to obtain $\mathfrak{s}(k\|k)$, i.e., $\mathbf{h}(k\|k)$, $\boldsymbol{\nu}(k\|k)$.
5. Refine (optional)	Re-equalize and decode the data using $\mathfrak{s}(k\|k)$ to improve the symbol error performance. Run one more time the EKF to improve the estimates.

Table 5.1: Pseudo-code of the EKF-based joint channel and CFO estimation algorithm.

5.2.4 Computational complexity

The major computational cost in EKF lies in the matrix inversion needed for the calculation of the Kalman gain. By applying the matrix inversion lemma, the number of required operations can be made proportional to $(L_h + 1)N^2$ when tracking is done in the time domain. The complexity is proportional to N^3 when the processing takes place in the frequency domain. In practice $L_h \ll N$, hence significantly lower complexity is achieved. Smaller parameter space compared to frequency domain tracking ($N_t N_r(L_h+1) \times 1$ versus $N_t N_r(N+1) \times 1$ state vector) leads also to smaller variance for the estimated values of the channel coefficients.

Pre-DFT compensation for frequency offsets prior to equalization cannot be performed in the considered scenario: having one offset per MIMO branch makes the problem non-separable and equalization for both channels and offsets needs to be done simultaneously. Because of multiple CFOs, equalization becomes computationally expensive. Pre-DFT compensation is possible however, if there is only one CFO per multi-antenna receiver. The complexity of the subsequent channel equalizer is then significantly reduced, due to the absence of ICI. The proposed state-space model may be easily modified to any of these scenarios.

5.3 Time domain channel estimation and tracking in MIMO OFDM

Assuming perfect carrier frequency synchronization, we describe briefly time domain channel estimation and tracking via Kalman filtering in MIMO OFDM transmissions. The proposed technique is a special case of the previously presented general method (Section 5.1). Channel estimation takes place in the time domain, whereas equalization and symbol detection are performed in the frequency domain. Detailed description, additional derivations and simulation results are reported in Publication I. The proposed algorithm may be applied to SISO OFDM transmissions as well. In the latter case, it reduces to the method introduced in [226].

Let us assume a state vector comprised of the MIMO channel coefficients only, i.e., $\mathfrak{s}(k) = \mathbf{h}(k)$. Assuming perfect frequency synchronization, i.e., $\boldsymbol{\nu}(k) = \mathbf{0}_{N_t N_r \times 1}$, the state-space model of equations (5.2) and (5.6) reduces to

$$\mathfrak{s}(k) = \mathbf{A}_{\mathfrak{s}}\, \mathfrak{s}(k-1) + \mathbf{v}(k) \tag{5.17}$$

$$\mathbf{y}(k) = \tilde{\mathbf{X}}(k)\mathbf{h}(k) + \mathbf{w}(k), \tag{5.18}$$

where the matrix $\tilde{\mathbf{X}}(k)$ is obtained from (5.7) by setting the values of the CFOs to zero. The state transition matrix in (5.3) becomes $\mathbf{Q}_{\mathbf{v}} = \mathbf{Q}_{\mathbf{h}}$, and the state noise vector $\mathbf{v}$ is of size $N_t N_r L_h \times 1$.

Since the model in (5.17)-(5.18) is linear and the noise is assumed to be Gaussian, Kalman filter may be directly applied to estimate and track the state vector $\mathfrak{s}$ over time. The well-known Kalman filter equations may be obtained by setting $\mathbf{G}_{\mathfrak{s}(k|k-1)} = \tilde{\mathbf{X}}(k)$ in equations (5.12)-(5.16). Indeed, KF and EKF have equivalent expressions in the case of linear state-space models.

As perfect frequency synchronization is assumed, the initial frequency selective channel is turned into a set of frequency flat subchannels. The equalizer is needed to compensate the flat fading experienced on each subcarrier as well as to separate the transmitted data streams. Hence, low complexity equalization may be performed in the frequency domain.

5.4 Discussion

In this chapter, a novel algorithm is presented for tracking jointly time-frequency selective channels and time-varying CFO parameters in MIMO OFDM systems. Detailed derivation is given in Publications I-III. The method stems from extended Kalman filtering. The estimation and tracking stage operates in the time domain while equalization is performed in the frequency domain. A few known training symbols at the beginning of the transmission are used to acquire initial estimates for the channel and CFO parameters. Then, the algorithm may switch to decision-directed mode and use the decoded symbols for keeping the track. The MMSE equalizer was chosen just for demonstration purposes to provide some indication about the bit error rate performance. However, there exist other equalization schemes in the literature [104, 157], which can be applied to the proposed state-space framework. For instance, ML or sub-optimal QRD-M data detection algorithms may be combined together with a KF MIMO channel estimation stage [148]. Also, a coded transmission may accommodate a time domain KF-based channel estimator [14].

Each transmitter-receiver pair is assumed to introduce its own carrier frequency offset [32]. This modeling is general while versatile at the same time. It is justified by mobility together with the large angle spread and rich scattering environment typically assumed in

MIMO systems (Section 2.2.2). Also, oscillator frequency mismatches may arise between each transmitter and receiver pair in case of separate RF-IF chains. Papers [32, 225] as well as Publication III presented in this chapter were among the first ones to advocate the use of multiple CFO parameters in mobile MIMO OFDM. With a single CFO per multi-antenna receiver, channel equalization and CFO compensation operations decouple, leading to low complexity equalization.

The use of recursive estimators such as Kalman filters for channel estimation purposes in OFDM has gained growing interest over the past years [9, 14, 39, 40, 48, 50, 80, 145–148, 225, 226, 236, 250, 297, 298]. Vector KF processing in the frequency domain may be replaced by a set of parallel Kalman filters running on each subcarrier [39, 48]. The latter approach has much lower complexity, but also much worse performance [226], unless the correlation among the estimated values of the CFR is restored through a MMSE combiner [48]. However, time domain processing remains an appealing option, since no degradation in performance takes place [50].

Extended Kalman filter may be used for nonlinear state-space models. The feasibility of EKF-based carrier phase and frequency estimation and tracking in digital communication systems was demonstrated in [7]. In addition, estimation of channel and delay parameters using EKF was proposed for code division multiple access (CDMA) [132] and OFDM systems as well [145, 147]. Particle filters (PF), also known as sequential Monte-Carlo methods, provide another way to address the estimation of the channel and delay [146] parameters, the carrier frequency offset [200] or the carrier phase offset [209]. However, the computational complexity of PFs is often prohibitive. Their use may only be justified for heavy-tailed noise distributions and multi-modal or skewed parameter distributions [200]. Indeed, the measurement noise may be non-Gaussian in practice, due largely to impulsive phenomena [278]. A thorough performance/complexity comparison of various Bayesian receivers versus conventional KF/EKF is given in [117, Fig.7].

Reliable channel and CFO estimation as well as bandwidth efficient transmission are achieved with the proposed method, especially in low mobility scenarios. Extensive simulation results and performance studies may be found in Publications I-III. However, decision-directed processing experiences performance loss at high terminal velocities, which leads to high time-variation of the wireless channel. Thus, the filtered estimates of the channel and CFO parameters at the previous block time instance may not be sufficiently good estimates to reliably decode the symbols, especially for higher-order modulations. An outer channel code may solve this problem at the cost of an increased latency [14]. A well-designed pilot structure in time-frequency domain is naturally needed in this case to obtain a reliable tracking performance [29, 66, 196]. Kalman-filters may accommodate pilot data for channel estimation purposes as well [9, 11, 80, 236, 250, 297, 298]. It leads to more reliable operation compared to pure decision-directed processing. In addition, the placement of pilots may be optimized in order to achieve the best tracking of time-varying channels. Assuming a first-order Gauss-Markov channel process, transmitting pilot symbols frequently achieves a lower steady-state MSE for the Kalman filter channel estimator compared to sending larger clusters of pilot symbols at a lower retraining rate [72, 73]. The problem of choosing how often training is required in time selective MIMO channels is addressed in [115, 216, 255]. More frequent training provides obviously with better channel tracking performance: the optimal training interval decreases as the Doppler frequency increases [255, Fig.3]. Over a short training interval, the symbol error performance is mainly governed by the noise, while the interference due to the temporal change of the channel coefficients increases as time proceeds (see e.g., [216, Fig.1] and [255, Fig.2]). The optimal training length/interval is difficult to obtain in a closed-form as it depends on various

system parameters such as the SNR, the channel spread, the modulation as well as the antenna configuration [216]. However, the combination of DD and KF processing chosen for the proposed algorithm allows updating the channel and CFO estimates on a block basis. This overcomes the problem of outdated estimates to a large extent. Combining pilot-aided and DD channel estimation is another possibility [250]. Alternatively, two KF stages may be operated in parallel, one using exclusively pilot symbols and the other one running on the estimated data [298]. Kalman filtering on pilot data may allow estimating the fading coefficient as well [80]. However, at very high terminal velocities the assumption of block fading channel may not hold anymore. Consequently, tracking of the channel coefficients within the time duration of the OFDM block may become mandatory [249].

It could be argued that the proposed first order auto-regressive channel modeling is not very accurate. However, is seems to be extremely difficult to accommodate an advanced channel model in the algorithm design, as it depends on the propagation environment. Nevertheless, low-order auto-regressive models are widely used in the literature [72, 73, 117, 132, 265]. Higher-order AR models allow describing the Doppler spectrum more precisely [132, 151, 265]. One option to select the modeling parameters would be to use existing and pre-established channel models, e.g. ITU models [133]. Another approach is to allow a set of different models, and perform KF channel estimation via multiple hypothesis testing [145]. One should recall that the state noise covariance matrix describes to some extent the uncertainty in modeling the state vector over time. Also, the maximum channel length should be estimated in practice. Alternatively, it may be upper-bounded by the CP length, with lower performance though. Thus, a general and perhaps simplistic channel model helps keeping the complexity at reasonable levels, while offering improved performance over no modeling at all. Robust channel estimation may be achieved by following the H_∞ approach [41], which aims at minimizing the effect of the worst possible finite energy disturbances including both state and measurement noise. Hence, both channel modeling errors and additive noise are taken into account and no a priori knowledge of the noise source statistics is required. Kalman filtering and H_∞ estimation are based upon the same state-space model. KF is optimal in the sense that is minimizes the error covariance, assuming known statistics for the state-space model. Hence, the intrinsic difference between them is that KF stems from MMSE estimation while H_∞ follows a minimax strategy.

Also, one may argue on whether to estimate and track either the CIR or the CFR parameters. The benefits of time domain versus frequency domain channel estimation are threefold. First, there are fewer channel parameters in time domain, hence the smaller dimension of the state vector. This leads to both reduced complexity and lower variance of the estimates. Second, the frequency correlation among the channel taps can be efficiently exploited. Indeed, the interpolation capabilities of the DFT are implicitly exploited. There is hence no need to restore the correlation structure in frequency domain explicitly [39, 40, 48, 50]. Kalman filter based channel estimation provides equal performance in both time and frequency domain, as long as the channel correlation features are properly described in both domains. Proper initialization of the filters plays an important role [50]. Third and last, channel estimation errors are spread over the whole transmission spectrum and not concentrated on a given set of subcarriers.

To conclude, a proper channel estimation algorithm for OFDM systems should capture both the time and frequency domain characteristics. In addition, carrier frequency synchronization must be maintained. The algorithm introduced in this chapter complies with those requirements as it allows tracking both time-varying channel and CFO parameters reliably in mobile MIMO OFDM systems. Moreover, time domain processing reduces the

number of state parameters to be estimated and tracked. Then, a significant reduction in the computational complexity of KF/EKF may be achieved via the matrix inversion lemma. Finally, the proposed state-space model may be extended to include the presence of pilot symbols as well as several other parameters of interest, e.g. the timing and carrier phase offsets.

Chapter 6

Blind frequency synchronization algorithms for OFDM and performance bounds

In this chapter, the contributions of this thesis to the area of blind carrier offset estimation for SISO OFDM systems are presented. They may be stated as follows:

- A blind fine CFO estimation/compensation algorithm based on the diagonality of the received signal covariance matrix is developed.
- A blind subspace fine CFO estimator for OFDM using real- or complex-valued constant modulus modulations is derived.
- Large sample properties of proposed blind CFO estimators are established.
- A stochastic Cramér-Rao bound for the blind carrier offset estimation problem in OFDM with real- or complex-valued modulations is derived.

In the following sections, the core ideas of the proposed algorithms are introduced. The derived performance bounds are expressed as well, and the key results and contributions are highlighted. Detailed mathematical proofs and derivations as well as simulation results may be found in Publications IV-VII.

6.1 Blind CFO estimation via diagonality criterion

In this section, we introduce a carrier frequency offset (CFO) estimator for OFDM based on the signal covariance matrix. Hence, it applies to both real- and complex-valued modulations schemes. Without loss of generality, we assume that unit energy QPSK modulation is used. However, even though the QPSK case is considered only, results presented in this section extend to other kind of real- or complex-valued modulation schemes, e.g., BPSK, 8PSK, 16QAM, 64QAM. The proposed algorithm is intended for estimating small CFOs. As a consequence, it may track small CFO or the residual offset when the initially larger CFO has been significantly reduced by other means [102, 190, 238].

6.1.1 Second order statistics for real and complex random vectors

In order to fully characterize the second order statistics of a complex-valued random vector $\mathbf{u}$, two matrices are needed [215]:

$$\begin{aligned} \operatorname{cov}(\mathbf{u}) &\triangleq \mathrm{E}\left[(\mathbf{u}-\mathrm{E}[\mathbf{u}])(\mathbf{u}-\mathrm{E}[\mathbf{u}])^H\right] && (6.1)\\ \operatorname{pcov}(\mathbf{u}) &\triangleq \mathrm{E}\left[(\mathbf{u}-\mathrm{E}[\mathbf{u}])(\mathbf{u}-\mathrm{E}[\mathbf{u}])^T\right], && (6.2) \end{aligned}$$

where $\operatorname{cov}(\mathbf{u})$ is the covariance matrix of $\mathbf{u}$ and $\operatorname{pcov}(\mathbf{u})$ is the pseudo-covariance matrix of $\mathbf{u}$. The pseudo-covariance matrix is sometimes also referred to as conjugate covariance matrix or complementary covariance matrix [195, 214, 215]. A complex-valued random vector $\mathbf{u}$ is called second-order circular [214] (or proper [195]) random vector if its pseudo-covariance vanishes, i.e., $\operatorname{pcov}(\mathbf{u}) = \mathbf{0}_{N\times N}$. When the real and the imaginary parts of $\mathbf{u}$ are statistically independent and have equal variance, the received signal becomes second-order circular. Otherwise, it is non-circular. Hence, complete second order statistics include both signal covariance and pseudo-covariance matrices [214, 215].

6.1.2 Signal model

Assuming a normalized carrier frequency offset ν, let us first recall the expression in (2.26) for the CFO-corrupted SISO OFDM received signal,

$$\mathbf{y}_\nu(k) = \varphi_k(\nu)\mathbf{C}(\nu)\tilde{\mathbf{H}}\mathbf{F}\mathbf{s}(k) + \mathbf{w}(k). \tag{6.3}$$

The CFO is introduced by both the diagonal matrix $\mathbf{C}(\nu)$ of size $N \times N$ defined in (2.13) and the block dependent term $\varphi_k(\nu) = \exp(j2\pi(kP + L_{\mathrm{CP}})\nu/N)$. The channel is assumed to be frequency selective and quasi-stationary over the observation period, i.e., the circulant channel matrix $\tilde{\mathbf{H}}$ does not depend on the block index k. The CFO is assumed to be time-invariant as well. No null-subcarriers are used, although their presence would not affect the following analysis.

Given an estimate $\hat{\nu}$ of the true value ν, CFO compensation may be performed in time domain at the receiver prior to the discrete Fourier transform. Based on (6.3), the resulting CFO-compensated received vector, $\mathbf{v}_{\hat{\nu}\nu}$, may be expressed as

$$\begin{aligned} \mathbf{v}_{\hat{\nu}\nu}(k) &= \varphi_k^*(\hat{\nu})\mathbf{F}^H\mathbf{C}^*(\hat{\nu})\mathbf{y}_\nu(k) && (6.4)\\ &= \varphi_k^*(\hat{\nu}-\nu)\mathbf{F}^H\mathbf{C}^*(\hat{\nu}-\nu)\tilde{\mathbf{H}}\mathbf{F}\mathbf{s}(k) + \varphi_k^*(\hat{\nu})\mathbf{F}^H\mathbf{C}^*(\hat{\nu})\mathbf{w}(k). && (6.5) \end{aligned}$$

6.1.3 Algorithm

Signal covariance matrix

Let $\tilde{\mathbf{Q}}_k(\mu) = \operatorname{cov}(\mathbf{v}_{\mu\nu}(k))$, where $\mathbf{v}_{\mu\nu}$ denotes $\mathbf{v}_{\hat{\nu}\nu}$ in (6.4) evaluated at $\hat{\nu} = \mu$. Then, let $\mathbf{Q} = \operatorname{cov}(\mathbf{y}_0(k)) = \tilde{\mathbf{H}}\tilde{\mathbf{H}}^H + \sigma^2\mathbf{I}_N$, where $\mathbf{y}_0(k)$ is the received signal in time domain assuming perfect frequency synchronization (see eq. (6.3) with $\nu = 0$). Now, $\tilde{\mathbf{Q}}_k(\mu)$ and $\mathbf{Q}$ are related by

$$\begin{aligned} \tilde{\mathbf{Q}}_k(\mu) &= \mathbf{F}^H\mathbf{C}^*(\mu-\nu)\tilde{\mathbf{H}}\tilde{\mathbf{H}}^H\mathbf{C}(\mu-\nu)\mathbf{F} + \sigma^2\mathbf{I}_N && (6.6)\\ &= \mathbf{F}^H\mathbf{C}^*(\mu-\nu)\,\mathbf{Q}\,\mathbf{C}(\mu-\nu)\mathbf{F} && (6.7)\\ &\triangleq \tilde{\mathbf{Q}}(\mu). && (6.8) \end{aligned}$$

We assumed zero-mean independent data and noise processes, with covariance matrices $\mathrm{cov}\left(\mathbf{s}(k)\right) = \mathbf{I}_N$ and $\mathrm{cov}\left(\mathbf{w}(k)\right) = \sigma^2\mathbf{I}_N$, respectively. Notice that the block dependent phase term $\varphi_k(\nu)$ in (6.4) cancels out in the derivation of $\tilde{\mathbf{Q}}_k\left(\mu\right)$. Hence the matrix $\tilde{\mathbf{Q}}_k\left(\mu\right)$ does not depend on the block index k and will be further denoted by $\tilde{\mathbf{Q}}\left(\mu\right)$.

Cost function minimizing the total off-diagonal power

Null or perfectly compensated frequency offset ($\mu = \nu$) leads to a perfectly orthogonal transmission, and $\tilde{\mathbf{Q}}(\mu)$ becomes diagonal. Proof is straightforward and may be found in Publication IV, Appendix I. Off-diagonal elements are introduced by intercarrier interference and should be minimized. Hence, for a given offset compensation value μ, we choose the total off-diagonal power $\mathcal{J}\left(\mu\right)$ of $\tilde{\mathbf{Q}}(\mu)$ as a cost function to be minimized:

$$\mathcal{J}\left(\mu\right) = \left\| \tilde{\mathbf{Q}}\left(\mu\right) \odot \left(\mathbb{1}_N - \mathbf{I}_N\right) \right\|_F^2, \quad \mu \in [0, 1[, \tag{6.9}$$

where $\odot$ stands for the Hadamard product and $\mathbb{1}_N$ denotes a $N \times N$ matrix of 1's. Notice that the noise does not have any influence in theory provided that its covariance matrix is diagonal, i.e., it is uncorrelated.

In order to guarantee the identifiability of the CFO parameter, the channel covariance matrix $\tilde{\mathbf{H}}\tilde{\mathbf{H}}^H$ should have at least one non-zero off-diagonal entry[1]. Otherwise, the matrix $\mathbf{Q}$ is diagonal and $\mathbf{C}(\nu)\mathbf{Q}\mathbf{C}^*(\nu)$ does not contain information on ν anymore. Now, Theorem 3 proves the existence of a unique minimum of $\mathcal{J}$ at ν in $[0, 1[$.

Theorem 3 *Let $\mathcal{J} : \mu \mapsto \mathcal{J}\left(\mu\right)$ be defined as in (6.9). Then, assuming a non-diagonal channel covariance matrix $\tilde{\mathbf{H}}\tilde{\mathbf{H}}^H$,*

1. $\mathcal{J}\left(\nu\right) = 0$.
2. $\mathcal{J}\left(\mu\right) > 0$, $\forall\, \mu \neq \nu$, $\mu \in [0, 1[$.

Proof is given in Publication IV, Appendix I.

As a consequence of Theorem 3, the true CFO may be found by driving $\mathcal{J}\left(\mu\right)$ to zero. In practice, only an estimate $\widehat{\tilde{\mathbf{Q}}}_K\left(\mu\right)$ of $\tilde{\mathbf{Q}}\left(\mu\right)$ is available through the sample covariance matrix (subscript K refers to the sample size). Then, an estimate $\hat{\nu}$ of the CFO ν may found by

$$\hat{\nu}_K = \underset{\mu \in [0,1[}{\arg\min}\, \widehat{\mathcal{J}}_K\left(\mu\right), \tag{6.10}$$

where the estimated cost function $\widehat{\mathcal{J}}_K$ after K received OFDM blocks is given as

$$\widehat{\mathcal{J}}_K\left(\mu\right) = \left\| \widehat{\tilde{\mathbf{Q}}}_K\left(\mu\right) \odot \left(\mathbb{1}_N - \mathbf{I}_N\right) \right\|_F^2, \quad \mu \in [0, 1[. \tag{6.11}$$

The cost function $\widehat{\mathcal{J}}_K$ penalizes the total off-diagonal power of $\widehat{\tilde{\mathbf{Q}}}_K$. It measures the loss of orthogonality due to CFO. The proposed method is blind in a sense that minimization of $\widehat{\mathcal{J}}_K$ may be performed without any knowledge of the wireless channel $\tilde{\mathbf{H}}$ or pilot symbols.

Note that exploiting the pseudo-covariance matrix alone instead of the covariance is not a viable choice here. In theory, $\tilde{\mathbf{P}}_k\left(\mu\right) = \mathrm{pcov}\left(\mathbf{v}_{\mu\nu}(k)\right)$ contains information on the CFO for real-valued modulations. However, the block dependent phase term $\varphi_k(\nu)$ in (6.4) drives its sample estimate to zero for large sample sizes.

[1]The channel is required to be multipath, i.e., it has at least two non-zero taps in the time domain. The latter assumption is fulfilled in practical OFDM transmissions.

Closed-form expression for the cost function

In order to find a computationally efficient way to estimate the CFO, a closed-form expression of the cost function is derived next. It proves that the estimate $\widehat{\mathcal{J}}_K$ of the cost function in (6.11) may be expressed as

$$\widehat{\mathcal{J}}_K(\mu) = a + b\cos(2\pi\mu) + c\sin(2\pi\mu), \quad a, b, c \in \mathbb{R}. \tag{6.12}$$

The proof as well as expressions for a, b and c are given in Publication IV, Appendix II.

It can be seen from (6.12) that $\widehat{\mathcal{J}}_K$ is a periodic function of μ with period 1. Hence, we may further restrict our analysis to the interval $[0, 1[$, or equivalently $[-1/2, 1/2[$. The proposed algorithm is aimed at estimating small CFOs. Consequently, it may track small CFO or the residual offset after coarse CFO estimation has been accomplished by other means [102, 190, 238]. An example of the cost function is depicted in Figure 6.1, at 15 dB SNR and with $K = 200$ observed blocks. The minimum is reached at $\mu = 0.4379$, while the true offset is $\nu = 0.43$. The sinusoidal form may be clearly observed, which is in par with the result in (6.12).

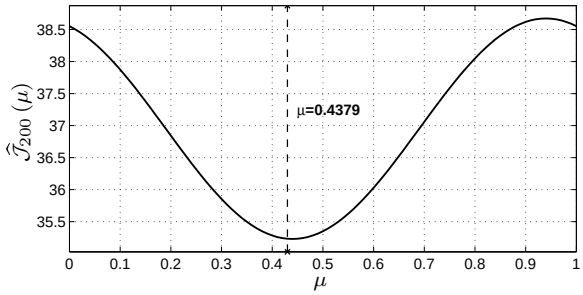

Figure 6.1: Estimate of cost function $\widehat{\mathcal{J}}_{200}(\mu)$, $K = 200$, $\nu = 0.43$ and SNR=15 dB. The cost function is sinusoidal.

Given the form in (6.12), it is sufficient to evaluate $\widehat{\mathcal{J}}_K$ at three points in order to solve for a, b and c. We choose the following equi-spaced points[2] 0, 1/3 and 2/3 within the interval $[0, 1[$. Hence, the extrema of $\widehat{\mathcal{J}}_K$ may be given in closed form by

$$\hat{\nu}_{K_i} = \frac{1}{2\pi}\arctan\left\{\frac{\sqrt{3}\left(\widehat{\mathcal{J}}_K\left(\frac{1}{3}\right) - \widehat{\mathcal{J}}_K\left(\frac{2}{3}\right)\right)}{2\,\widehat{\mathcal{J}}_K(0) - \widehat{\mathcal{J}}_K\left(\frac{1}{3}\right) - \widehat{\mathcal{J}}_K\left(\frac{2}{3}\right)}\right\} + \frac{i}{2} \mod 1, \quad i = 0, 1. \tag{6.13}$$

Finally, the frequency offset estimate is found by choosing the value corresponding to the minimum of the cost function

$$\hat{\nu}_K = \begin{cases} \hat{\nu}_{K_0} & \text{if } \widehat{\mathcal{J}}_K(\hat{\nu}_{K_0}) < \widehat{\mathcal{J}}_K(\hat{\nu}_{K_1}), \\ \hat{\nu}_{K_1} & \text{otherwise.} \end{cases} \tag{6.14}$$

6.1.4 Asymptotic analysis

We now investigate the large sample properties of the proposed CFO estimator, that is consistency, convergence in the mean square and rate of convergence. Proofs and additional derivations may be found in Publication IV, Appendix IV-VI.

[2] A similar minimization/maximization procedure in closed-form is found in [293].

Convergence

Theorem 4 establishes the convergence with probability one of the proposed CFO estimate to the true CFO. Proof is given in Publication IV, Appendix IV.

Theorem 4 (Strong consistency) *As* $K \to \infty$,

$$\hat{\nu}_K \to \nu \text{ w. p. } 1 .$$

As convergence with probability one implies convergence in probability [240, p.10], the proposed estimator yields a consistent estimate of the CFO. In addition, convergence in the mean square follows from Theorem 4 and from the fact that $\hat{\nu}_K$ is bounded to $[0, 1[$. See Appendix V in Publication IV as well as [240, p.11].

Corollary 1 *$\hat{\nu}_K$ converges to ν in the mean square.*

Consequently, the proposed estimator is asymptotically unbiased. We next study the convergence rate of the estimator.

Convergence rate

Let us define the MSE after K received blocks by

$$\text{MSE}_K = \text{E}\left[(\nu - \hat{\nu}_K)^2 \right]. \tag{6.15}$$

For large sample size K, the MSE may be approximated as a quotient of polynomials by

$$\text{MSE}_K \cong \frac{1}{4\pi^2} \frac{\mathcal{P}^{(\leq 3)}(K)}{\mathcal{Q}^{(4)}(K)} \propto 1/K, \tag{6.16}$$

where $\mathcal{Q}^{(4)}$ is a polynomial of degree four in K, while the polynomial $\mathcal{P}^{(\leq 3)}$ is of degree at most three. See Appendix VI in Publication IV for a detailed derivation. Hence, it follows that for K sufficiently large, the rate of convergence in MSE is proportional to $1/K$.

6.1.5 Discussion

In this section, we presented a novel blind frequency offset estimator for OFDM systems under frequency selective fading. Detailed derivations may be found in Publication IV. The proposed algorithm applies to both real (e.g., BPSK, PAM) and complex modulations (e.g., QPSK, 8PSK, 16QAM, 64QAM), and extends to asymmetric modulations as well. Hence it may be used in a wide range of OFDM transceivers. The method is applicable to fine estimation of the normalized CFO in the range of $[-1/2, 1/2[$ with respect to the intercarrier spacing. Information on the CFO is embedded in the received signal covariance matrix. Based on that property, a cost function may be derived, and the sample covariance matrix may be used to estimate the CFO in practice. The cost function minimizes the total off-diagonal power induced by ICI in the frequency domain. Enforcing a diagonal structure aims at restoring the orthogonality of the transmission inherent to perfectly synchronized OFDM modulation. The method does not require a priori knowledge of the transmitted data or the multipath channel. Channel estimation may then be performed as a subsequent step, after the frequency synchronization is achieved. Bandwidth efficiency remains high as no pilot or null-subcarrier are needed. A closed-form expression is found for the cost function which leads to low complexity and accurate computational solution. The cost function needs to be evaluated in three points in order to obtain the CFO estimate

in practice. Note that the covariance matrix may already be available to the receiver: it is commonly needed for channel estimation for instance. However, the proposed approach suffers from a few drawbacks. The small estimation range limits the use to small frequency offsets or refinement purposes. Note that the method could be potentially extended to slowly time-varying channels, with fixed CFO. However, the convergence rate in $1/K$ would not allow for estimation in highly time-varying environments. For this purpose, estimators that need only small sample support should be preferred.

The proposed estimator exploits the structure of the covariance matrix in CFO estimation. The proposed cost function yields in fact a measure of the transmission orthogonality in frequency domain, or equivalently, it characterizes in time domain how far the covariance matrix is from a circulant matrix. The derived concepts apply to cyclic prefix based transmissions in general. A few similarities exist with some algorithms in the literature [158, 224, 274, 290, 293]. While [224] focuses on reducing the total ICI power, the method in Publication IV minimizes the power of cross-correlation terms in the frequency domain in order to restore an orthogonal transmission. The idea of restoring the orthogonality among the OFDM subcarriers is also found in [274], where an adaptive decorrelator corrects for the CFO-induced ICI. The problem is solved using a recursive update. No closed-form solution is available, unlike in Publication IV. The idea of CFO estimation via ICI reduction is also exploited by the minimum output variance (MOV) estimator [290]. CFO does not change the total received power of received symbols. However, the variance on a given subcarrier increases when the CFO gets larger. At the same time, the expected value of the amplitude decreases because of the attenuation due to the CFO. Minimum output variance occurs for zero CFO, which leads to the MOV estimator [290]. The difference to Publication IV is that [290] operates on the received signal magnitude in the frequency domain. Also, no closed-form solution is available for the MOV estimator. The explicit use of the signal covariance matrix for carrier frequency synchronization was proposed in [158]. The idea is to match the sample correlations to their theoretical values in the weighted least-squares sense. However, unlike the proposed estimator, the CIR needs to be known a-priori, which is a major drawback. Finally, Publication IV has also some similarities in the sinusoidal cost function and related minimization with the kurtosis based estimator [293]. Both algorithms rely on fourth-order statistics. However, the cost functions are intrinsically different since off-diagonal power of covariance matrix is considered instead of sample Kurtosis.

Simulation studies are presented in detail in Publication IV, where the proposed estimator is tested under various channel and noise conditions. On average, the residual error on the CFO falls below 5% after 100 received blocks. After 600 blocks, it is less than 2% for both QPSK and 16QAM modulations. As OFDM systems are commonly considered to tolerate synchronization errors up to a few percents of the carrier spacing, the proposed approach is a feasible solution for practical receivers. Unlike subspace estimators for example, the algorithm performs well for multipath channels with unknown channel length, provided that the channel is shorter than the duration of the cyclic prefix. In addition, simulation studies show that CFO estimation performs equally well with QPSK or 16QAM modulations. Also, a test run with complex Gaussian distributed signals did not show any difference in performance. This is not surprising since the algorithm does not exploit the finite symbol alphabet or the constant modulus property. Then, in theory, the covariance matrix of the noise is diagonal on average for complex white noise. Hence, the performance of the algorithm should not depend on the SNR if noise is uncorrelated. However, in practice, the sample estimates of the covariance matrix experience perturbations because of small sample size and low SNR. Simulation results do not show any significant

dependence of the performance on the noise level. Thus, reliable CFO estimation may be achieved at low SNR regime, where decision-directed methods are likely to fail. Moreover, the proposed estimator yields a consistent estimate of the CFO. Hence, it is asymptotically unbiased. Finally, simulations show that it performs close to the stochastic Cramér-Rao bound established at the end of this chapter.

6.2 Subspace technique for blind CFO estimation for OFDM with constant modulus modulations

In this section, we describe the novel subspace based approaches for blind carrier frequency offset estimation in OFDM with constant modulus modulations proposed in Publications VI-VII. Correlation in squared amplitude spectrum of the channel is exploited. Low rank signal model is thereby obtained without null-subcarriers. The proposed estimator accomplishes fine frequency synchronization with a single OFDM block in the range $[-1/2, 1/2[$. Small sample support reduces the need of time averaging, which makes the approach very attractive for time selective channels and time-varying CFOs. Detailed description of the related algorithms, proofs and derivations as well as simulation results may be found in Publications VI-VII. First, the subspace structures of both the channel frequency response and the channel squared amplitude spectrum are shortly described. Then, the subspace CFO estimation algorithm for constant modulus modulations is presented, and its extension to case of real-valued modulations is briefly outlined. Finally, the relation to existing algorithms [97] in the literature is investigated.

6.2.1 Correlation in channel frequency response

An important property in OFDM transmission is the frequency correlation of the channel among subcarriers induced by the DFT and the FIR communication channel. Let $\mathbf{h}(k)$ be the $L_h \times 1$ channel impulse response in time domain corresponding to the $N \times 1$ channel frequency response vector $\tilde{\mathbf{h}}(k)$. Since typically $L_h \ll N$, vectors $\mathbf{h}(k)$ and $\tilde{\mathbf{h}}(k)$ are related by an N-point DFT as

$$\tilde{\mathbf{h}}(k) = \sqrt{N} \left[\mathbf{F}^H\right]_{\{:,1:L_h\}} \mathbf{h}(k), \tag{6.17}$$

where the $N \times L_h$ matrix $\left[\mathbf{F}^H\right]_{\{:,1:L_h\}}$ is made from the L_h first columns of the DFT matrix $\mathbf{F}^H$. Then, the $L_h \times 1$ vector $\mathbf{h}(k)$ may be obtained from $\tilde{\mathbf{h}}(k)$ via IDFT as

$$\mathbf{h}(k) = \frac{1}{\sqrt{N}} \mathbf{F}_{\{1:L_h,:\}} \tilde{\mathbf{h}}(k). \tag{6.18}$$

Now, the following relationship may be established:

$$\begin{aligned} \tilde{\mathbf{h}}(k) &= \left[\mathbf{F}^H\right]_{\{:,1:L_h\}} \mathbf{F}_{\{1:L_h,:\}} \tilde{\mathbf{h}}(k) && (6.19) \\ &= \mathbf{A}\tilde{\mathbf{h}}(k), && (6.20) \end{aligned}$$

where the DFT/IDFT pair is denoted by $\mathbf{A} = \left[\mathbf{F}^H\right]_{\{:,1:L_h\}} \mathbf{F}_{\{1:L_h,:\}}$. Since both the truncated DFT and IDFT matrices are of rank L_h, we also have $\text{rank}\{\mathbf{A}\} = L_h$ [125].

6.2.2 Correlation in channel squared amplitude spectrum

In the following, we denote by $\odot$ the Hadamard (i.e., element-wise) product [125]. Channel spectrum may not be uniquely determined from the squared spectrum (ambiguity in

phase). Therefore we study and characterize the correlation properties of the squared amplitude spectrum $\tilde{\mathbf{h}}(k) \odot \tilde{\mathbf{h}}^*(k)$. First, by using Theorem 5 below, we identify the vector subspace of channel squared amplitude spectrum.

Theorem 5 *Let* $\mathbf{x}$ *be a* $N \times 1$ *vector such that* $\mathbf{x} = \mathbf{A}\mathbf{x}$*, where* $\mathbf{A}$ *is a* $N \times N$ *matrix of rank* $L \leq N$*. Then, the vector* $\mathbf{x} \odot \mathbf{x}^*$ *of squared amplitudes lies in the column space of* $\mathbf{A} \odot \mathbf{A}^*$*.*

Proof is given in Publication VII. From (6.20), $\tilde{\mathbf{h}}(k) = \mathbf{A}\tilde{\mathbf{h}}(k)$, and according to the above theorem, the squared amplitude spectrum $\tilde{\mathbf{h}}(k) \odot \tilde{\mathbf{h}}^*(k)$ lies in the column space of $\mathbf{A} \odot \mathbf{A}^*$. Next, Theorem 6 below provides us with a basis for this column space.

Theorem 6 *Let* $\mathbf{A} = \left[\mathbf{F}^H\right]_{\{:,1:L_h\}} \mathbf{F}_{\{1:L_h,:\}}$ *with* $\left[\mathbf{F}^H\right]_{\{:,1:L_h\}} = \left[\overline{\mathbf{f}}_1, \overline{\mathbf{f}}_2, \ldots, \overline{\mathbf{f}}_{L_h}\right]$*, where* $\overline{\mathbf{f}}_k$ *is the* k^{th} *column vector of the DFT matrix* $\mathbf{F}^H$*. Then, let us construct the basis* $\mathcal{G} = \left\{\mathbf{g}_{-(L_h-1)}, \ldots, \mathbf{g}_{(L_h-1)}\right\}$ *from the* $2L_h - 1$ *vectors* $\mathbf{g}_d$ *defined as* $\mathbf{g}_d \triangleq \sqrt{N}\left(\overline{\mathbf{f}}_k \odot \overline{\mathbf{f}}_l^*\right)$*,* $k, l = 1, \ldots, L_h$*,* $d = k - l$*,* $d = -(L_h - 1), \ldots, (L_h - 1)$*. Then,* $\mathcal{G}$ *forms an orthonormal basis of the column space of* $\mathbf{A} \odot \mathbf{A}^*$*.*

Proof is given in Publication VII. Therefore, the channel squared amplitude spectrum lies in a subspace of dimension $2L_h - 1$. We conclude that $\operatorname{rank}\{\mathbf{A} \odot \mathbf{A}^*\} = 2L_h - 1$. Because $2L_h - 1 < N$ in practice, a low rank model arises from correlation in channel squared amplitude spectrum. Based on this property, we propose next a subspace method for blind frequency synchronization in OFDM.

6.2.3 Subspace method for blind CFO estimation for constant modulus modulations

Let us first make the following assumptions under which the proposed subspace based algorithm is derived:

1. All the N subcarriers are assumed to be active. The vector $\mathbf{s}(k)$ in (2.31) becomes the $N \times 1$ symbol vector $\mathbf{a}(k) = [a_1(k), \ldots, a_N(k)]^T$. The implications of the presence of null-subcarriers will be discussed at the end of this section.

2. We consider complex-valued constant modulus modulations. Without loss of generality, let us assume the symbols have unit energy, i.e., $|a_n(k)|^2 = 1$, $n = 0, \ldots, N-1$.

Let us assume that the received signal is subject to a carrier frequency offset ν, and consider the model in (2.27) for the CFO-corrupted signal. Given an estimate μ of the true value ν, let us recall from (6.4) the expression for the CFO-compensated vector in the frequency domain:

$$\begin{aligned} \mathbf{v}_{\mu\nu}(k) &= \varphi_k^*(\mu)\mathbf{F}^H\mathbf{C}^*(\mu)\mathbf{y}_\nu(k) && (6.21)\\ &= \varphi_k^*(\mu)\mathbf{F}^H\mathbf{C}^*(\mu)\mathbf{C}(\nu)\mathbf{F}\mathbf{D}_{\tilde{\mathbf{h}}}(k)\mathbf{a}(k) + \tilde{\mathbf{w}}(k), && (6.22)\end{aligned}$$

where $\tilde{\mathbf{w}}(k) = \varphi_k^*(\mu)\mathbf{F}^H\mathbf{C}^*(\mu)\mathbf{w}(k)$ is complex circular AWGN with covariance matrix $\operatorname{cov}(\tilde{\mathbf{w}}(k)) = \sigma^2\mathbf{I}_N$. From now on, we consider a single OFDM block at the time. Hence, we drop the time index k, for simplicity. In the noise-free case, let us compute the Hadamard product $\mathbf{v}_{\mu\nu} \odot \mathbf{v}_{\mu\nu}^*$ as

$$\mathbf{v}_{\mu\nu} \odot \mathbf{v}_{\mu\nu}^* = \left(\mathbf{M}_{\mu-\nu}\mathbf{D}_{\tilde{\mathbf{h}}}\mathbf{a}\right) \odot \left(\mathbf{M}_{\mu-\nu}^*\mathbf{D}_{\tilde{\mathbf{h}}}^*\mathbf{a}^*\right), \quad (6.23)$$

where we defined $\mathbf{M}_{\mu-\nu} = \mathbf{F}^H \mathbf{C}^*(\mu)\mathbf{C}(\nu)\mathbf{F}$ and the diagonal matrix $\mathbf{D}_{\tilde{\mathbf{h}}} = \text{diag}\{\tilde{\mathbf{h}}\}$ of size $N \times N$.

In case of perfect frequency synchronization, $\mu = \nu$ and $\mathbf{M}_{\mu-\nu} = \mathbf{I}_N$, where $\mathbf{I}_N$ is the $N \times N$ identity matrix. Then, in a noise-free situation, equation (6.23) reduces to

$$\mathbf{v}_{\nu\nu} \odot \mathbf{v}^*_{\nu\nu} = \left(\mathbf{D}_{\tilde{\mathbf{h}}}\mathbf{a}\right) \odot \left(\mathbf{D}^*_{\tilde{\mathbf{h}}}\mathbf{a}^*\right) \tag{6.24}$$

$$= \tilde{\mathbf{h}} \odot \tilde{\mathbf{h}}^*, \tag{6.25}$$

since the matrix $\mathbf{D}_{\tilde{\mathbf{h}}}$ is diagonal and $\mathbf{a} \odot \mathbf{a}^* = [1, \ldots, 1]^T$ under the CM assumption. Therefore $\mathbf{v}_{\nu\nu} \odot \mathbf{v}^*_{\nu\nu}$ is equal to the squared amplitude spectrum $\tilde{\mathbf{h}} \odot \tilde{\mathbf{h}}^*$, in the noise-free case. Frequency mismatch ($\mu \neq \nu$) leads to intercarrier interference (ICI) and alters the components of $\mathbf{v}_{\mu\nu} \odot \mathbf{v}^*_{\mu\nu}$, which does not lie in the correct subspace anymore, i.e., the one of $\tilde{\mathbf{h}} \odot \tilde{\mathbf{h}}^*$. The spanned subspaces are depicted in Figure 6.2. From Theorem 5, the vector $\tilde{\mathbf{h}} \odot \tilde{\mathbf{h}}^*$ lies in the column space of $\mathbf{A} \odot \mathbf{A}^*$. The latter has dimension $2L_h - 1 < N$, as a consequence of Theorem 6. Hence, a subspace-based blind CFO estimator may be proposed.

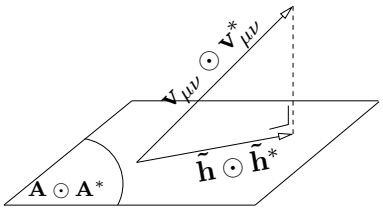

Figure 6.2: Subspaces used in proposed blind CFO estimation. Projection of $\mathbf{v}_{\mu\nu} \odot \mathbf{v}^*_{\mu\nu}$ to subspace of $\tilde{\mathbf{h}} \odot \tilde{\mathbf{h}}^*$ is maximized, or equivalently projection to orthogonal subspace is minimized.

In the noisy case, this leads to the idea of restoring the subspace structure induced by Fourier transforms and FIR communication channels. For this purpose, let us define the squared norm of the projection of $\mathbf{v}_{\mu\nu} \odot \mathbf{v}^*_{\mu\nu}$ to the orthogonal subspace of $\mathbf{A} \odot \mathbf{A}^*$ as cost function $\mathcal{C}$. Consequently, the carrier frequency offset may be estimated by minimizing the projection of $\mathbf{v}_{\mu\nu} \odot \mathbf{v}^*_{\mu\nu}$ to the orthogonal subspace of $\mathbf{A} \odot \mathbf{A}^*$, as a function of μ. The value achieving the minimum of $\mathcal{C}$ provides us with an estimate of the CFO as follows,

$$\hat{\nu} = \underset{\mu \in \left[-\frac{1}{2}, \frac{1}{2}\right[}{\arg\min}\, \mathcal{C}(\mu), \quad \mathcal{C}(\mu) = \left\| \mathbf{\Pi}^{\perp}_{\mathbf{A}\odot\mathbf{A}^*} \left(\mathbf{v}_{\mu\nu} \odot \mathbf{v}^*_{\mu\nu}\right) \right\|^2. \tag{6.26}$$

Now, the following clarifying remarks are in order:

1. The cost function $\mathcal{C}(\mu)$ is periodic with period 1, because replacing μ by $\mu + 1$ only produces a shift by one of the OFDM subcarriers, and therefore does not alter the subspace structure.

2. Numerical solution to (6.26) may be found, e.g., by using a gradient descent method. Computational cost is not prohibitive due to a one dimensional search space with unique minimum in $[-1/2, 1/2[$. See the plot of the cost function in Figure 6.3 (Section 6.2.5).

3. Since Theorem 6 provides us with an orthonormal basis for the column subspace of $\mathbf{A} \odot \mathbf{A}^*$, we may express the projection matrix $\mathbf{\Pi}^{\perp}_{\mathbf{A}\odot\mathbf{A}^*}$ in a closed-form as $\mathbf{\Pi}^{\perp}_{\mathbf{A}\odot\mathbf{A}^*} =$

$\mathbf{I}_N - \mathbf{G}\mathbf{G}^H$, where the $N \times (2L_h - 1)$ matrix $\mathbf{G}$ is constructed from the basis vectors of $\mathcal{G}$ stacked in matrix form. Hence, the projection matrix $\mathbf{\Pi}^{\perp}_{\mathbf{A}\odot\mathbf{A}^*}$ may be efficiently computed off-line.

4. One may also maximize the projection to the subspace of $\mathbf{A} \odot \mathbf{A}^*$ in order estimate the CFO.

5. Null-subcarriers are not needed to ensure a low rank model. Low rank model naturally arises from correlation in channel spectrum.

6.2.4 Blind subspace-based CFO estimation for real-valued constant modulus modulations

The CFO estimator in (6.26) applies to complex-valued CM modulations in general, including real-valued binary phase shift keying. However, the BPSK modulation requires a specific treatment, since the component-wise squared symbol vector is non-zero in this case, i.e., $\mathbf{a} \odot \mathbf{a} = [1, \ldots, 1]^T$. Hence, a low rank model is also found in the subspace of channel squared spectrum. In the following, we briefly highlight the differences between the two approaches.

The counterpart of Theorem 5 for channel squared spectra is found in Publication VI. As a result, the squared spectrum $\mathbf{h} \odot \mathbf{h}$ lies in the column space of $\mathbf{A} \odot \mathbf{A}$. Now, Theorem 6 may easily be extended as follows:

Theorem 7 *Let* $\mathbf{A}$ *and* $\bar{\mathbf{f}}_k$ *be defined as in Theorem 6. Then,* $\mathcal{G}_{BPSK} = \{\mathbf{g}_{BPSK,1}, \ldots, \mathbf{g}_{BPSK,2L_h-1}\}$ *with* $\mathbf{g}_{BPSK,d} \triangleq \sqrt{N}\left(\bar{\mathbf{f}}_k \odot \bar{\mathbf{f}}_l\right)$, $k, l = 1, \ldots, L_h$, $d = k + l - 1$, *forms an orthonormal basis of the column space of* $\mathbf{A} \odot \mathbf{A}$.

Hence, in case of BSPK modulation, the CFO may be found by minimizing the projection to the orthogonal subspace of $\mathbf{A} \odot \mathbf{A}$. The CFO estimator and the related cost function take the following form:

$$\hat{\nu} = \underset{\mu \in \left[-\frac{1}{2}, \frac{1}{2}\right[}{\arg\min} \left\| \mathbf{\Pi}^{\perp}_{\mathbf{A}\odot\mathbf{A}} \left(\mathbf{v}_{\mu\nu} \odot \mathbf{v}_{\mu\nu}\right) \right\|^2 . \tag{6.27}$$

As previously, the projection matrix may be computed off-line. As a consequence of Theorem 7 the latter projection matrix is found by $\mathbf{\Pi}^{\perp}_{\mathbf{A}\odot\mathbf{A}} = \mathbf{I}_N - \mathbf{G}_{\text{BPSK}}\mathbf{G}^H_{\text{BPSK}}$, where $\mathbf{G}_{\text{BPSK}}$ stacks the basis vector of $\mathcal{G}_{\text{BPSK}}$ in matrix form. Detailed analysis and simulation results may be found in Publication VI.

6.2.5 Relation to existing algorithms

Other algorithms exploiting the CM assumption

The CFO estimator in (6.26) is closely related to the work by Ghogho and Swami [97]. Assuming a single received block with a number $N_v = N - N_a$ of VSCs at the edges, the following composite criterion exploiting both VSCs and the CM property is proposed [97]:

$$\mathcal{J}_{\text{VSC+CM}}(\mu) = \mathcal{J}_{\text{VSC}}(\mu) + \mathcal{J}_{\text{CM}}(\mu), \tag{6.28}$$

with

$$\mathcal{J}_{\text{VSC}}(\mu) = \sum_{n \notin \mathcal{N}_{\text{A}}} \left| \mathbf{f}_n^H \mathbf{C}^*(\mu) \mathbf{y}_\nu \right|^2 \tag{6.29}$$

$$\mathcal{J}_{\text{CM}}(\mu) = \sum_{n \in \mathcal{N}_{\text{A}}} \left(\left| \mathbf{f}_n^H \mathbf{C}^*(\mu) \mathbf{y}_\nu \right| - \sqrt{\mathbf{c}_n^T \hat{\boldsymbol{\lambda}}(\mu)} \right)^2, \tag{6.30}$$

and where

$$\begin{aligned}
\hat{\boldsymbol{\lambda}}(\mu) &= \mathbf{G}_{\text{CM}_2}^{\dagger} \sum_{n' \in \mathcal{N}_{\text{A}}} \left| \mathbf{f}_{n'}^H \mathbf{C}^*(\mu) \mathbf{y}_\nu \right|^2 \mathbf{c}_{n'} \\
\mathbf{G}_{\text{CM}_2} &= \sum_{n \in \mathcal{N}_{\text{A}}} \mathbf{c}_n \mathbf{c}_n^T \\
\mathbf{c}_n &= \sqrt{2} \left[\frac{1}{\sqrt{2}}, \cos\left(\frac{2\pi n}{N}\right), \ldots, \cos\left(\frac{2\pi n L_h'}{N}\right), \sin\left(\frac{2\pi n}{N}\right), \ldots, \sin\left(\frac{2\pi n L_h'}{N}\right) \right]^T.
\end{aligned}$$

The criterion $\mathcal{J}_{\text{VSC}}$ is equivalent to Tureli's NSC-based cost function [167], while $\mathcal{J}_{\text{CM}}$ exploits the CM property [97]. The estimate of the CFO is then obtained as

$$\hat{\nu}_{\text{VSC+CM}} = \arg\min_{\mu} \mathcal{J}_{\text{VSC+CM}}(\mu). \tag{6.31}$$

The flexibility of the above estimator is worth to be noted, as it may perform with or without VSCs. Without virtual subcarrier, it exploits the constant modulus assumption solely.

The likelihood function depends in fact on both the CFO and the values $|\tilde{h}_n|$ of the channel amplitude spectrum, where $\tilde{\mathbf{h}} = [\tilde{h}_0, \ldots, \tilde{h}_{N-1}]^T$ is the CFR vector defined in (6.17). In order to obtain a scalar optimization procedure, the search over the values $|\tilde{h}_n|$ needs to be eliminated. Both Publications VII and [97] rely on equivalent parametrization of the squared amplitude spectrum $|\tilde{h}_n|^2$. For this reason, the considered criteria are not ML anymore, although they lead to consistent estimates of the CFO.

Link to the proposed algorithm

Let us now describe the relation of the algorithm in Publication VII and the related geometrical approach to the estimator in [97]. Under the assumptions of Publication VII, i.e., CM modulations and no virtual subcarrier, the cost function in (6.28) reduces to $\mathcal{J}_{\text{CM}}$ solely. Then, similarly to [97], let us consider the following modified criterion:

$$\mathcal{J}'_{\text{CM}}(\mu) = \sum_{n=0}^{N-1} \left(\left| \mathbf{f}_n^H \mathbf{C}^*(\mu) \mathbf{y}_\nu \right|^2 - \mathbf{c}_n^T \hat{\boldsymbol{\lambda}}(\mu) \right)^2. \tag{6.32}$$

One may easily show that $\mathcal{J}'_{\text{CM}}$ is equivalently expressed as

$$\mathcal{J}'_{\text{CM}}(\mu) = \left\| \boldsymbol{\Pi}_{\text{CM}}^{\perp} \left(\mathbf{v}_{\mu\nu} \odot \mathbf{v}_{\mu\nu}^* \right) \right\|^2, \tag{6.33}$$

where $\boldsymbol{\Pi}_{\text{CM}}^{\perp} = \mathbf{I_N} - \frac{1}{N} \mathbf{C}_{\text{CM}}^T \mathbf{C}_{\text{CM}}$ is the projection matrix to the orthogonal subspace of $\mathbf{C}_{\text{CM}} = [\mathbf{c}_1, \ldots, \mathbf{c}_N]$.

As discussed previously, equivalent parametrization of the subspace of squared channel amplitude spectrum implies that $\boldsymbol{\Pi}_{\text{CM}}^{\perp} = \boldsymbol{\Pi}_{\mathbf{A} \odot \mathbf{A}^*}^{\perp}$. Consequently, the modified criterion

leads to the cost function proposed in Publication VII. The link with the projection argument is therefore established (see (6.26)). The difference between [97] and the method in Publication VII lies in the square-root operation in (6.30). While adding to the computational complexity, it makes the criterion closer to the ML solution [97]. Nevertheless, both Publications VII and [97] rely on the modified criterion of equation (6.32). For this reason, they yield approximate ML estimates only. In practice, however, simulations studies show that the gap to the CRB is very small. The cost functions for the proposed method as well as the criteria relying on the CM property, VSCs and the combination of them are illustrated in Figure 6.3 below.

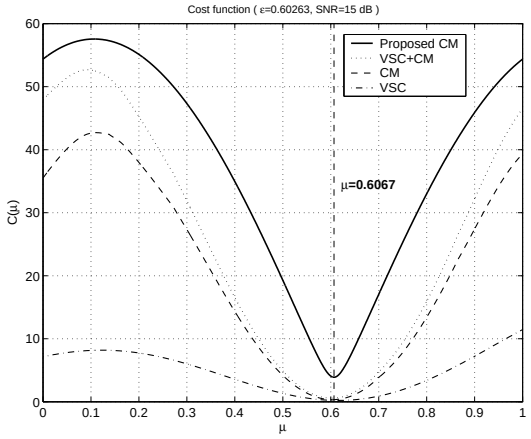

Figure 6.3: Cost functions for proposed subspace based blind CFO estimation, joint VSC and CM criterion [97], CM [97] and VSC criteria [167] only; $\nu = 0.60263$, SNR=15 dB.

6.2.6 Discussion

In this section, we presented novel subspace-based algorithms for blind carrier frequency offset estimation in OFDM using real- or complex-valued constant modulus modulations. See Publications VI-VII for a detailed derivation. Exploiting correlation in squared or squared amplitude spectrum of the channel is the key idea of the methods. Due to DFT and IDFT operations, low rank model is feasible in OFDM transmission provided that the channel length L_h is such that $2L_h - 1 < N$. This is generally the case for a well designed OFDM system since $L_h \leq L_{\mathrm{CP}} < (N+1)/2$. Low rank signal model is therefore obtained without null-subcarriers.

Unlike majority of blind CFO recovery techniques, the proposed estimator needs only a single OFDM block to perform fine frequency synchronization. Thus, no time averaging is needed, unlike in correlation and SOCS-based methods which typically require up to a hundred of received blocks. Hence, the proposed algorithms may be used to find an estimate for each block independently. This is obviously significant advantage in the case of time selective channels. Numerical solution to (6.26) or (6.27) may be found, e.g., using a gradient descent method. Computational cost is not prohibitive due to the one-dimensional search space and unique minimum in $[-1/2, 1/2[$. Notice that the geometrical projection argument is different compared to [45]: the subspace of squared or squared amplitude channel spectra is considered here instead of the subspace of null-subcarriers [45].

However, as for any subspace method, the dimensions of subspaces have to be known a priori for optimal performance. The proposed estimator as well as [97] need the channel length as input parameter. The performance of both methods suffers from under-estimated

delay spread, while both still perform well with slightly over-estimated assumed channel length. The length of the cyclic prefix yields a reasonable upper limit in practice. Note that purely NSC-based estimators are not affected by an unknown channel length, as the subspace structure is determined by the location of null-subcarriers, assumed to be known a priori. The proposed approach could be potentially extended to include NSCs as in [97]. For this purpose, the subspace description of channel squared spectra needs to be modified to accommodate for the presence of NSCs. The extension to non-constant modulus modulation may be feasible as well. However, the subspaces become data dependent in this case.

The performance of the proposed algorithms is analyzed in simulations. The results are reported in Publications VI-VII. Close to optimal estimation of time-varying carrier offset in time-frequency selective channels is achieved. Performance is comparable to the methods developed in [97], and more than 10 dB gain is achieved over NSC-based estimators [167]. To conclude, estimation using a constant modulus criterion is more effective than exploiting null-subcarriers solely. CM-based estimators are especially suited to time selective channels as estimators requiring small sample support are highly desired. However, they are restricted to CFO refinement, as the estimation range for the normalized CFO is within $[-1/2, 1/2[$. However, by adding NSCs and choosing the composite criterion in [97], the estimation range may be increased.

Finally, the relationship to the estimator in [97] as well as with ML estimation was established. Also, it proves that [97] is a projection-based algorithm as well. It appears that the approaches in [97] and Publication VII are extremely close together from the algorithm and performance standpoints. Despite being approximate ML methods, they lead to highly accurate and consistent estimation of the CFO under time-frequency selective fading.

6.3 Large sample performance

In this section, we assess the large sample performance by deriving the Cramér-Rao bound. Detailed derivations as well as simulation results may be found in Publications IV-V. The CRB gives the minimum variance an unbiased estimator may achieve. The CRB is established for the blind CFO estimation problem in OFDM, under the three following assumptions:

1. Channel parameters are treated as deterministic nuisance parameters, and are assumed to be constant over the observation period.

2. The noise is assumed to be complex circular Gaussian and uncorrelated.

3. Data symbols are i.i.d. complex random variables drawn from either real- or complex-valued constellations.

Under the stochastic approach, we model the transmitted data $\tilde{\mathbf{x}}(k) = \mathbf{F}\mathbf{s}(k)$ in (2.7) as a complex Gaussian random vector. In this way, we get rid of both the data and channel dependencies. For this reason, the related CRB will be further referred to as stochastic CRB. The Gaussian approximation has been widely used in the OFDM literature [188, 272]. This approximation is justified by the central limit theorem. Here, we assume that the vector $\mathbf{r}(k) = \tilde{\mathbf{H}}\tilde{\mathbf{x}}(k)$ is multivariate Gaussian. Then, the OFDM transmission with imperfect frequency synchronization in (2.26) may be written as

$$\mathbf{y}_\nu(k) = \bar{\mathbf{C}}_{\nu,k}\mathbf{r}(k) + \mathbf{w}(k), \tag{6.34}$$

where $\bar{\mathbf{C}}_{\nu,k} = \varphi_k(\nu)\mathbf{C}(\nu)$ and $\mathbf{w}$ is the complex circular Gaussian noise vector. Since we are interested in both real and complex modulations, $\tilde{\mathbf{x}}(k)$ cannot always be modeled as a complex circular random vector. Complete second order statistics of complex random vectors require both signal covariance and pseudo-covariance matrices (see Section 6.1.1 and [215]). Hence, we also define

$$\mathbf{Q} = \mathrm{cov}\left(\mathbf{r}(k)\right) \tag{6.35}$$

$$\mathbf{P} = \mathrm{pcov}\left(\mathbf{r}(k)\right). \tag{6.36}$$

Notice that the pseudo-covariance matrix $\mathbf{P}$ vanishes for circular random vectors, i.e., $\mathbf{P} = \mathbf{0}_{N\times N}$. This happens for instance with complex modulations having independent and identically distributed I an Q branches. We further assume that the entire statistics $\{\mathbf{P}, \mathbf{Q}\}$ depend only on a finite number M of real-valued unknown parameters stacked into the vector $\boldsymbol{\rho} = [\rho_1, \ldots, \rho_M]^T$.

Let us define the parameter vector as $\boldsymbol{\theta} = [\nu, \boldsymbol{\rho}^T, \alpha]^T$, where $\alpha = \sigma^2$ the variance of the noise. The CFO ν is the parameter of interest while $\boldsymbol{\rho}$ and α are nuisance parameters. The CRB for blind frequency offset estimation in OFDM and the associated Fisher information matrix (FIM) with finite sample size K are respectively given by

$$\mathrm{CRB}_K\left(\nu\right) = \left[\mathrm{FIM}_K^{-1}\right]_{1,1} \tag{6.37}$$

$$\mathrm{FIM}_K = \frac{1}{2}\sum_{k=0}^{K-1}\begin{bmatrix}\mathbf{g}_k^H \\ \boldsymbol{\Delta}_k^H\end{bmatrix}\begin{bmatrix}\mathbf{g}_k & \boldsymbol{\Delta}_k\end{bmatrix}, \quad \mathrm{FIM}_K \in \mathbb{C}^{(M+2)\times(M+2)}, \tag{6.38}$$

with the following notation and definitions:

$$\mathbf{g}_k = \mathrm{vec}(\boldsymbol{\Omega}_k^{-1/2}(\tilde{\mathbf{D}}_{\nu,k}\tilde{\boldsymbol{\Omega}}\tilde{\mathbf{C}}_{\nu,k}^H + \tilde{\mathbf{C}}_{\nu,k}\tilde{\boldsymbol{\Omega}}\tilde{\mathbf{D}}_{\nu,k}^H)\boldsymbol{\Omega}_k^{-1/2}), \quad \mathbf{g}_k \in \mathbb{C}^{4N^2\times 1} \tag{6.39}$$

$$\boldsymbol{\Delta}_k = \begin{bmatrix}\mathbf{V}_k & \mathbf{u}_k\end{bmatrix}, \quad \mathbf{V}_k \in \mathbb{C}^{4N^2\times M}, \quad \mathbf{u}_k \in \mathbb{C}^{4N^2\times 1} \tag{6.40}$$

$$\tilde{\mathbf{C}}_{\nu,k} = \begin{bmatrix}\bar{\mathbf{C}}_{\nu,k} & \mathbf{0}_{N\times N} \\ \mathbf{0}_{N\times N} & \bar{\mathbf{C}}_{\nu,k}^*\end{bmatrix}, \; \tilde{\mathbf{D}}_{\nu,k} = \frac{\partial}{\partial\nu}\tilde{\mathbf{C}}_{\nu,k} \tag{6.41}$$

$$\boldsymbol{\Omega}_k = \tilde{\mathbf{C}}_{\nu,k}\tilde{\boldsymbol{\Omega}}\tilde{\mathbf{C}}_{\nu,k}^H + \sigma^2\mathbf{I}_{2N} \tag{6.42}$$

$$\tilde{\boldsymbol{\Omega}} = \begin{bmatrix}\mathbf{Q} & \mathbf{P} \\ \mathbf{P}^H & \mathbf{Q}^*\end{bmatrix} \tag{6.43}$$

$$\mathbf{u}_k = \mathrm{vec}\left(\boldsymbol{\Omega}_k^{-1}\right) \tag{6.44}$$

$$\mathbf{V}_k = \left((\boldsymbol{\Omega}_k^{-1/2}\tilde{\mathbf{C}}_{\nu,k}^*) \otimes (\boldsymbol{\Omega}_k^{-1/2}\tilde{\mathbf{C}}_{\nu,k})\right)\mathbf{J}, \quad \mathbf{J} \in \mathbb{C}^{4N^2\times M}. \tag{6.45}$$

The matrix $\mathbf{J}$ in (6.45) is such that $\mathrm{vec}(\tilde{\boldsymbol{\Omega}}) = \mathbf{J}\boldsymbol{\rho}$. Detailed derivations may be found in Publications IV and V. Note that an alternate expression for the CRB for a similar model has also been independently derived in [58]. Even though the component-wise Gaussian approximation is reasonable, the assumption on the joint Gaussianity of the components is more questionable, and this may lead to slight differences compared to the exact CRB. Notice finally that the quantities defined in (6.39)-(6.45) are not block dependent anymore when the transmitted signal becomes circular. In this case, the computation of the CRB is of significantly lower complexity.

It is interesting to compare the obtained bounds for the circular and non-circular cases. The curves presented in Publication V highlight a significant difference in performance between the circular and non-circular case, which is in par with the results in [58]. Much lower CRBs are observed whenever the signal is non-circular. Moreover, for finite sample

size, the Cramér-Rao bound tends to zero as the SNR tends to infinity for non-circular signals, which does not hold true for the circular case. This implies that blind CFO estimators may be significantly improved by exploiting a complete second order statistics, in place of the covariance matrix only, when real modulations are in use. The improvement has been already noted in practice, for instance in [63].

Another approach for deriving the CRB is to assume that the received signal affected by both channel fading and CFO is a deterministic unknown vector, i.e., the vector $\bar{\mathbf{C}}_{\nu,k}\mathbf{r}(k)$ in (6.34) is non-random. The related Cramér-Rao bound is referred to as conditional CRB (CCRB). It is also called deterministic CRB. Detailed derivations for the case of OFDM may be found in [101, 8.8.1]. The CCRB is a useful tool in order to lower-bound the CFO estimation performance for particular channel and data realizations. A channel and data independent bound must be derived to assess the large sample performance for random channel and data processes. It is then referred to as unconditional or stochastic CRB. Such bound is derived in [101, 8.8.2], whereas the CRB herein applies to deterministic channel and random data processes.

6.4 Concluding remarks

In this chapter, the contributions of this thesis to the field of blind CFO estimation for OFDM were presented. A blind CFO estimator based on the diagonality of the received signal covariance matrix was derived. Intuitively, the value of the CFO is found by restoring the orthogonality of the transmission. The proposed estimator was shown to provide consistent estimates of the CFO under frequency selective fading, and achieves almost equal performance regardless of the noise level. A subspace-based blind CFO estimator exploiting the constant modulus property was also proposed as part of this thesis work. It was shown that a low rank signal model arises from correlation in channel spectrum. Hence, NSCs are not necessarily needed to allow blind subspace CFO estimation in OFDM. However, they may be exploited jointly with the CM assumption [97].

The proposed covariance- and subspace-based estimators may be applied to fine CFO estimation in the range of $[-1/2, 1/2[$ with respect to the intercarrier spacing. Hence, they may be used in practice for refinement purposes or in the face of small carrier frequency mismatches. Both estimators assume frequency selective fading, and no performance degradation is observed compared to the AWGN case. For instance, some other CFO estimators in the literature exhibit error floors in multipath fading [272]. The design of channel independent estimators is of high importance indeed. NSC-based estimators fall into this category as well. The proposed subspace CFO estimation requires significantly smaller sample size compared to the method based on the covariance matrix (1 block versus 30-100 blocks, respectively). Thus, in highly time selective environments, estimators with small sample support should be preferred. NSC-based estimation [167] or the combined NSC and CM approach [97] as well as the proposed subspace estimator require only small sample support.

Finally, in order to assess the large sample performance, the stochastic Cramér-Rao bound was established. As real-valued modulations induce non-circularity in the received signal, the derivation of the CRB was conducted for the general complex multivariate Gaussian distribution [215].

Chapter 7

Summary

The wireless telecommunication industry has grown at fast pace since the beginning of the 1980's. The Internet has enjoyed a similar growth over the last decade. The next stage will be the convergence of fixed and mobile Internet systems, which means making the Internet and high data rate multimedia applications available to mobile users in addition to digital speech and text messaging services. The telecommunication standards and systems have already evolved toward this step, with the enhancements of third generation communication networks such as the high speed data packet access (HSDPA). Packet data is expected to become soon a significant part of the total wireless traffic. Beyond 3G and 4G systems are targeting far higher data rates, spectral efficiency and mobility requirements. MIMO multicarrier wireless transmission techniques are strong candidates for radio access technology in such systems.

Advanced signal processing techniques are needed at the physical layer level in order to ensure reliable data transmission. Receiver algorithms are required to cope with impairments specific to wireless broadband channels characterized by time, frequency and space selectivity. Spatial multiplexing and transmit diversity techniques allow increasing the spectral efficiency and the link reliability of multi-antenna systems [126]. They rather exploit than combat the channel selectivity, which is also a source of diversity. In order to fully capitalize on MIMO multicarrier transmissions, channel estimation and frequency synchronization should be accomplished with high fidelity. The parameters should not only be acquired, but they should also be tracked over time as the wireless environment may be time-varying. At the same time, the overhead of pilot symbols should be kept as low as possible to maintain high effective data rates. Computational complexity should also remain at low levels, which is an important issue in battery operated terminals especially.

The work reported in this thesis provides new solutions for practical MIMO OFDM receivers operating in time-varying wireless environments. State-space models are used for modeling the transmission and its time evolution under imperfect frequency synchronization. The proposed state-space model was among the first ones to consider separate frequency offset parameter for each MIMO branch, which is justified by separate RF-IF transmission chains, mobility and rich scattering together with large angle spread. A novel algorithm for the joint estimation and tracking of time and frequency offset parameters in mobile MIMO OFDM systems is introduced. The algorithm performs recursive estimation of the state parameters using Kalman and extended Kalman filters, which is a natural way to deal with state-space models. Since the 1960's, Kalman filter has been applied in control theory and to signal processing problems. Hence, it proves to be a valuable tool which is now highly popular in the wireless communications community. In the derived algorithm, the estimation and tracking is done in time domain. Time domain processing leads

to lower computational complexity, lower estimation variance and increased robustness against estimation errors compared to frequency domain estimation and tracking. Equalization takes place in the frequency domain, as it is usually the case in OFDM systems. A few training blocks are needed to acquire initial estimates for channel and synchronization parameters. Then, the method switches to decision-directed mode and uses the decoded symbols for keeping the track. Training symbols need to be sent periodically in order to avoid loosing the track, which could occur in case of a deep channel fade. In highly time selective channels more pilot symbols are naturally needed. Also, Kalman filters may easily accommodate pilot data for channel estimation purposes. Experimental results show good overall performance of the proposed algorithm in the face of noise and multiple carrier frequency mismatches as well as time, frequency and space selective fading. Moreover, the method requires only a few percents training overhead. Hence, it yields a feasible solution for practical mobile multi-antenna OFDM transceivers with high effective data rates.

Novel approaches for blind fine frequency synchronization are proposed in this thesis. The decoupling of data and pilot information may be difficult in the presence of CFO. For this reason, blind frequency synchronization is appealing as no pilot symbol needs to be extracted. It is shown that the sample covariance matrix contains information on the carrier frequency offset in OFDM transmissions with cyclic-prefix. Consequently, the CFO may be estimated by exploiting the structure and properties of this matrix. By choosing the off-diagonal power as cost function, a novel algorithm for fine carrier frequency synchronization is derived. Estimation of the CFO is entirely accomplished in a closed-form, which leads to low complexity solution as well as low estimation variance. The proposed algorithm is a consistent estimator of the CFO under multipath fading. In theory, the performance does not depend on the signal-to-noise ratio. This is a significant advantage at low SNR regime. The tolerance to multipath propagation is also a key property, as channel state information is usually not available at this stage. Channel estimation is typically performed as a subsequent step. In this dissertation, contributions are also made in the area of subspace-based CFO estimation. Assuming constant modulus modulations, low rank signal model arises in almost any OFDM transmission because of the finite CIR length much shorter than the DFT window. Based on this property, a novel fine CFO estimator is introduced. Close-to-optimal estimation of the carrier frequency offset is achieved under time-frequency selective fading. The small sample support needed by the technique is a key advantage in time selective channels. Finally, the large sample performance of blind CFO estimators for OFDM is investigated. The Cramér-Rao bound is derived under the general multivariate Gaussian assumption. In this way, the non-circularity of the received signal due to the potential use of real-valued modulations is also taken into account. It is shown that the performance of blind carrier frequency synchronizers may be significantly improved in the non-circular case by using complete second-order statistics, i.e., covariance and pseudo-covariance matrices.

Possible topics of future research include channel estimation and synchronization for multi-user MIMO systems and multicarrier CDMA systems. MC-CDMA combines the advantages of both CDMA and OFDM in order to provide a high data rate multi-user air interface. However, MC-CDMA also inherits the drawbacks of both systems. It is thus very sensitive to synchronization errors. The state-space models developed in this thesis may further be extended to describe MC-CDMA transmissions impaired by carrier frequency offsets. Time synchronization may be considered as well. The proposed KF/EKF estimation framework may then be adapted to estimate and track channel and synchronization parameters in MC-CDMA.

OFDMA is another popular and active field of research. In the uplink of an OFDMA

system, each user modulates a subset of subcarriers that is impaired by a specific carrier frequency offset. Hence, the synchronization of such systems is much more demanding compared to conventional OFDM. Low synchronization errors guarantee both efficient user separation and high data rates. Reliable CFO and timing estimators with low overhead are desired. Theoretical performance bounds as well as identifiability conditions are of high importance, especially in a blind estimation framework.

A multiband version of OFDM (MB-OFDM) is gaining momentum as a candidate standard to be adopted for ultrawideband (UWB) communications [129]. The popularity of MB-OFDM stems from its abilities to address data throughput and range requirements, while maintaining low cost, computational complexity and power consumption. Also, the transmission spectrum may be easily shaped to comply with international regulations and may be extended as well for future enhancements. Frequency hopping across multiple bands offers improved diversity and multi-user access, but gives rise to new challenges in channel estimation and carrier frequency synchronization. Very efficient signal processing techniques are therefore necessary to allow the practical deployment of such systems.

Bibliography

[1] IEEE standard for local and metropolitan area networks part 16: Air interface for fixed broadband wireless access systems. *IEEE Std 802.16-2004 (Revision of IEEE Std 802.16-2001)*, pages 0 – 857, 2004.

[2] 3GPP - Technical Specification Group Radio Access Network. Physical layer aspects for evolved UTRA. *3GPP TR 25.814*, R7. Available for download at: http://www.3gpp.org/.

[3] 3GPP - Third Generation Partnership Project. Url: http://www.3gpp.org/.

[4] T. Abrudan, M. Sirbu, and V. Koivunen. A block-toeplitz VCMA equalizer for MIMO-OFDM systems. In *Conference Record of the Thirty-Seventh Asilomar Conference on Signals, Systems and Computers*, volume 1, pages 1037–1041, Nov. 2003.

[5] S. Adireddy, L. Tong, and H. Viswanathan. Optimal embedding of known symbols for OFDM. In *Proc. of the IEEE International Conference on Acoustics, Speech, and Signal Processing*, volume 5, pages 2541–2544, Jun. 2000.

[6] S. Adireddy, L. Tong, and H. Viswanathan. Optimal placement of training for frequency-selective block-fading channels. *IEEE Transactions on Information Theory*, 48(8):2338–2353, Aug. 2002.

[7] A. Aghamohammadi, H. Meyr, and G. Ascheid. Adaptive synchronization and channel parameter estimation using an extended Kalman filter. *IEEE Transactions on Communications*, 37(11):1212–1219, Nov. 1989.

[8] S. Ahmed, S. Lambotharan, A. Jakobsson, and J.A. Chambers. Parameter estimation and equalization techniques for communication channels with multipath and multiple frequency offsets. *IEEE Transactions on Communications*, 53(2):219–223, Feb. 2005.

[9] T.Y. Al-Naffouri, O. Awoniyi, O. Oteri, and A. Paulraj. Receiver design for MIMO-OFDM transmission over time variant channels. In *Proc. of the IEEE Global Telecommunications Conference*, volume 4, pages 2487–2492, Dec. 2004.

[10] T.Y. Al-Naffouri, A. Bahai, and A. Paulraj. Semi-blind channel identification and equalization in OFDM: an expectation-maximization approach. In *Proc. of the IEEE Vehicular Technology Conference*, volume 1, pages 13–17, Sept. 2002.

[11] T.Y. Al-Naffouri and A. Paulraj. A forward-backward Kalman for the estimation of time-variant channels in OFDM. In *Proc. of the IEEE Workshop on Signal Processing Advances in Wireless Communications*, pages 670–674, Jun. 2005.

[12] T.Y. Al-Naffouri, D. Toumpakaris, A. Bahai, and A. Paulraj. An adaptive semi-blind algorithm for channel identification in OFDM. In *Conference Record of the Thirty-Fifth Asilomar Conference on Signals, Systems and Computers*, volume 2, pages 921–925, Nov. 2001.

[13] G.A. Al-Rawi, T.Y. Al-Naffouri, A. Bahai, and J. Cioffi. Exploiting error-control coding and cyclic-prefix in channel estimation for coded OFDM systems. *IEEE Communications Letters*, 7(8):388–390, Jul. 2003.

[14] G.A. Al-Rawi, T.Y. Al-Naffouri, A. Bahai, and J. Cioffi. An iterative receiver for coded OFDM systems over time-varying wireless channels. In *Proc. of the IEEE International Conference on Communications*, volume 5, pages 3371–3376, May 2003.

[15] E. Al-Susa and R.F. Ormondroyd. A predictor-based decision feedback channel estimation method for COFDM with high resilience to rapid time-variations. In *Proc. of the IEEE Vehicular Technology Conference*, volume 1, pages 273–278, Sept. 1999.

[16] H. Ali, J.H. Manton, and Y. Hua. A SOS subspace method for blind channel identification and equalization in bandwidth efficient OFDM systems based on receive antenna diversity. In *Proc. of the 11th IEEE Signal Processing Workshop on Statistical Signal Processing*, pages 401–404, Aug. 2001.

[17] ANSI. Network and customer installation interfaces - asymmetric digital subscriber line (ADSL). *T1.413*, 1998.

[18] J. Armstrong. Analysis of new and existing methods of reducing intercarrier interference due to carrier frequency offset in OFDM. *IEEE Transactions on Communications*, 47(3):365–369, Mar. 1999.

[19] P. Arun, R. Venkatesh, S. Karthikeyan, and S. Srikanth. Multiple access schemes for OFDM based indoor wireless systems. In *Proc. of the 8th National conference on communications, Mumbai, India*, pages 488–492, Jan. 2002.

[20] C.R.N. Athaudage and A.D.S. Jayalath. Enhanced MMSE channel estimation using timing error statistics for wireless OFDM systems. *IEEE Transactions on Broadcasting*, 50(4):369–376, Dec. 2004.

[21] S. Attallah. Blind estimation of residual carrier offset in OFDM systems. *IEEE Signal Processing Letters*, 11(2):216–219, Feb. 2004.

[22] G. Auer. Analysis of pilot-symbol aided channel estimation for OFDM systems with multiple transmit antennas. In *Proc. of the IEEE International Conference on Communications*, volume 6, pages 3221–3225, Jun. 2004.

[23] B. Bai, X. Xu, Y. Cai, and Z. Ii. Optimal pilot patterns for OFDM system based on two-dimension sampling theory. In *Proc. of the International Conference on Neural Networks and Signal Processing*, volume 1, pages 663–666, Dec. 2003.

[24] W. Bai and Z. Bu. Subspace based channel estimation in MIMO-OFDM systems. In *Proc. of the IEEE Vehicular Technology Conference*, volume 2, pages 598–602, May 2004.

[25] W. Bai, C. He, L.G. Jiang, and H.W. Zhu. Blind channel estimation in MIMO-OFDM systems. In *Proc. of the IEEE Global Telecommunications Conference*, volume 1, pages 317–321, Nov. 2002.

[26] W. Bai, H. Yang, and Z. Bu. Blind channel identification in SIMO-OFDM systems. In *Proc. of the International Conference on Communications, Circuits and Systems*, volume 1, pages 318–321, Jun. 2004.

[27] A. Barabell. Improving the resolution performance of eigenstructure-based direction-finding algorithms. In *Proc. of the IEEE International Conference on Acoustics, Speech, and Signal Processing*, volume 8, pages 336–339, Apr. 1983.

[28] S. Barbarossa, M. Pompili, and G.B. Giannakis. Channel-independent synchronization of orthogonal frequency division multiple access systems. *IEEE Journal on Selected Areas in Communications*, 20(2):474–486, Feb. 2002.

[29] I. Barhumi, G. Leus, and M. Moonen. Optimal training design for MIMO OFDM systems in mobile wireless channels. *IEEE Transactions on Signal Processing*, 51(6):1615–1624, Jun. 2003.

[30] I. Barhumi, G. Leus, and M. Moonen. Time-domain channel shortening and equalization of OFDM over doubly-selective channels. In *Proc. of the IEEE International Conference on Acoustics, Speech, and Signal Processing*, volume 3, pages 801–804, May 2004.

[31] K. Barner and A. Gonzalo. *Nonlinear Signal and Image Processing: Theory, Methods, and Applications*. CRC Press, 2004.

[32] O. Besson and P. Stoica. On parameter estimation of MIMO flat-fading channels with frequency offsets. *IEEE Transactions on Signal Processing*, 51(3):602–613, Mar. 2003.

[33] J.A.C. Bingham. Multicarrier modulation for data transmission: an idea whose time has come. *IEEE Communications Magazine*, 28(5):5–14, May 1990.

[34] H. Bölcskei. Blind high-resolution uplink synchronization of OFDM-based multiple access schemes. In *Proc. of the IEEE Workshop on Signal Processing Advances in Wireless Communications*, pages 166–169, May 1999.

[35] H. Bölcskei. Blind estimation of symbol timing and carrier frequency offset in wireless OFDM systems. *IEEE Transactions on Communications*, 49(6):988–999, Jun. 2001.

[36] H. Bölcskei, P. Duhamel, and R. Hleiss. A subspace-based approach to blind channel identification in pulse shaping OFDM/OQAM systems. *IEEE Transactions on Signal Processing*, 49(7):1594–1598, Jul. 2001.

[37] H. Bölcskei, R.W. Jr. Heath, and A.J. Paulraj. Blind channel identification and equalization in OFDM-based multiantenna systems. *IEEE Transactions on Signal Processing*, 50(1):96–109, Jan. 2002.

[38] A. Bria, F. Gessler, O. Queseth, R. Stridh, M. Unbehaun, J. Wu, J. Zander, and M. Flament. 4th-generation wireless infrastructures: scenarios and research challenges. *IEEE Personal Communications*, 8(6):25–31, Dec. 2001.

[39] S. B. Bulumulla, S. A. Kassam, and S. S. Venkatesh. An adaptive diversity receiver for OFDM in fading channels. In *Proc. of the IEEE International Conference on Communications*, volume 3, pages 1325–1329, Jun. 1998.

[40] S. B. Bulumulla, S. A. Kassam, and S. S. Venkatesh. A systematic approach to detecting OFDM signals in a fading channel. *IEEE Transactions on Communications*, 48(5):725–728, May 2000.

[41] J. Cai, X. Shen, and J.W. Mark. Robust channel estimation for OFDM wireless communication systems - An H_∞ approach. *IEEE Transactions on Wireless Communications*, 3(6):2060–2071, Nov. 2004.

[42] X. Cai and A.N. Akansu. A subspace method for blind channel identification in OFDM systems. In *Proc. of the IEEE International Conference on Communications*, volume 2, pages 929–933, Jun. 2000.

[43] M.X. Chang and Y.T. Su. Model-based channel estimation for OFDM signals in Rayleigh fading. *IEEE Transactions on Communications*, 50(4):540–544, Apr. 2002.

[44] R.W. Chang. Synthesis of band-limited orthogonal signals for multichannel data transmission. *Bell Syst. Tech. Journal*, 45:1775–1796, Dec. 1966.

[45] B. Chen. Maximum likelihood estimation of OFDM carrier frequency offset. *Signal Processing Letters*, 9(4):123–126, Apr. 2002.

[46] B. Chen and H. Wang. Blind estimation of OFDM carrier frequency offset via oversampling. *IEEE Transactions on Signal Processing*, 52(7):2047–2057, Jul. 2004.

[47] N. Chen and G.T. Zhou. A superimposed periodic pilot scheme for semi-blind channel estimation of OFDM systems. In *Proc. of the Digital Signal Processing Workshop*, pages 362–365, Oct. 2002.

[48] W. Chen and R. Zhang. Kalman-filter channel estimator for OFDM systems in time and frequency-selective fading environment. In *Proc. of the IEEE International Conference on Acoustics, Speech, and Signal Processing*, volume 4, pages iv–377–iv–380, May 2004.

[49] Y.Y. Cheng, Y. Lee, and H.J. Li. Subspace-MMSE blind channel estimation for multiuser OFDM with receiver diversity. In *Proc. of the IEEE Global Telecommunications Conference*, volume 4, pages 2295–2299, Dec. 2003.

[50] Z. Cheng and D. Dahlhaus. Time versus frequency domain channel tracking using Kalman filters for OFDM systems with antenna arrays. In *Proc. of the IEEE Vehicular Technology Conference, VTC 2003-Spring*, volume 1, pages 651–655, Apr. 2003.

[51] L. Chengyang and S. Roy. Subspace-based blind channel estimation for OFDM by exploiting virtual carriers. *IEEE Transactions on Wireless Communications*, 2(1):141–150, Jan. 2003.

[52] H. Cheon and D. Hong. A blind spatio-temporal equalizer using cyclic prefix in OFDM systems. In *Proc. of the IEEE International Conference on Acoustics, Speech, and Signal Processing*, volume 5, pages 2957–2960, Jun. 2000.

[53] E. Chiavaccini and G.M. Vitetta. Maximum-likelihood frequency recovery for OFDM signals transmitted over multipath fading channels. *IEEE Transactions on Communications*, 52(2):244–251, Feb. 2004.

[54] J.W. Choi and Y.H. Lee. Design of the optimum pilot pattern for channel estimation in OFDM systems. In *Proc. of the IEEE Global Telecommunications Conference*, volume 6, pages 3661–3665, Dec. 2004.

[55] Y. S. Choi, P.J. Voltz, and F.A. Cassara. ML estimation of carrier frequency offset for multicarrier signals in Rayleigh fading channels. *IEEE Transactions on Vehicular Technology*, 50(2):644–655, Mar. 2001.

[56] N. Chotikakamthorn and H. Suzuki. On identifiability of OFDM blind channel estimation. In *Proc. of the Vehicular Technology Fall Conference*, volume 4, pages 2358–2361, Sept. 1999.

[57] C. K. Chui and G. Chen. *Kalman Filtering with Real-Time Applications*. Springer, 3rd edition, 1999.

[58] P. Ciblat and M. Ghogho. Harmonic retrieval in non-circular complex-valued multiplicative noise: Cramér-Rao bound. In *Proc. of the IEEE International Conference on Acoustics, Speech, and Signal Processing*, volume 2, pages II 489–II 492, May 2004.

[59] P. Ciblat, M. Ghogho, P. Larzabal, and P. Forster. Harmonic retrieval in the presence of non-circular gaussian multiplicative noise: Performance bounds. *Elsevier Signal Processing*, 85(4):737–749, Apr. 2005.

[60] P. Ciblat, P. Loubaton, E. Serpedin, and G.B. Giannakis. Performance analysis of blind carrier frequency offset estimators for noncircular transmissions through frequency-selective channels. *IEEE Transactions on Signal Processing*, 50(1):130–140, Jan. 2002.

[61] P. Ciblat and E. Serpedin. A fine blind frequency offset estimator for OFDM/OQAM systems. *IEEE Transactions on Signal Processing*, 52(1):291–296, Jan. 2004.

[62] P. Ciblat, E. Serpedin, and Y. Wang. On a blind fractionally sampling-based carrier frequency offset estimator for noncircular transmissions. *IEEE Signal Processing Letters*, 10(4):89–92, Apr. 2003.

[63] P. Ciblat and L. Vandendorpe. Blind carrier frequency offset estimation for non-circular constellation-based transmissions. *IEEE Transactions on Signal Processing*, 51(5):1378–1389, May 2003.

[64] L. Cimini. Analysis and simulation of a digital mobile channel using orthogonal frequency division multiplexing. *IEEE Transactions on Communications*, 33(7):665–675, Jul. 1985.

[65] H. A. Cirpan and M. K. Tsatsanis. Maximum likelihood blind channel estimation in the presence of Doppler shifts. *IEEE Transactions on Signal Processing*, 47(6):1559–1569, Jun. 1999.

[66] S. Coleri, M. Ergen, A. Puri, and A. Bahai. Channel estimation techniques based on pilot arrangement in OFDM systems. *IEEE Transactions on Broadcasting*, 48(3):223–229, Sept. 2002.

[67] A.J. Coulson. Maximum likelihood synchronization for OFDM using a pilot symbol: algorithms. *IEEE Journal on Selected Areas in Communications*, 19(12):2486–2494, Dec. 2001.

[68] F. Daffara and O. Adami. A new frequency detector for orthogonal multicarrier transmission techniques. In *proc. of the IEEE Vehicular Technology Conference*, volume 2, pages 804–809, Jul. 1995.

[69] F. Daffara and A. Chouly. Maximum likelihood frequency detectors for orthogonal multicarrier systems. In *Proc. of the IEEE International Conference on Communications*, volume 2, pages 766–771, May 1993.

[70] M. de Courville, P. Duhamel, P. Madec, and J. Palicot. Blind equalization of OFDM systems based on the minimization of a quadratic criterion. In *Proc. of the IEEE International Conference on Communications*, volume 3, pages 1318–1322, Jun. 1996.

[71] L. Deneire, P. Vandenameele, L. van der Perre, B. Gyselinckx, and M. Engels. A low-complexity ML channel estimator for OFDM. *IEEE Transactions on Communications*, 51(2):135–140, Feb. 2003.

[72] M. Dong, L. Tong, and B.M. Sadler. Optimal pilot placement for channel tracking in OFDM. In *Proc. of MILCOM*, volume 1, pages 602–606, Oct. 2002.

[73] M. Dong, L. Tong, and B.M. Sadler. Optimal insertion of pilot symbols for transmissions over time-varying flat fading channels. *IEEE Transactions on Signal Processing*, 52(5):1403–1418, May 2004.

[74] X.G. Doukopoulos and G.V. Moustakides. Adaptive algorithms for blind channel estimation in OFDM systems. In *Proc. of the IEEE International Conference on Communications*, volume 4, pages 2377–2381, Jun. 2004.

[75] J. Du, Q. Peng, and H. Zhang. Adaptive blind channel identification and equalization for OFDM-MIMO wireless communication systems. In *IEEE Proc. on Personal, Indoor and Mobile Radio Communications*, volume 3, pages 2078–2082, Sept. 2003.

[76] O. Edfors. Low-complexity algorithms in digital receivers. Doctoral Thesis 1996:206 D, ISSN 0348-8373, Lulea University of Technology, Sept. 1996.

[77] O. Edfors, M. Sandell, J.-J. van de Beek, S.K. Wilson, and P. Ola Börjesson. OFDM channel estimation by singular value decomposition. *IEEE Transactions on Communications*, 46(7):931–939, Jul. 1998.

[78] M. Enescu, M. Herdin, T. Roman, and V. Koivunen. Parameter estimation of measured channels in mobile MIMO OFDM system. In *Proc. of the IEEE International Symposium on Signal Processing and Information Technology*, pages 123–126, Dec. 2004.

[79] M. Enescu and V. Koivunen. On the estimation of state matrix and noise statistics in state-space models. In *Proc. of the IEEE Vehicular Technology Fall Conference*, volume 4, pages 2192–2196, Sept. 2002.

[80] M. Enescu and V. Koivunen. Estimating the fading coefficient in mobile OFDM systems using state-space model. In *Proc. of the IEEE International Symposium on Circuits and Systems*, volume 6, pages 6094–6097, May 2005.

[81] M. Enescu, T. Roman, and M. Herdin. Kalman-based estimation of measured channels in mobile MIMO OFDM system. In *Proc. of the European Signal Processing Conference*, pages 1865–1868, Sept. 2004.

[82] M. Enescu, T. Roman, and V. Koivunen. Channel estimation and tracking in spatially correlated MIMO OFDM systems. In *Proc. of the IEEE Workshop on Statistical Signal Processing*, pages 347–350, Oct. 2003.

[83] M. Engels. *Wireless OFDM systems - How to make them work?* Kluwer Academic Publishers, 2002.

[84] ETSI. Broadband radio access networks (BRAN); HIPERLAN type 2; physical (PHY) layer. *TS 101 475 V1.1.1*, 2000-2004.

[85] ETSI. Radio broadcasting systems; digital audio broadcasting (DAB) to mobile, portable and fixed receivers. *EN 300 401 V1.3.3*, May 2001.

[86] ETSI. Digital video broadcasting (DVB); framing structure, channel coding and modulation for digital terrestrial television. *EN 300 744 V1.5.1*, Nov. 2004.

[87] P. Frenger and A. Svensson. A decision directed coherent detector for OFDM. In *Proc. of the IEEE Vehicular Technology Conference*, volume 3, pages 1584–1588, May 1996.

[88] M.J. Fernandez-Getino Garcia, O. Edfors, and J.M. Paez-Borrallo. Frequency offset correction for coherent OFDM in wireless systems. *IEEE Transactions on Consumer Electronics*, 47(1):187–193, Feb. 2001.

[89] M.J.F.G. Garcia, J.M. Paez-Borrallo, and S. Zazo. Efficient pilot patterns for channel estimation in OFDM systems over HF channels. In *Proc. of the IEEE Vehicular Technology Conference*, volume 4, pages 2193–2197, Sept. 1999.

[90] M.J.F.G. Garcia, J.M. Paez-Borrallo, and S. Zazo. DFT-based channel estimation in 2D-pilot-symbol-aided OFDM wireless systems. In *Proc. of the IEEE Vehicular Technology Conference*, volume 2, pages 810–814, May 2001.

[91] M.J.F.G. Garcia, S. Zazo, and J.M. Paez-Borrallo. Pilot patterns for channel estimation in OFDM. *IEE Electronics Letters*, 36(12):1049–1050, Jun. 2000.

[92] W.A. Gardner. *Cyclostationarity in Communications and Signal Processing.* Piscataway (N.J.), IEEE Press, 1994.

[93] H. Ge and K. Wang. Efficient method for carrier offset correction in OFDM system. In *Proc. of the IEEE International Conference on Acoustics, Speech, and Signal Processing*, volume 5, pages 2467–2470, Mar. 1999.

[94] I. Ghaleb, O.A. Alim, and K. Gomaa. A new finite alphabet based blind channel estimation algorithm for OFDM systems. In *Proc. of the Twenty-First National Radio Science Conference*, volume C10, pages 1–7, Mar. 2004.

[95] M. Ghogho. On blind frequency-offset synchronization for OFDM communications. In *European Signal Processing Conference (invited paper)*, Sept. 2002. Available at *http://www.personal.leeds.ac.uk/~eenmg/publications.html*.

[96] M. Ghogho and A. Swami. Blind frequency-offset estimation for OFDM and related multicarrier systems. In *IEEE International Symposium on Signal Processing and Information Technology (invited paper)*, 2002. Available at *http://www.personal.leeds.ac.uk/~eenmg/publications.html*.

[97] M. Ghogho and A. Swami. Blind frequency-offset estimator for OFDM systems transmitting constant-modulus symbols. *IEEE Communications Letters*, 6(8):343–345, Aug. 2002.

[98] M. Ghogho and A. Swami. Semi-blind frequency offset synchronization for OFDM. In *Proc. of the IEEE International Conference on Acoustics, Speech, and Signal Processing*, volume 3, pages III–2333–III–2336, May 2002.

[99] M. Ghogho and A. Swami. Blind channel identification for OFDM systems with receive antenna diversity. In *Proc. of the IEEE Workshop Signal Processing Advances in Wireless Communications*, pages 378–382, Jun. 2003.

[100] M. Ghogho and A. Swami. Unified framework for a class of frequency-offset estimation techniques for OFDM. In *Proc. of the IEEE International Conference on Acoustics, Speech, and Signal Processing*, volume 4, pages iv–361–iv–364, May 2004.

[101] M. Ghogho and A. Swami. Carrier frequency synchronization for OFDM systems. In M. Ibnkahla, editor, *Signal Processing for mobile communications handbook*, chapter 8. CRC Press, 2005.

[102] M. Ghogho, A. Swami, and G.B. Giannakis. Optimized null-subcarrier selection for CFO estimation in OFDM over frequency-selective fading channels. In *Proc. of the IEEE Global Telecommunications Conference*, volume 1, pages 202–206, Nov. 2001.

[103] A. Ghosh, D.R. Wolter, J.G. Andrews, and R. Chen. Broadband wireless access with WiMax/802.16: current performance benchmarks and future potential. *IEEE Communications Magazine*, 43(2):129–136, Feb. 2005.

[104] G.B. Giannakis, Y. Hua, P. Stoica, and L. Tong, editors. *Signal Processing Advances in Wireless and Mobile Communications, Volume 1: Trends in Channel Estimation and Equalization*. Prentice Hall, 2000.

[105] G.H. Golub and C.F. van Loan. *Matrix computations*. The Johns Hopkins University Press, 3rd edition, 1996.

[106] Y. Gong and K.B. Letaief. Low rank channel estimation for space-time coded wideband OFDM systems. In *Proc. of the IEEE Vehicular Technology Conference*, volume 2, pages 772–776, Oct. 2001.

[107] A. Gorokhov. Blind equalization in SIMO OFDM systems with frequency domain spreading. *IEEE Transactions on Signal Processing*, 48(12):3536–3549, Dec. 2000.

[108] B. Guo, H. Lin, and K. Yamashita. Blind signal recovery in multiuser MIMO-OFDM system. In *Proc. of the Midwest Symposium on Circuits and Systems*, volume 2, pages II–637 – II–640, Jul. 2004.

[109] J. Guo, D. Wang, and C. Ran. Simple channel estimator for STBC-based OFDM systems. *IEE Electronics Letters*, 39(5):445–447, Mar. 2003.

[110] A. W. Habboosh, R. J. Vaccaro, and S. Kay. An algorithm for detecting closely spaced delay/Doppler components. In *Proc. of the IEEE International Conference on Acoustics, Speech, and Signal Processing*, volume 1, pages 535–538, 1997.

[111] T. Han and X. Li. Minimum-output-energy method for blind equalization of OFDM and systems with sufficient or insufficient cyclic prefix. In *Proc. of the IEEE International Conference on Acoustics, Speech, and Signal Processing*, volume 4, pages IV–225 – IV–228, Apr. 2003.

[112] T. Han and X. Li. Blind adaptive equalization of OFDM transmission with insufficient cyclic prefix. In *Proc. of the International Conference of Modern Problems of Radio Engineering, Telecommunications and Computer Science*, pages 213–216, Feb. 2004.

[113] L. Hanzo, M. Münster, B.J. Choi, and T. Keller. *OFDM and MC-CDMA for Broadband Multi-User Communications, WLANs and Broadcasting.* Wiley, IEEE Press, 2003.

[114] S. Hara and R. Prasad. Overview of multicarrier CDMA. *IEEE Communications Magazine*, 35(12):126–133, Dec. 1997.

[115] B. Hassibi and B.M. Hochwald. How much training is needed in multiple-antenna wireless links? *IEEE Transactions on Information Theory*, 49(4):951–963, Apr. 2003.

[116] S. Haykin. *Adaptive filter theory.* Prentice-Hall, 3rd edition, 1996.

[117] S. Haykin, K. Huber, and Z. Chen. Bayesian sequential state estimation for MIMO wireless communications. *Proceedings of the IEEE*, 92(3):439–454, Mar. 2004.

[118] R.W.Jr. Heath and G.B. Giannakis. Exploiting input cyclostationarity for blind channel identification in OFDM systems. *IEEE Transactions on Signal Processing*, 47(3):848–856, Mar. 1999.

[119] J. Heiskala and J. Terry. *OFDM Wireless LANs: A theoretical and practical guide.* SAMS Publishing, 2001.

[120] T.C. Hewavithana and D.M. Brookes. Blind adaptive channel equalization for OFDM using the cyclic prefix data. In *Proc. of the IEEE Global Telecommunications Conference*, volume 4, pages 2376–2380, Dec. 2004.

[121] B. Hirosaki. An orthogonally multiplexed QAM system using the discrete Fourier transform. *IEEE Transactions on Communications*, 29(7):982–989, Jul. 1981.

[122] C.K. Ho, B. Farhang-Boroujeny, and F. Chin. Added pilot semi-blind channel estimation scheme for OFDM in fading channels. In *Proc. of the IEEE Global Telecommunications Conference*, volume 5, pages 3075–3079, Nov. 2001.

[123] P. Hoeher, S. Kaiser, and P. Robertson. Two-dimensional pilot-symbol-aided channel estimation. In *Proc. of the IEEE International Symposium on Information Theory*, volume 3, pages 1845–1848, Apr. 1997.

[124] P. Hoeher, S. Kaiser, and P. Robertson. Two-dimensional pilot-symbol-aided channel estimation by Wiener filtering. In *Proc. of the IEEE International Conference on Acoustics, Speech, and Signal Processing*, volume 3, pages 1845–1848, Apr. 1997.

[125] R.A. Horn and C.R. Johnson. *Topics in Matrix Analysis*. Cambridge University Press, 1991.

[126] A. Hottinen, O. Tirkkonen, and R. Wichman. *Multi-antenna Transceiver Techniques for 3G and Beyond*. Wiley, Jan. 2003.

[127] M.H. Hsieh and C.H. Wei. Channel estimation for OFDM systems based on comb-type pilot arrangement in frequency selective fading channels. *IEEE Transactions on Consumer Electronics*, 44(1):217–225, Feb. 1998.

[128] M.H. Hsieh and C.H. Wei. A low-complexity frame synchronization and frequency offset compensation scheme for OFDM systems over fading channels. *IEEE Transactions on Vehicular Technology*, 48(5):1596–1609, Sept. 1999.

[129] IEEE. Multiband OFDM proposal overview. *IEEE P802.15 Working Group for Wireless Personal Area Networks*, Jan. 2005. Doc. number IEEE 802.15-05-0081. Available for download at: http://grouper.ieee.org/groups/802/15/pub/2005/.

[130] IEEE 802.11 standard. Available at:. *http://grouper.ieee.org/groups/802/11/*.

[131] IEEE P802.11, Task group N, Status of Project IEEE 802.11n. Available at:. *http://grouper.ieee.org/groups/802/11/Reports/tgn_update.htm*.

[132] R. A. Iltis. Joint estimation of PN code delay and multipath using the extended Kalman filter. *IEEE Transactions on Communications*, 38(10):1677–1685, Oct. 1990.

[133] International Telecommunication Union. Guideline for evaluation of radio transmission technologies for IMT-2000. 1997.

[134] W.C. Jakes. *Microwave Mobile Communications*. New York, Wiley, 1974.

[135] A. Jakobsson, A. L. Swindlehurst, and P. Stoica. Resolution of overlapping Doppler shifted echoes. In *Proc. of the IEEE International Conference on Acoustics, Speech, and Signal Processing*, volume 4, pages 2417–2420, May 1998.

[136] A. Jakobsson, A. L. Swindlehurst, and P. Stoica. Subspace-based estimation of time delays and Doppler shifts. *IEEE Transactions on Signal Processing*, 46(9):2472–2482, Sept. 1998.

[137] W. G. Jeon, K. H. Paik, and Y. S. Cho. An efficient channel estimation technique for OFDM systems with transmitter diversity. In *Proc. of the IEEE International Symposium on Personal, Indoor and Mobile Radio Communications*, volume 2, pages 1246–1250, Sept. 2000.

[138] S. Jun-Zhao, J. Sauvola, and D. Howie. Features in future: 4G visions from a technical perspective. In *Proc. of the IEEE Global Telecommunications Conference*, volume 6, pages 3533–3537, Nov. 2001.

[139] S. Kai and E. Serpedin. Coarse frame and carrier synchronization of OFDM systems: a new metric and comparison. *IEEE Transactions on Wireless Communications*, 3(4):1271 – 1284, Jul. 2004.

[140] I. Kalet. The multitone channel. *IEEE Transactions on Communications*, 37(2):119–124, Feb. 1989.

[141] S. G. Kang, Y. M. Ha, and E. K. Joo. A comparative investigation on channel estimation algorithms for OFDM in mobile communications. *IEEE Transactions on Broadcasting*, 49(2):142–149, Jun. 2003.

[142] S. G. Kang, Y. M. Ha, and E. K. Joo. Corrections to "A comparative investigation on channel estimation algorithms for OFDM in mobile communications". *IEEE Transactions on Broadcasting*, 51(1):154–154, Mar. 2005.

[143] J. P. Kermoal, L. Schumacher, K. I. Pedersen, P. E. Mogensen, and F. Frederiksen. A stochastic MIMO radio channel model with experimental validation. *IEEE Journal on Selected Areas in Communications*, 20(6):1211–1226, Aug. 2002.

[144] J. Kim, J. Park, and D. Hong. Performance analysis of channel estimation in OFDM systems. *IEEE Signal Processing Letters*, 12(1):60–62, Jan. 2005.

[145] K.J. Kim and T. Reid. Multiple hypothesis channel estimation for the MIMO-OFDM system. In *Proc. of the IEEE Global Telecommunications Conference*, volume 4, pages 2674–2678, Dec. 2004.

[146] K.J. Kim, T. Reid, and R.A. Iltis. A sequential Monte-Carlo Kalman filter based delay and channel estimation method in the MIMO-OFDM system. In *Proc. of the IEEE Vehicular Technology Conference*, volume 1, pages 573–577, Sept. 2004.

[147] K.J. Kim and J. Yue. Joint channel estimation and data detection algorithms for MIMO-OFDM systems. In *Conference Record of the Thirty-Sixth Asilomar Conference on Signals, Systems and Computers*, volume 2, pages 1857–1861, Nov. 2002.

[148] K.J. Kim, J. Yue, R.A. Iltis, and J.D. Gibson. A QRD-M/Kalman filter-based detection and channel estimation algorithm for MIMO-OFDM systems. *IEEE Transactions on Wireless Communications*, 4(2):710–721, Mar. 2005.

[149] C.C. Ko, R. Mo, and M. Shi. A new data rotation based CP synchronization scheme for OFDM systems. *IEEE Transactions on Broadcasting*, 51(3):315–321, Sept. 2005.

[150] I. Koffman and V. Roman. Broadband wireless access solutions based on OFDM access in IEEE 802.16. *IEEE Communications Magazine*, 40(4):96 – 103, Apr. 2002.

[151] C. Komninakis, C. Fragouli, A. H. Sayed, and R.D. Wesel. Multi-Input Multi-Output fading channel tracking and equalization using Kalman estimation. *IEEE Transactions on Signal Processing*, 50(5):1065–1076, May 2002.

[152] L. Kuang, Z. Ni, J. Lu, and J. Zheng. A time-frequency decision-feedback loop for carrier frequency offset tracking in OFDM systems. *IEEE Transactions on Wireless Communications*, 4(2):367–373, Mar. 2005.

[153] D. Landstrom, S.K. Wilson, J.J. van de Beek, P. Odling, and P.O. Börjesson. Symbol time offset estimation in coherent OFDM systems. *IEEE Transactions on Communications*, 50(4):545–549, Apr. 2002.

[154] N. Lashkarian and S. Kiaei. Class of cyclic-based estimators for frequency-offset estimation of OFDM systems. *IEEE Transactions on Communications*, 48(12):2139–2149, Dec. 2000.

[155] K.F. Lee and D.B. Williams. A multirate pilot-symbol-assisted channel estimator for OFDM transmitter diversity systems. In *Proc. of the IEEE Conference on Acoustics, Speech, and Signal Processing*, volume 4, pages 2409–2412, May 2001.

[156] J. Lei and T.S. Ng. A consistent OFDM carrier frequency offset estimator based on distinctively spaced pilot tones. *IEEE Transactions on Wireless Communications*, 3(2):588–599, Mar. 2004.

[157] G. Leus and M. Moonen. Per-tone equalization for MIMO OFDM systems. *IEEE Transactions on Signal Processing*, 51(11):2965–2975, Nov. 2003.

[158] G. Levin and D. Wulich. Frequency offset estimation in OFDM using sample covariance. In *Proc. of the IEEE Military Communications Conference*, volume 2, pages 688–692, Oct. 1998.

[159] J. Li, G. Liu, and G.B. Giannakis. Carrier frequency offset estimation for OFDM-based WLANs. *IEEE Signal Processing Letters*, 8(3):80–82, Mar. 2001.

[160] Y. Li. Pilot-symbol-aided channel estimation for OFDM in wireless systems. *IEEE Transactions on Vehicular Technology*, 49(4):1207–1215, Jul. 2000.

[161] Y. Li. Simplified channel estimation for OFDM systems with multiple transmit antennas. *IEEE Transactions on Wireless Communications*, 1(1):67–75, Jan. 2002.

[162] Y. Li, L.J.Jr. Cimini, and N.R. Sollenberger. Robust channel estimation for OFDM systems with rapid dispersive fading channels. *IEEE Transactions on Communications*, 46(7):902–915, Jul. 1998.

[163] Y. G. Li, N. Seshadri, and S. Ariyavisitakul. Channel estimation for OFDM systems with transmitter diversity in mobile wireless channels. *IEEE Journal on Selected Areas in Communications*, 17:461–471, Mar. 1999.

[164] Y. G. Li, J. H. Winters, and N. R. Sollenberger. MIMO-OFDM for wireless communications: Signal detection with enhanced channel estimation. *IEEE Transactions on Communications*, 50(9):1471–1477, Sep. 2002.

[165] J.C. Lin. Maximum-likelihood frame timing instant and frequency offset estimation for OFDM communication over a fast Rayleigh-fading channel. *IEEE Transactions on Vehicular Technology*, 52(4):1049–1062, Jul. 2003.

[166] R. Lin and A.P. Petropulu. Linear block precoding for blind channel estimation in OFDM systems. In *Proc. of the Seventh International Symposium on Signal Processing and Its Applications*, volume 2, pages 395–398, Jul. 2003.

[167] H. Liu and U. Tureli. A high-efficiency carrier estimator for OFDM communications. *IEEE Communications Letters*, 2(4):104–106, Apr. 1998.

[168] Z. Liu, G. B. Giannakis, and B. L. Hughes. Double differential space-time block coding for time-selective fading channels. *IEEE Transactions on Communications*, 49(9):1529–1539, Sept. 2001.

[169] Z. Liu, B. Weng, and Q. Zhu. Frequency offset estimation for differential OFDM. *IEEE Transactions on Wireless Communications*, 4(4):1737–1748, Jul. 2005.

[170] M. Luise, M. Marselli, and R. Reggiannini. Low-complexity blind carrier frequency recovery for OFDM signals over frequency-selective radio channels. *IEEE Transactions on Communications*, 50(7):1182–1188, Jul. 2002.

[171] M. Luise and R. Reggiannini. Carrier frequency acquisition and tracking for OFDM systems. *IEEE Transactions on Communications*, 44(11):1590–1598, Nov. 1996.

[172] M. Luise, R. Reggiannini, and G.M. Vitetta. Blind equalization/detection for OFDM signals over frequency-selective channels. *IEEE Journal on Selected Areas in Communications*, 16(8):1568–1578, Oct. 1998.

[173] X. Ma, M.K. Oh, G.B. Giannakis, and D.J. Park. Hopping pilots for estimation of frequency-offset and multiantenna channels in MIMO-OFDM. *IEEE Transactions on Communications*, 53(1):162–172, Jan. 2005.

[174] X. Ma, C. Tepedelenlioglu, G.B. Giannakis, and S. Barbarossa. Non-data-aided carrier offset estimators for OFDM with null subcarriers: identifiability, algorithms, and performance. *IEEE Journal on Selected Areas in Communications*, 19(12):2504–2515, Dec. 2001.

[175] Y. Ma. Modified nonlinear least square approaches to carrier frequency offset estimation in OFDM systems. *IEEE Communications Letters*, 7(4):177–179, Apr. 2003.

[176] Y. Ma and Y. Huang. Blind estimation of carrier frequency offset for OFDM in unknown multipath channels. *Electronics Letters*, 39(1):128–130, Jan. 2003.

[177] Y. Ma, Y. Huang, and N. Yi. Exploiting subcarrier correlation for blind channel estimation in block precoded OFDM systems. In *Proc. of the 5th International Symposium on Multi-Dimensional Mobile Communications*, volume 1, pages 338–342, Sept. 2004.

[178] L. Maniatis, T. Weber, A. Sklavos, and Y. Liu. Pilots for joint channel estimation in multi-user OFDM mobile radio systems. In *Proc. of the IEEE International Symposium on Spread Spectrum Techniques and Applications*, volume 1, pages 44–48, Sept. 2002.

[179] J. Mannerkoski and V. Koivunen. Autocorrelation properties of channel encoded sequences-applicability to blind equalization. *IEEE Transactions on Signal Processing*, 48(12):3501–3507, Dec. 2000.

[180] J.H. Manton. Optimal training sequences and pilot tones for OFDM systems. *IEEE Communications Letters*, 5(4):151–153, Apr. 2001.

[181] L. Mazet, V. Buzenac-Settineri, M. de Courville, and P. Duhamel. An EM based semi-blind channel estimation algorithm designed for OFDM systems. In *Conference Record of the Thirty-Sixth Asilomar Conference on Signals, Systems and Computers*, volume 2, pages 1642–1646, Nov. 2002.

[182] B. McNair, L.J.Jr. Cimini, and N. Sollenberger. A robust timing and frequency offset estimation scheme for orthogonal frequency division multiplexing (OFDM) systems. In *Proc. of the IEEE Vehicular Technology Conference*, volume 1, pages 690–694, May 1999.

[183] V. Mignone and A. Morello. CD3-OFDM: a novel demodulation scheme for fixed and mobile receivers. *IEEE Transactions on Communications*, 44(9):1144–1151, Sept. 1996.

[184] H. Minn and N. Al-Dhahir. Optimal training signals for MIMO OFDM channel estimation. In *Proc. of the IEEE Global Telecommunications Conference*, volume 1, pages 219–224, Dec. 2004.

[185] H. Minn and V.K. Bhargava. An investigation into time-domain approach for OFDM channel estimation. *IEEE Transactions on Broadcasting*, 46(4):240–248, Dec. 2000.

[186] H. Minn, V.K. Bhargava, and K.B. Letaief. A robust timing and frequency synchronization for OFDM systems. *IEEE Transactions on Wireless Communications*, 2(4):822–839, Jul. 2003.

[187] H. Minn, D.I. Kim, and V.K. Bhargava. A reduced complexity channel estimation for OFDM systems with transmit diversity in mobile wireless channels. *IEEE Transactions on Communications*, 50(5):799–807, May 2002.

[188] P.H. Moose. A technique for orthogonal frequency division multiplexing frequency offset correction. *IEEE Transactions on Communications*, 42(10):2908–2914, Oct. 1994.

[189] M. Morelli, A.N. D'Andrea, and U. Mengali. Frequency ambiguity resolution in OFDM systems. *IEEE Communications Letters*, 4(4):134–136, Apr. 2000.

[190] M. Morelli and U. Mengali. An improved frequency offset estimator for OFDM applications. *IEEE Communications Letters*, 3(3):75–77, Mar. 1999.

[191] M. Morelli and U. Mengali. A comparison of pilot-aided channel estimation methods for OFDM systems. *IEEE Transactions on Signal Processing*, 49(12):3065–3073, Dec. 2001.

[192] B. Muquet, M. de Courville, and P. Duhamel. Subspace-based blind and semi-blind channel estimation for OFDM systems. *IEEE Transactions on Signal Processing*, 50(7):1699–1712, Jul. 2002.

[193] M.C. Necker and F. Sanzi. Generalized 8-PSK for totally blind channel estimation in OFDM. In *Proc. of the IEEE Vehicular Technology Conference*, volume 2, pages 924–928, May 2004.

[194] M.C. Necker and G.L. Stuber. Totally blind channel estimation for OFDM on fast varying mobile radio channels. *IEEE Transactions on Wireless Communications*, 3(5):1514–1525, Sept. 2004.

[195] F.D. Neeser and J.L. Massey. Proper complex random processes with applications to information theory. *IEEE Transactions on Information Theory*, 39(4):1293–1302, Jul. 1993.

[196] R. Negi and J. Cioffi. Pilot tone selection for channel estimation in a mobile OFDM system. *IEEE Transactions on Consumer Electronics*, 44(3):1122–1128, Aug. 1998.

[197] K. Nikitopoulos and A. Polydoros. Phase-impairment effects and compensation algorithms for OFDM systems. *IEEE Transactions on Communications*, 53(4):698–707, Apr. 2005.

[198] H. Nishookar and R. Prasad. On the sensitivity of multicarrier transmission over multipath channels to phase noise and frequency offset. In *Proc. IEEE International Symposium on Personal, Indoor and Mobile Radio Communications, PIMRC*, volume 1, pages 68–72, Oct. 1996.

[199] H. Nogami and T. Nagashima. A frequency and timing period acquisition technique for OFDM systems. In *Proc. of the IEEE International Symposium on Personal, Indoor and Mobile Radio Communications*, volume 3, pages 1010–1015, Sept. 1995.

[200] T. Nyblom, T. Roman, M. Enescu, and V. Koivunen. Time-varying carrier offset tracking in OFDM systems using particle filtering. In *Proc. of the IEEE Symposium on Signal Processing and Information Technology*, volume 2, pages 1934–1938, Dec. 2004.

[201] N. Ohkubo and T. Ohtsuki. Added pilot semi-blind iterative channel estimation for OFDM packet transmission. In *Proc. of the IEEE Global Telecommunications Conference*, volume 2, pages 878–882, Dec. 2003.

[202] N. Ohkubo and T. Ohtsuki. Space-time trellis coded OFDM system with added pilot semi-blind iterative channel estimation. In *Proc. of the IEEE Global Telecommunications Conference*, volume 6, pages 3546–3550, Dec. 2004.

[203] S. Ohno and G.B. Giannakis. Capacity maximizing MMSE-optimal pilots for wireless OFDM over frequency-selective block Rayleigh-fading channels. *IEEE Transactions on Information Theory*, 50(9):2138–2145, Sept. 2004.

[204] A. Pandharipande. Principles of OFDM. *IEEE Potentials*, 21(2):16–19, Apr.-May 2002.

[205] B. Park, H. Cheon, E. Ko, C. Kang, and D. Hong. A blind OFDM synchronization algorithm based on cyclic correlation. *IEEE Signal Processing Letters*, 11(2):83–85, Feb. 2004.

[206] S.Y. Park, B.S. Seo, and C.G. Kang. Effects of frequency offset compensation error on channel estimation for OFDM system under mobile radio channels. *Signal Processing*, 83:2621–2630, Dec. 2003.

[207] A.J. Paulraj, D.A. Gore, R.U. Nabar, and H. Bölcskei. An overview of MIMO communications - a key to gigabit wireless. *Proc. of the IEEE*, 92(2):198–218, Feb. 2004.

[208] A. Peled and A. Ruiz. Frequency domain data transmission using reduced computational complexity algorithms. In *Proc. of the IEEE International Conference on Acoustics, Speech, and Signal Processing*, volume 5, pages 964–967, Apr. 1980.

[209] R. Perets and B.Z. Bobrovsky. A new phase and frequency offset estimation algorithm for OFDM systems applying Kalman filter. In *Proc. of the 22nd Convention of Electrical and Electronics Engineers in Israel*, pages 300–302, Dec. 2002.

[210] T. Petermann, S. Vogeler, K.D. Kammeyer, and D. Boss. Blind turbo channel estimation in OFDM receivers. In *Conference Record of the Thirty-Fifth Asilomar Conference on Signals, Systems and Computers*, volume 2, pages 1489–1493, Nov. 2001.

[211] A. Petropulu and R. Zhang. Blind channel estimation for OFDM systems. In *Proc. of the 2002 IEEE 10th Digital Signal Processing Workshop*, pages 366–370, Oct. 2002.

[212] A. Petropulu, R. Zhang, and R. Lin. Blind OFDM channel estimation through simple linear precoding. *IEEE Transactions on Wireless Communications*, 3(2):647–655, Mar. 2004.

[213] L. Piazzo and P. Mandarini. Analysis of phase noise effects in OFDM modems. *IEEE Transactions on Communications*, 50(10):1696–1705, Oct. 2002.

[214] B. Picinbono. On circularity. *IEEE Transactions on Signal Processing*, 42(12):3473–3482, Dec. 1994.

[215] B. Picinbono. Second-order complex random vectors and normal distributions. *IEEE Transactions on Signal Processing*, 44(10):2637–2640, Oct. 1996.

[216] V. Pohl, P. H. Nguyen, V. Jungnickel, and C. von Helmolt. Continuous flat-fading MIMO channels: achievable rate and optimal length of the training and data phases. *IEEE Transactions on Wireless Communications*, 4(4):1889–1900, Jul. 2005.

[217] T. Pollet, M. Van Bladel, and M. Moeneclaey. BER sensitivity of OFDM systems to carrier frequency offset and Wiener phase noise. *IEEE Transactions on Communications*, 43:191–193, Feb.-Mar.-Apr. 1995.

[218] H.V. Poor. *An introduction to signal detection and estimation*. Springer Verlag, 2nd edition, 1994.

[219] S. Prasad and A.S. Varikat. Semi-blind equalization at the symbol rate with application to OFDM. *Elsevier Signal Processing*, 83(5):1105–1115, May 2003.

[220] J. G. Proakis. *Digital Communications*. McGraw-Hill, third edition, 1995.

[221] Y. Qiao, S. Yu, P. Su, and L. Zhang. Research on an iterative algorithm of LS channel estimation in MIMO OFDM systems. *IEEE Transactions on Broadcasting*, 51(1):149–153, Mar. 2005.

[222] J. Ran, R. Grunheid, H. Rohling, E. Bolinth, and R. Kern. Decision-directed channel estimation method for OFDM systems with high velocities. In *Proc. of the IEEE Vehicular Technology Conference*, volume 4, pages 2358–2361, Apr. 2003.

[223] J. Rinne and M. Renfors. Pilot spacing in orthogonal frequency division multiplexing systems on practical channels. *IEEE Transactions on Consumer Electronics*, 42(4):959–962, Nov. 1996.

[224] H. Roh, K. Cheun, and J. Park. An MMSE fine carrier frequency synchronization algorithm for OFDM systems. *IEEE Transactions on Consumer Electronics*, 43(3):761–766, Aug. 1997.

[225] T. Roman, M. Enescu, and V. Koivunen. Recursive estimation of time-varying channel and frequency offset in MIMO OFDM systems. In *Proc. of the IEEE Conference on Personal, Indoor and Mobile Radio Communications*, volume 2, pages 1934–1938, Sept. 2003.

[226] T. Roman, M. Enescu, and V. Koivunen. Time-domain method for tracking dispersive channels in OFDM systems. In *Proc. of the IEEE Vehicular Technology Spring Conference*, pages 1318–1321, Apr. 2003.

[227] S. Roy and L. Chengyang. A subspace blind channel estimation method for OFDM systems without cyclic prefix. *IEEE Transactions on Wireless Communications*, 1(4):572–579, Oct. 2002.

[228] L. Rugini, P. Banelli, and G. Leus. Block DFE and windowing for Doppler-affected OFDM systems. In *Proc. of the IEEE Workshop on Signal Processing Advances in Wireless Communications*, pages 470–474, Jun. 2005.

[229] L. Rugini, P. Banelli, and G. Leus. Simple equalization of time-varying channels for OFDM. *IEEE Communications Letters*, 9(7):619–621, Jul. 2005.

[230] B. Saltzberg. Performance of an efficient parallel data transmission system. *IEEE Transactions on Communications*, 15(6):805–811, Dec. 1967.

[231] M. Sandel. Design and analysis of estimators for multicarrier modulation and ultrasonic imaging. Doctoral thesis, Lulea University of Technology, Sept. 1996.

[232] F. Sanzi, S. Jelting, and J. Speidel. A comparative study of iterative channel estimators for mobile OFDM systems. *IEEE Transactions on Wireless Communications*, 2(5):849–859, Sept. 2003.

[233] F. Sanzi and M.C. Necker. Totally blind APP channel estimation for mobile OFDM systems. *IEEE Communications Letters*, 7(11):517–519, Nov. 2003.

[234] F. Sanzi and J. Speidel. An adaptive two-dimensional channel estimator for wireless OFDM with application to mobile DVB-T. *IEEE Transactions on Broadcasting*, 46(2):128–133, Jun. 2000.

[235] K. Sathananthan and C. Tellambura. Probability of error calculation of OFDM systems with frequency offset. *IEEE Transactions on Communications*, 49(11):1884–1888, Nov. 2001.

[236] D. Schafhuber, G. Matz, and F. Hlawatsch. Kalman tracking of time-varying channels in wireless MIMO-OFDM systems. In *Conference Record of the Thirty-Seventh Asilomar Conference on Signals, Systems and Computers*, volume 2, pages 1261–1265, Nov. 2003.

[237] T.C.W. Schenk, X.J. Tao, P.F.M. Smulders, and E.R. Fledderus. Influence and suppression of phase noise in multi-antenna OFDM. In *Proc. of the IEEE Vehicular Technology Conference*, volume 2, pages 1443–1447, Sept. 2004.

[238] T.M. Schmidl and D.C. Cox. Robust frequency and timing synchronization for OFDM. *IEEE Transactions on Communications*, 45(12):1613–1621, Dec. 1997.

[239] R. Schmidt. Multiple emitter location and signal parameter estimation. *IEEE Transactions on Antennas and Propagation*, 34(3):276–280, Mar. 1986.

[240] R. J. Serfling. *Approximation Theorems of Mathematical Statistics*. Wiley, 1980.

[241] A. Seyedi and G.J. Saulnier. General ICI self-cancellation scheme for OFDM systems. *IEEE Transactions on Vehicular Technology*, 54(1):198–210, Jan. 2005.

[242] K. Shi, E. Serpedin, and P. Ciblat. Decision-directed fine synchronization in OFDM systems. *IEEE Transactions on Communications*, 53(3):408–412, Mar. 2005.

[243] C. Shin and E.J. Powers. Blind channel estimation for MIMO-OFDM systems using virtual carriers. In *Proc. of the IEEE Global Telecommunications Conference*, volume 4, pages 2465–2469, Dec. 2004.

[244] M. Shin, H. Lee, and C. Lee. Enhanced channel-estimation technique for MIMO-OFDM systems. *IEEE Transactions on Vehicular Technology*, 53(1):261–265, Jan. 2004.

[245] O. Simeone, Y. Bar-Ness, and U. Spagnolini. Pilot-based channel estimation for OFDM systems by tracking the delay-subspace. *IEEE Transactions on Wireless Communications*, 3(1):315–325, Jan. 2004.

[246] O. Simeone and U. Spagnolini. Adaptive pilot pattern for OFDM systems. In *Proc. of the IEEE International Conference on Communications*, volume 2, pages 978–982, Jun. 2004.

[247] M. Sirbu. Channel and delay estimation algorithms for wireless communication systems. Doctoral Thesis, ISBN 951-22-6837-X, Helsinki University of Technology, Signal Processing Laboratory, Dec. 2003.

[248] H.K. Song, Y.H. You, J.H. Paik, and Y.S. Cho. Frequency-offset synchronization and channel estimation for OFDM-based transmission. *IEEE Communications Letters*, 4(3):95–97, Mar. 2000.

[249] W.G. Song and J.T. Lim. Pilot-symbol aided channel estimation for OFDM with fast fading channels. *IEEE Transactions on Broadcasting*, 49(4):398–402, Dec. 2003.

[250] M. Sternad and D. Aronsson. Channel estimation and prediction for adaptive OFDM downlinks. In *Proc. of the IEEE Vehicular Technology Conference*, volume 2, pages 1283–1287, Oct. 2003.

[251] P. Stoica and O. Besson. Training sequence design for frequency offset and frequency-selective channel estimation. *IEEE Transactions on Communications*, 51(11):1910–1917, Nov. 2003.

[252] P. Stoica and G. Ganesan. Trained space-time block decoding for flat fading channels with frequency offsets. *Kluwer Wireless Personal Communications*, 27(3):235–245, Sept. 2003.

[253] P. Stoica and R. Moses. *Introduction to Spectral Analysis*. Prentice Hall, 1997.

[254] T. Strohmer and S. Beaver. Optimal OFDM design for time-frequency dispersive channels. *IEEE Transactions on Communications*, 51(7):1111–1122, Jul. 2003.

[255] Q. Sun, D.C. Cox, H.C. Huang, and A. Lozano. Estimation of continuous flat fading MIMO channels. *IEEE Transactions on Wireless Communications*, 1(4):549–553, Oct. 2002.

[256] S. Sun, I. Wiemer, C.K. Ho, and T.T. Tjhung. Training sequence assisted channel estimation for MIMO OFDM. In *Proc. of the IEEE Wireless Communications and Networking Conference*, volume 1, pages 38–43, Mar. 2003.

[257] Y. Sun, Z. Xiong, and X. Wang. EM-based iterative receiver design with carrier-frequency offset estimation for MIMO OFDM systems. *IEEE Transactions on Communications*, 53(4):581–586, Apr. 2005.

[258] S. Takaoka and F. Adachi. Pilot-assisted adaptive interpolation channel estimation for OFDM signal reception. In *Proc. of the IEEE Vehicular Technology Conference*, volume 3, pages 1777–1781, May 2004.

[259] M. Tanda. Blind symbol-timing and frequency-offset estimation in OFDM systems with real data symbols. *IEEE Transactions on Communications*, 52(10):1609–1612, Oct. 2004.

[260] H. Tang, K.Y. Lau, and R.W. Brodersen. Interpolation-based maximum likelihood channel estimation using OFDM pilot symbols. In *Proc. of the IEEE Global Telecommunications Conference*, volume 2, pages 1860–1864, Nov. 2002.

[261] I.E. Telatar. Capacity of multi-antenna gaussian channels. *European Transactions on Telecommunications*, 10(6):585–595, Nov. 1999.

[262] T.A. Thomas, F.W. Vook, and K.L. Baum. Semi-blind channel identification in OFDM. In *Proc. of the IEEE Vehicular Technology Conference*, volume 4, pages 1747–1750, May 2002.

[263] L. Tong, B.M. Sadler, and M. Dong. Pilot-assisted wireless transmissions: general model, design criteria, and signal processing. *IEEE Signal Processing Magazine*, 21(6):12–25, Nov. 2004.

[264] P.Y. Tsai, H.Y. Kang, and T.D. Chiueh. Joint weighted least-squares estimation of carrier-frequency offset and timing offset for OFDM systems over multipath fading channels. *IEEE Transactions on Vehicular Technology*, 54(1):211–223, Jan. 2005.

[265] M. Tsatsanis, G. Giannakis, and G. Zhou. Estimation and equalization of fading channels with random coefficients. *Signal Processing*, 53(2-3):211–229, 1996.

[266] U. Tureli, P. Honan, and H. Liu. Low-complexity nonlinear least squares carrier offset estimator for OFDM: identifiability, diversity and performance. *IEEE Transactions on Signal Processing*, 52(9):2441–2452, Sept. 2004.

[267] U. Tureli, D. Kivanc, and H. Liu. Experimental and analytical studies on a high-resolution OFDM carrier frequency offset estimator. *IEEE Transactions on Vehicular Technology*, 50(2):629–643, Mar. 2001.

[268] U. Tureli, H. Liu, and M.D. Zoltowski. OFDM blind carrier offset estimation: ESPRIT. *IEEE Transactions on Communications*, 48(9):1459–1461, Sept. 2000.

[269] A. Vahlin and N. Holte. Optimal finite duration pulses for OFDM. *IEEE Transactions on Communications*, 44(1):10–14, Jan. 1996.

[270] M. Valkama, M. Renfors, and V. Koivunen. Advanced methods for I/Q imbalance compensation in communication receivers. *IEEE Transactions on Signal Processing*, 49(10):2335–2344, Oct. 2001.

[271] J.J. van de Beek, O. Edfors, M. Sandell, S.K. Wilson, and P.O. Börjesson. On channel estimation in OFDM systems. In *Proc. of the IEEE Vehicular Technology Conference*, volume 2, pages 815–819, July 1995.

[272] J.J. van de Beek, M. Sandell, and P.O. Börjesson. Ml estimation of time and frequency offset in OFDM systems. *IEEE Transactions on Signal Processing*, 45(7):1800–1805, Jul. 1997.

[273] R. van Nee and R. Prasad. OFDM for wireless multimedia communications. *Artech House*, 2000.

[274] M.A. Visser and Y. Bar-Ness. Frequency offset correction for OFDM using a blind adaptive decorrelator in a time-variant selective Rayleigh fading channel. In *Proc. of the IEEE Vehicular Technology Conference*, volume 2, pages 1281–1285, May 1999.

[275] S. Visuri and V. Koivunen. Resolving ambiguities in subspace-based blind receiver for MIMO channels. In *Conference Record of the Thirty-Sixth Asilomar Conference on Signals, Systems and Computers*, volume 1, pages 589–593, Nov. 2002.

[276] H. Wang, Y. Lin, and B. Chen. Data-efficient blind OFDM channel estimation using receiver diversity. *IEEE Transactions on Signal Processing*, 51(10):2613–2623, Oct. 2003.

[277] H.S. Wang and P.C. Chang. On verifying the first-order Markovian assumption for a Rayleigh fading channel model. *IEEE Transactions on Vehicular Technology*, 45(2):353–357, May 1996.

[278] X. Wang and H.V. Poor. Robust multiuser detection in non-Gaussian channels. *IEEE Transactions on Signal Processing*, 47(2):289–305, Feb. 1999.

[279] Z. Wang and G. B. Giannakis. Wireless multicarrier communications. *IEEE Signal Processing Magazine*, 17(3):29–48, May 2000.

[280] W.D. Warner and C. Leung. OFDM/FM frame synchronization for mobile radio data communication. *IEEE Transactions on Vehicular Technology*, 42(3):302–313, Aug. 1993.

[281] S. Wei, D. Goeckel, and P. Kelly. The complex envelope of a bandlimited OFDM signal converges weakly to a gaussian random process: Proof and application. Technical report, University of Massachusetts, Sept. 2002. Available at *http://www.ee.lsu.edu/swei/*.

[282] W. Weichselberger, M. Herdin, H. Özcelik, and E. Bonek. A stochastic MIMO channel model with joint correlation of both link ends. *IEEE Transactions on Wireless Communications*, 5(1):90–100, Jan. 2006.

[283] S. Weinstein and P. Ebert. Data transmission by frequency-division multiplexing using the discrete Fourier transform. *IEEE Transactions on Communications*, 19(5):628–634, Oct. 1971.

[284] S.K. Wilson, R.E. Khayata, and J.M. Cioffi. 16 QAM modulation with orthogonal frequency division multiplexing in a Rayleigh-fading environment. In *Proc. of the IEEE Vehicular Technology Conference*, volume 3, pages 1660–1664, Jun. 1994.

[285] WINNER - Wireless World Initiative New Radio project. Url: http://www.ist-winner.org/.

[286] Y. Xie and C.N. Georghiades. Two EM-type channel estimation algorithms for OFDM with transmitter diversity. *IEEE Transactions on Communications*, 51(1):106–115, Jan. 2003.

[287] H. Xuejun, B. Houjie, and Y. Songyu. A new subspace algorithm of blind channel estimation for OFDM systems. In *Proc. of IEEE Personal, Indoor and Mobile Radio Communications*, volume 2, pages 1105–1108, Sept. 2003.

[288] B. Yang, Z. Cao, and K.B. Letaief. Analysis of low-complexity windowed DFT-based MMSE channel estimator for OFDM systems. *IEEE Transactions on Communications*, 49(11):1977–1987, Nov. 2001.

[289] B. Yang, K.B. Letaief, R.S. Cheng, and Z. Cao. Channel estimation for OFDM transmission in multipath fading channels based on parametric channel modeling. *IEEE Transactions on Communications*, 49(3):467–479, Mar. 2001.

[290] F. Yang, K.H. Li, and K.C. Teh. A carrier frequency offset estimator with minimum output variance for OFDM systems. *IEEE Communications Letters*, 8(11):677–679, Nov. 2004.

[291] L. Yang, C. Ming, S. Cheng, and H. Wang. An iterative semi-blind channel estimation with decision-directed for OFDM systems in fading channels. In *Proc. of the Vehicular Technology Conference*, volume 2, pages 958–961, May 2004.

[292] Z. Yang and X. Wang. A sequential Monte Carlo blind receiver for OFDM systems in frequency-selective fading channels. *IEEE Transactions on Signal Processing*, 50(2):271–280, Feb. 2002.

[293] Y. Yao and G.B. Giannakis. Blind carrier frequency offset estimation in SISO, MIMO, and multiuser OFDM systems. *IEEE Transactions on Communications*, 53(1):173–183, Jan. 2005.

[294] S. Yatawatta and A.P. Petropulu. Blind channel equalization in a multiuser OFDM communications system. In *Conference Record of the Thirty-Sixth Asilomar Conference on Signals, Systems and Computers*, volume 2, pages 1709–1713, Nov. 2002.

[295] S. Yatawatta and A.P. Petropulu. Blind channel estimation in MIMO OFDM systems. In *Proc. of the IEEE Workshop on Statistical Signal Processing*, volume 2, pages 1709–1713, Oct. 2003.

[296] J.H. Yu and Y.T. Su. Pilot-assisted maximum-likelihood frequency-offset estimation for OFDM systems. *IEEE Transactions on Communications*, 52(11):1997–2008, Nov. 2004.

[297] Z. Yuanjin. A novel channel estimation and tracking method for wireless OFDM systems based on pilots and Kalman filtering. *IEEE Transactions on Consumer Electronics*, 49(2):275–283, May 2003.

[298] J. Yue, K.J. Kim, T. Reid, and J.D. Gibson. Joint semiblind channel estimation and data detection for MIMO-OFDM systems. In *Proc. of the IEEE Symposium on Circuits and Systems*, volume 2, pages 709–712, Jun. 2004.

[299] X. Yue and H.H. Fan. Linear smoothing method for blind equalization of OFDM systems without cyclic prefix. In *Proc. of the IEEE Wireless Communications and Networking Conference*, volume 4, pages 2313–2316, Mar. 2004.

[300] Y. Zeng and T. Ng. A subspace method for channel estimation of multi-user multi-antenna OFDM system. In *Proc. of the International Symposium on Circuits and Systems*, volume 3, pages III–52 – III–55, May 2003.

[301] Y. Zeng and T. S. Ng. Subspace-based semi-blind channel estimation for STC-OFDM. In *Proc. of the IEEE International Conference on Communications*, volume 4, pages 2422–2426, Jun. 2004.

[302] Y. Zeng and T.S. Ng. A proof of the identifiability of a subspace-based blind channel estimation for OFDM systems. *IEEE Signal Processing Letters*, 11(9):756–759, Sept. 2004.

[303] Y. Zeng and T.S. Ng. A semi-blind channel estimation method for multiuser multi-antenna OFDM systems. *IEEE Transactions on Signal Processing*, 52(5):1419–1429, May 2004.

[304] J. Zhang, G. Liao, and J. Wang. Efficient frequency offset resolution for OFDM systems based on ML principle. *IEEE Transactions on Consumer Electronics*, 50(3):799–806, Aug. 2004.

[305] R. Zhang. Blind OFDM channel estimation through linear precoding: a subspace approach. In *Conference Record of the Thirty-Sixth Asilomar Conference on Signals, Systems and Computers*, volume 1, pages 631–633, Nov. 2002.

[306] R. Zhang and W. Chen. A mixture Kalman filter approach for blind OFDM channel estimation. In *Conference Record of the Thirty-Eighth Asilomar Conference on Signals, Systems and Computers*, volume 1, pages 350–354, Nov. 2004.

[307] Z. Zhang, W. Jiang, H. Zhou, Y. Liu, and J. Ga. High accuracy frequency offset correction with adjustable acquisition range in OFDM systems. *IEEE Transactions on Wireless Communications*, 4(1):228–237, Jan. 2005.

[308] Z. Zhang, K. Long, and Y. Liu. Complex efficient carrier frequency offset estimation algorithm in OFDM systems. *IEEE Transactions on Broadcasting*, 50(2):159–164, Jun. 2004.

[309] Z. Zhang, K. Long, M. Zhao, and Y. Liu. Joint frame synchronization and frequency offset estimation in OFDM system. *IEEE Transactions on Broadcasting*, 51(3):389–394, Sept. 2005.

[310] Z. Zhang, M. Zhao, H. Zhou, Y. Liu, and J. Gao. Frequency offset estimation with fast acquisition in OFDM system. *IEEE Communications Letters*, 8(3):171–173, Mar. 2004.

[311] Y. Zhao and S.G. Haggman. Sensitivity to Doppler shift and carrier frequency errors in OFDM systems - the consequences and solutions. In *Proc. of the IEEE Vehicular Technology Conference*, volume 3, pages 1564–1568, May 1996.

[312] Y. Zhao and S.G. Haggman. Intercarrier interference self-cancellation scheme for OFDM mobile communication systems. *IEEE Transactions on Communications*, 49(7):1185–1191, Jul. 2001.

[313] S. Zhou and G.B. Giannakis. Finite-alphabet based channel estimation for OFDM and related multicarrier systems. *IEEE Transactions on Communications*, 49(8):1402–1414, Aug. 2001.

[314] S. Zhou, B. Muquet, and G.B. Giannakis. Subspace-based (semi-) blind channel estimation for block precoded space-time OFDM. *IEEE Transactions on Signal Processing*, 50(5):1215–1228, May 2002.

[315] X. Zhou and X. Wang. Channel estimation for OFDM systems using adaptive radial basis function networks. *IEEE Transactions on Vehicular Technology*, 52(1):48–59, Jan. 2003.

[316] X. Zhuang, Z. Ding, and A.L. Swindlehurtst. A statistical subspace method for blind channel identification in OFDM communications. In *Proc. of the IEEE International Conference on Acoustics, Speech, and Signal Processing*, volume 5, pages 2493–2496, Jun. 2000.